Jet Substructure and Tagging in pp collisions

On behalf of ALICE, ATLAS, CMS, and LHCb
LHCP 2024, Boston, MA

Ibrahim Chahrour, University of Michigan

Jets at the LHC

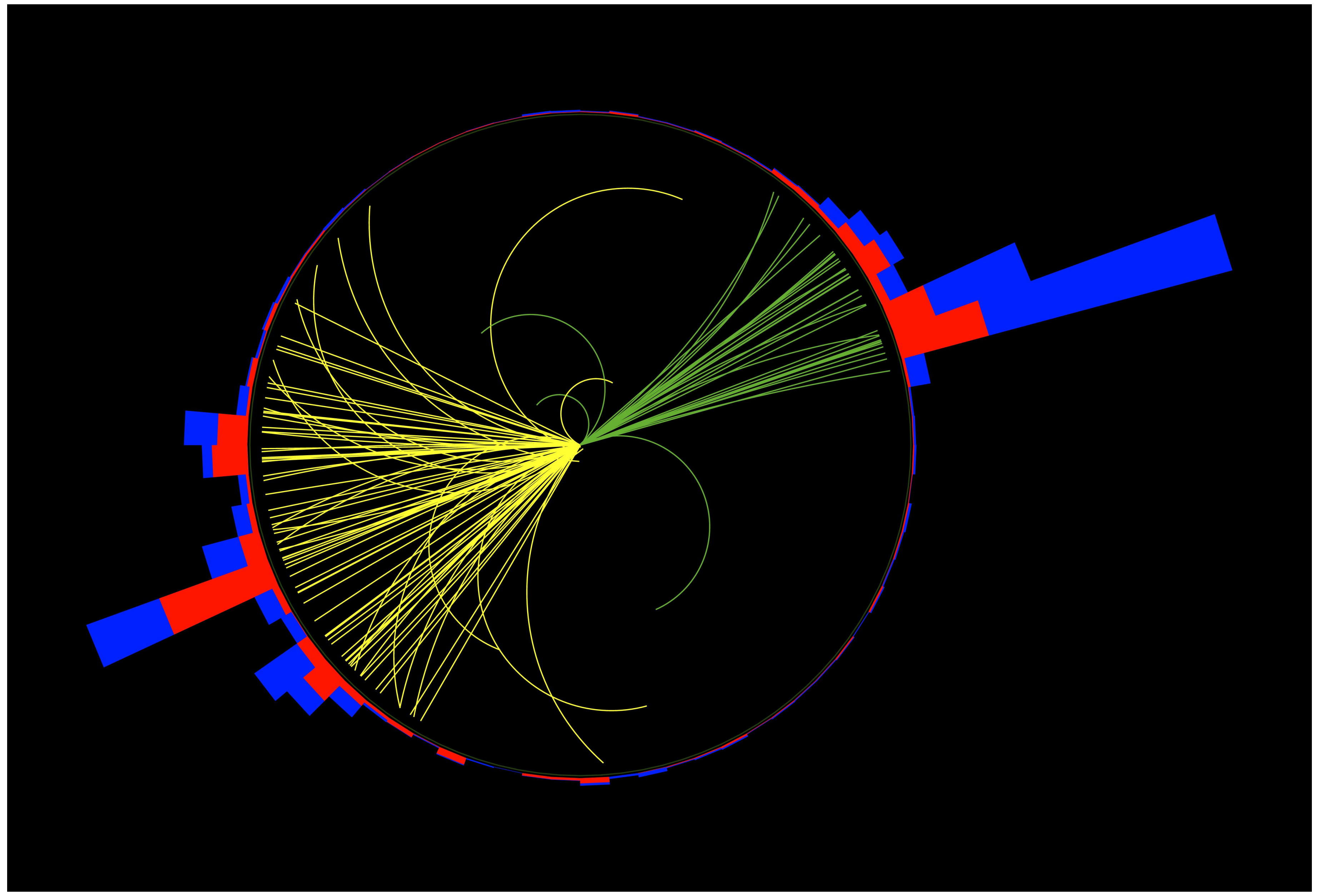

Credit: CMS Collaboration

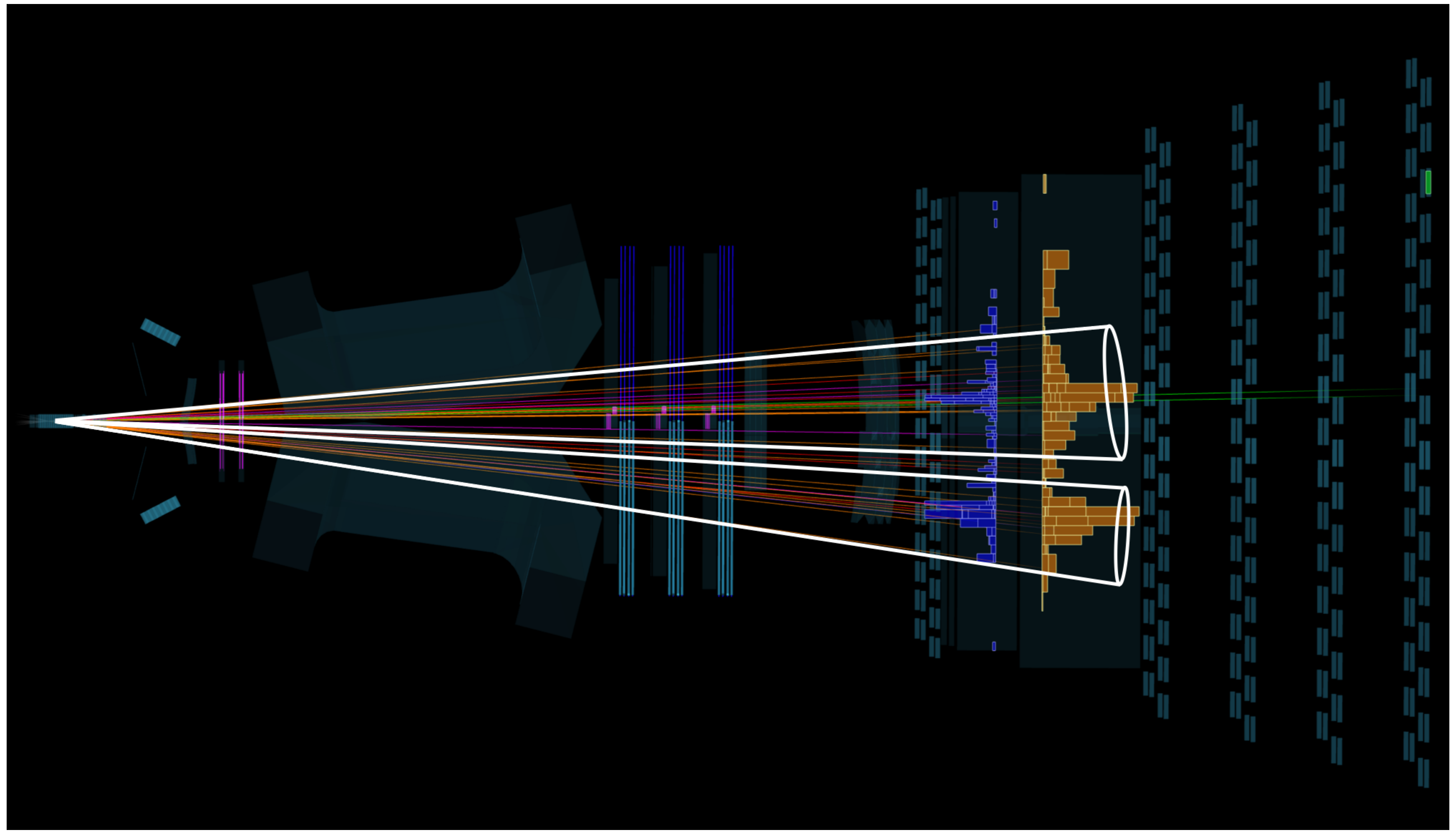

Credit: LHCb Collaboration

What can we learn from looking inside jets?

Jet Substructure: opening the QCD world

Heavy quark splitting functions

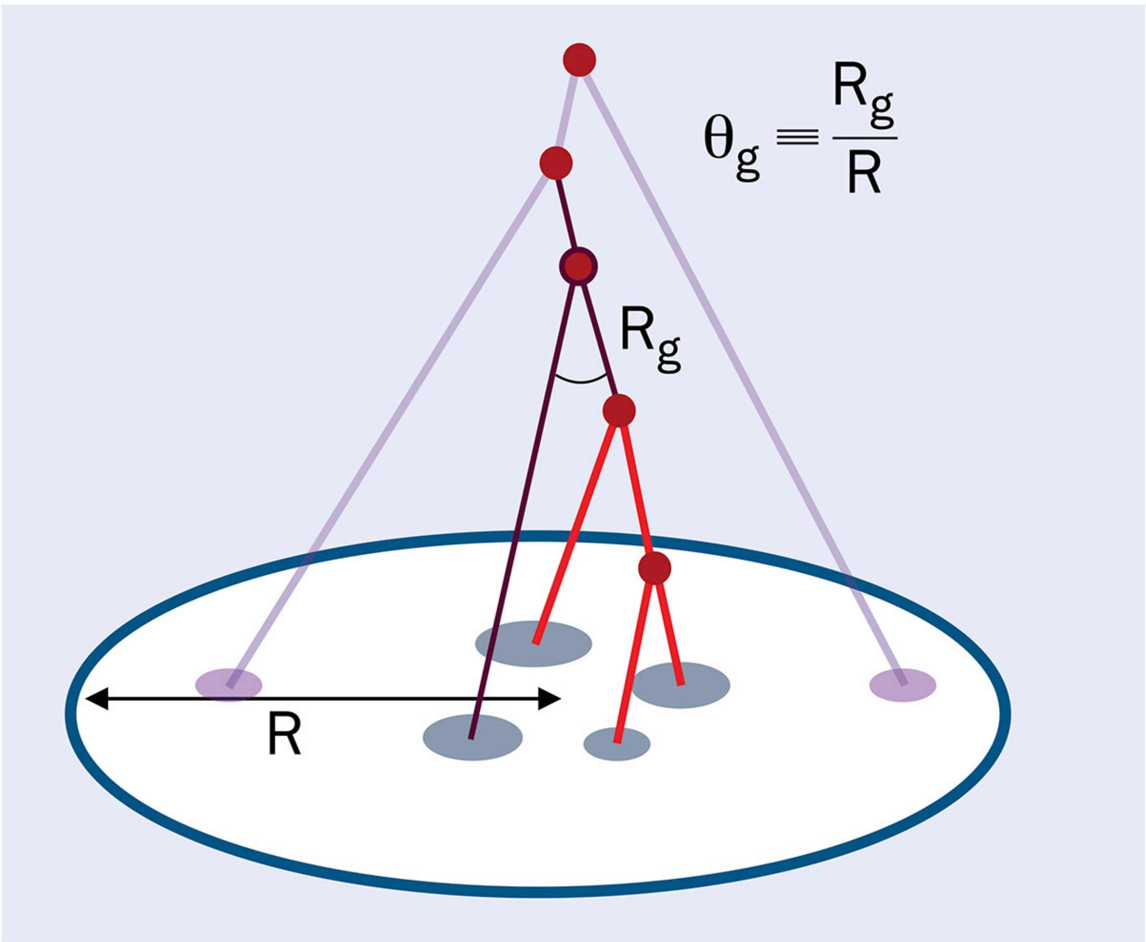

Credit: CERN

Fragmentation of hadrons

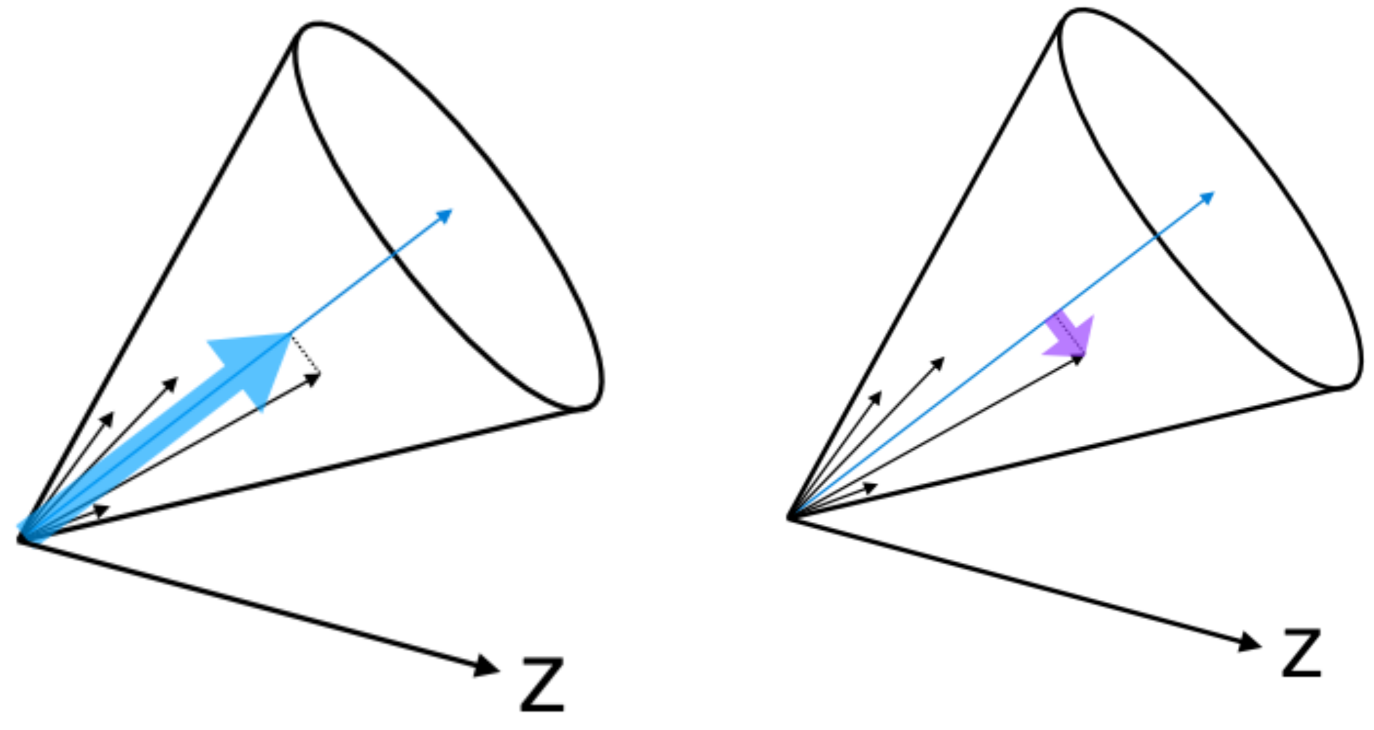

$$z = \frac{\mathbf{p_{jet}} \cdot \mathbf{p_{hadron}}}{|\mathbf{p_{jet}}|^2} \qquad j_T = \frac{|\mathbf{p_{jet}} \times \mathbf{p_{hadron}}|}{|\mathbf{p_{jet}}|}$$

Energy Correlators

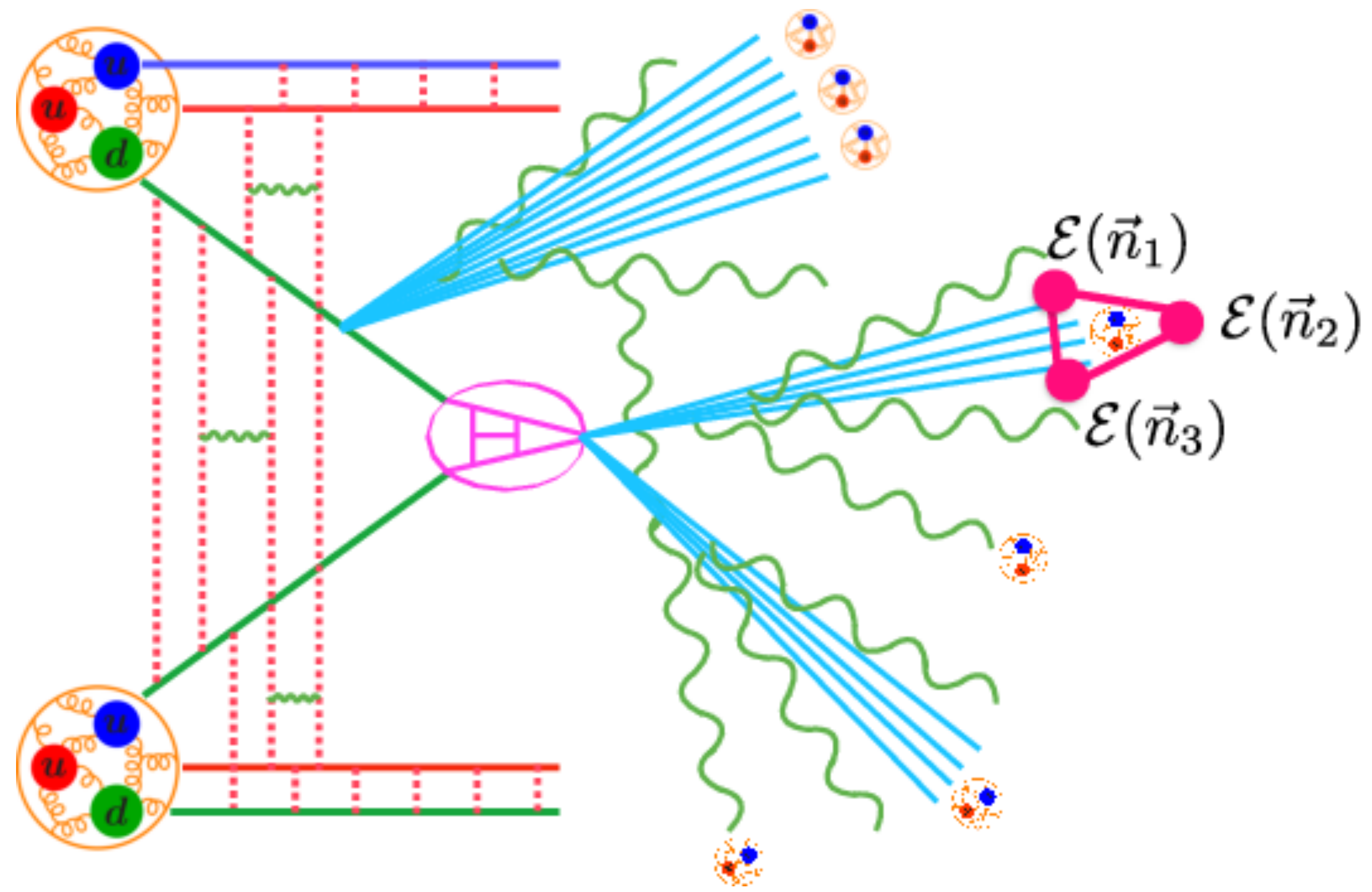

H Chen, I Moult, XY Zhang, HX Zhu , 2020

Boosted heavy-flavor jets

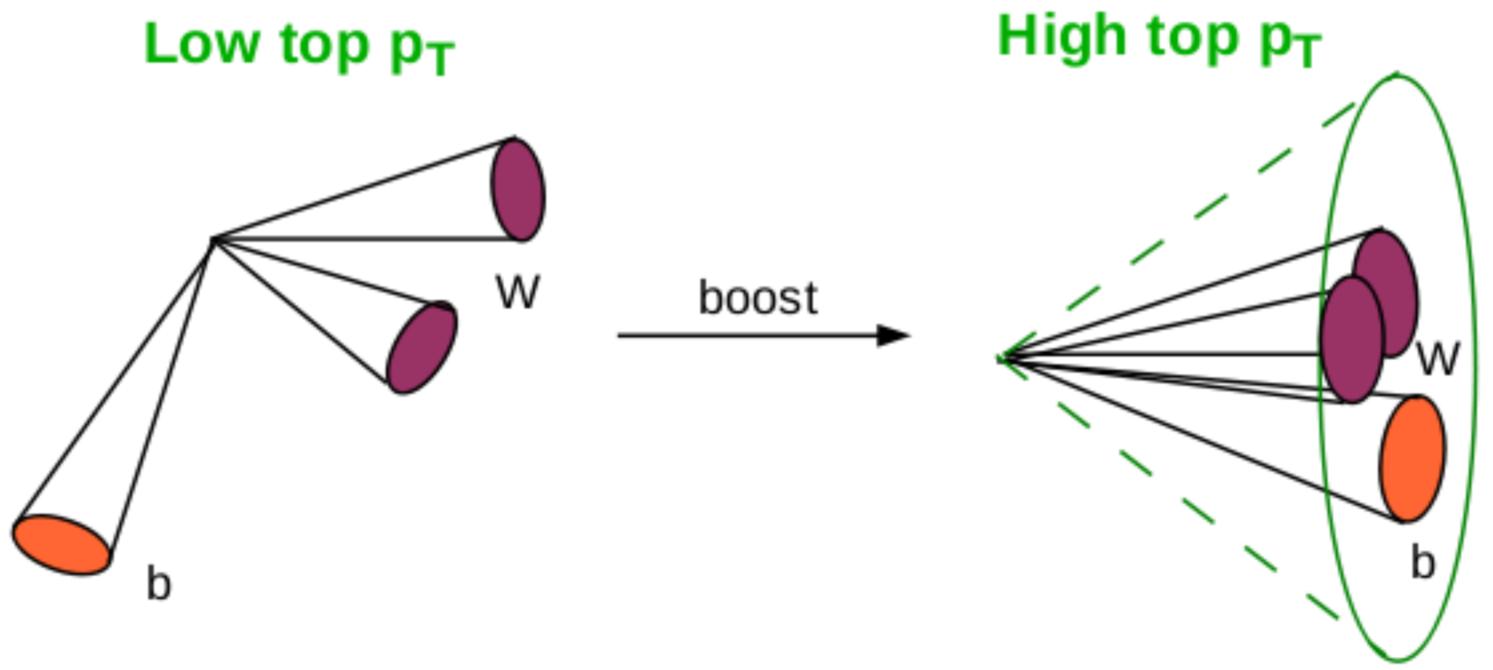

Credit: Matthew Anthony

Jet axes from underlying substructure

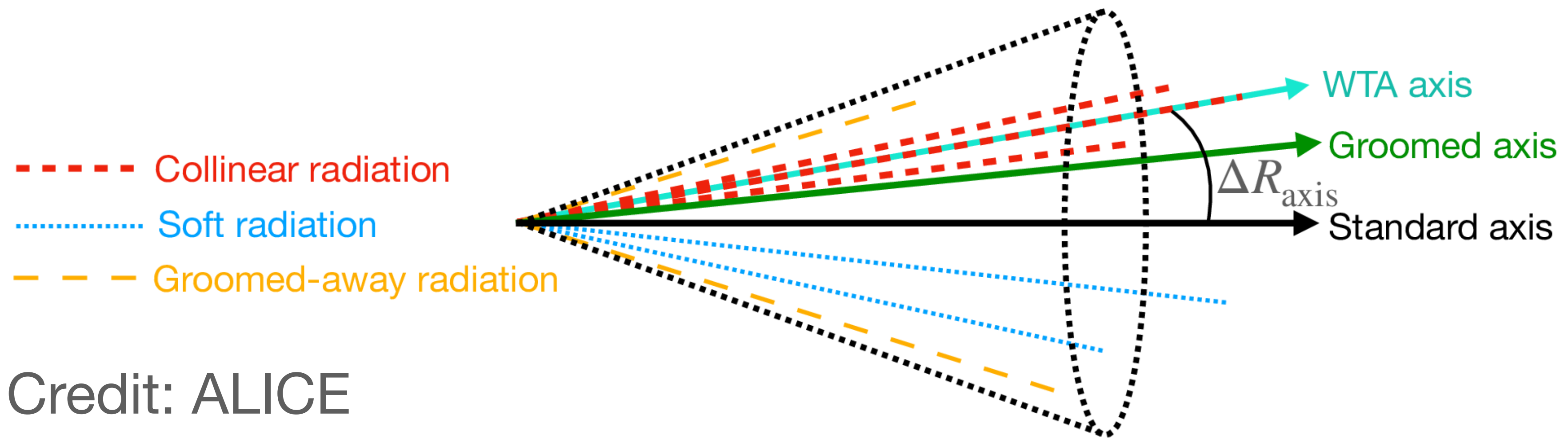

Credit: ALICE

Phase space structure: Lund planes

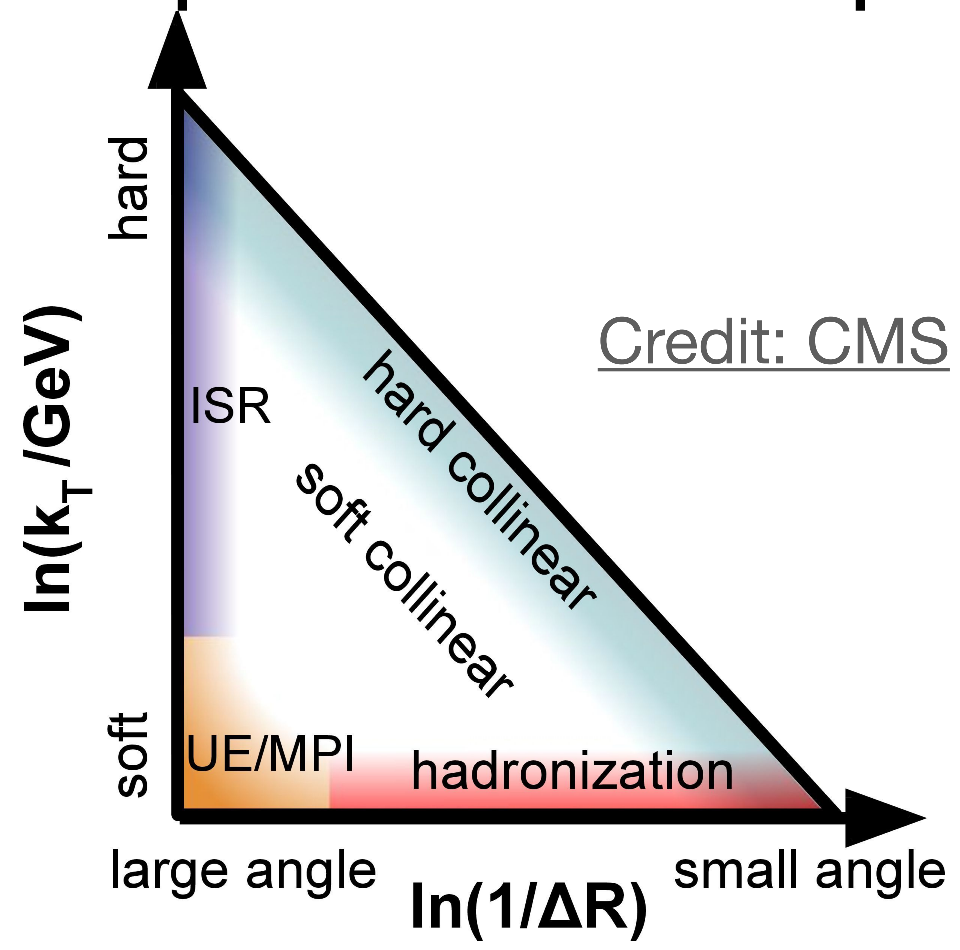

Credit: CMS

Jet Substructure: opening the QCD world

Heavy quark splitting functions

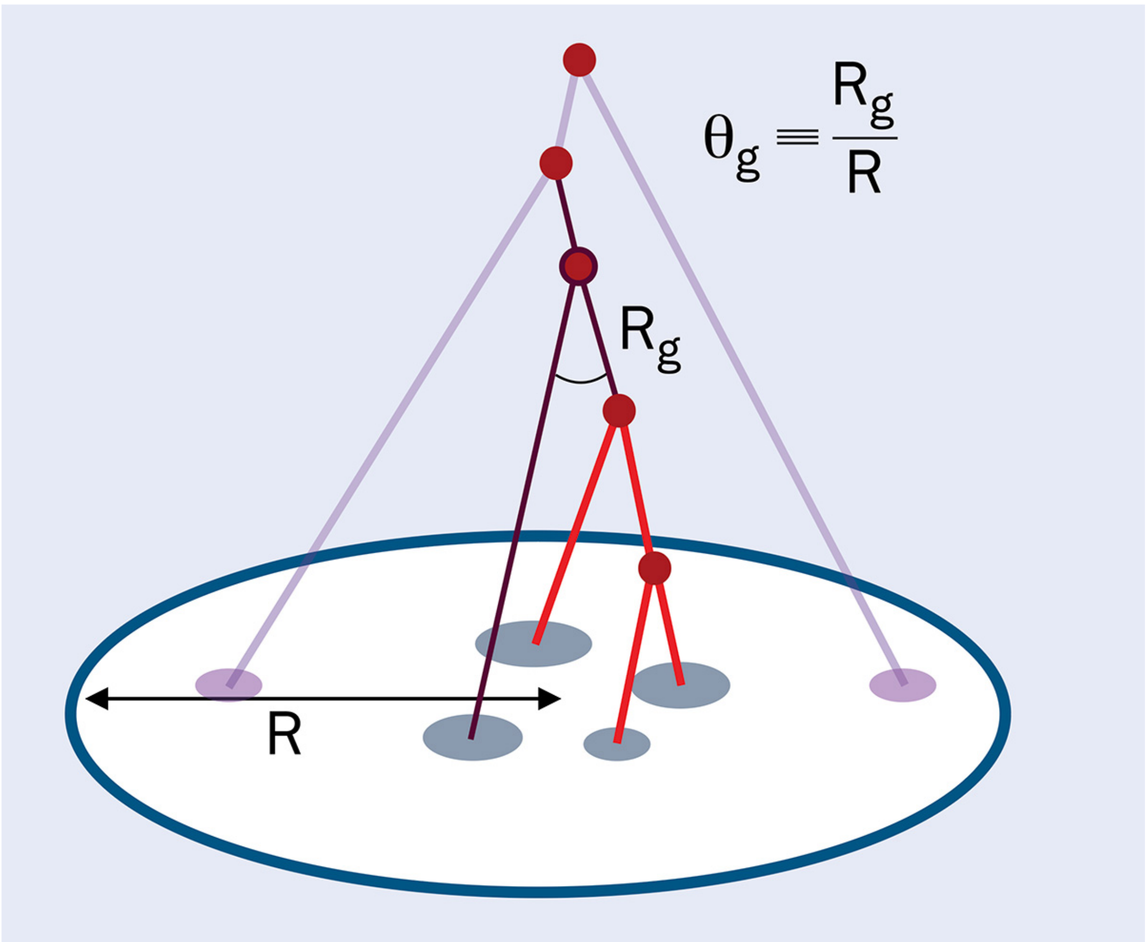

Credit: CERN

Fragmentation of hadrons

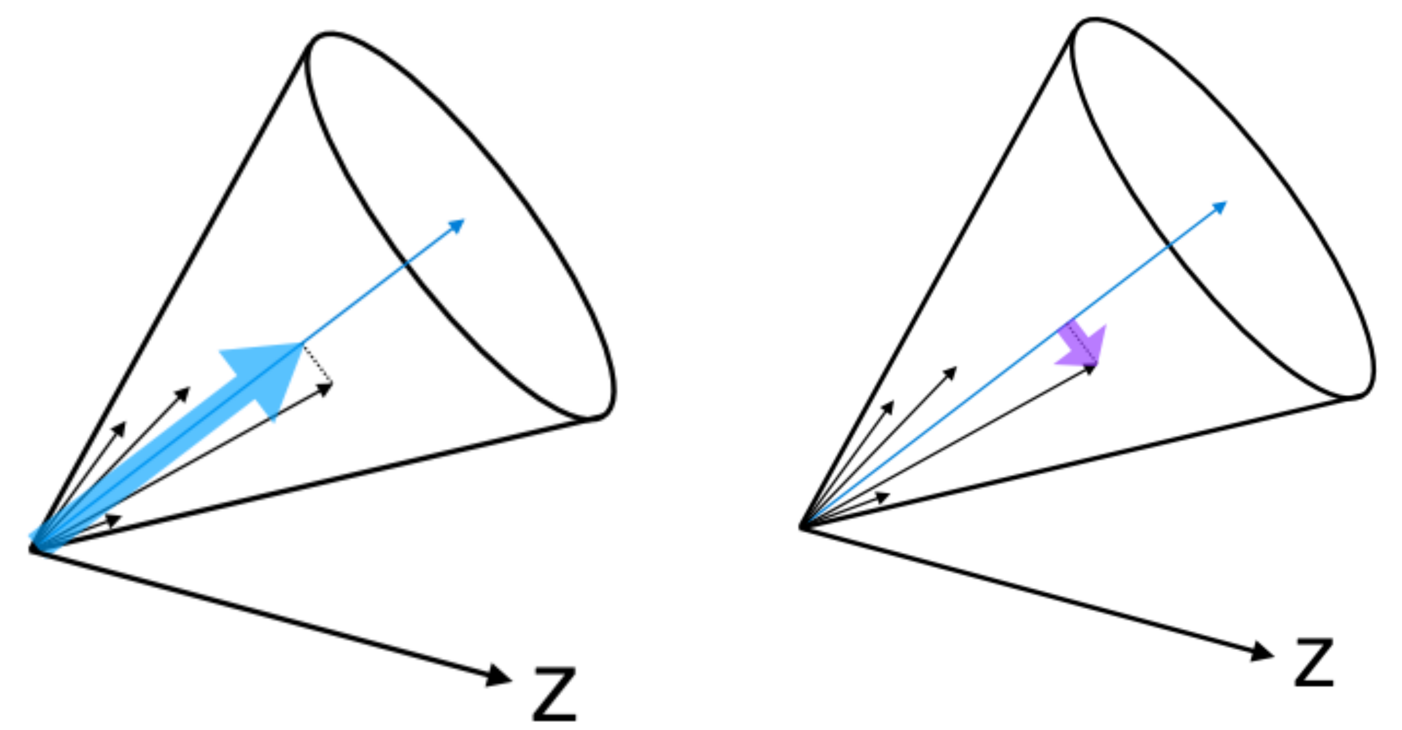

$$z = \frac{\mathbf{p}_{\text{jet}} \cdot \mathbf{p}_{\text{hadron}}}{|\mathbf{p}_{\text{jet}}|^2} \qquad j_T = \frac{|\mathbf{p}_{\text{jet}} \times \mathbf{p}_{\text{hadron}}|}{|\mathbf{p}_{\text{jet}}|}$$

Energy Correlators

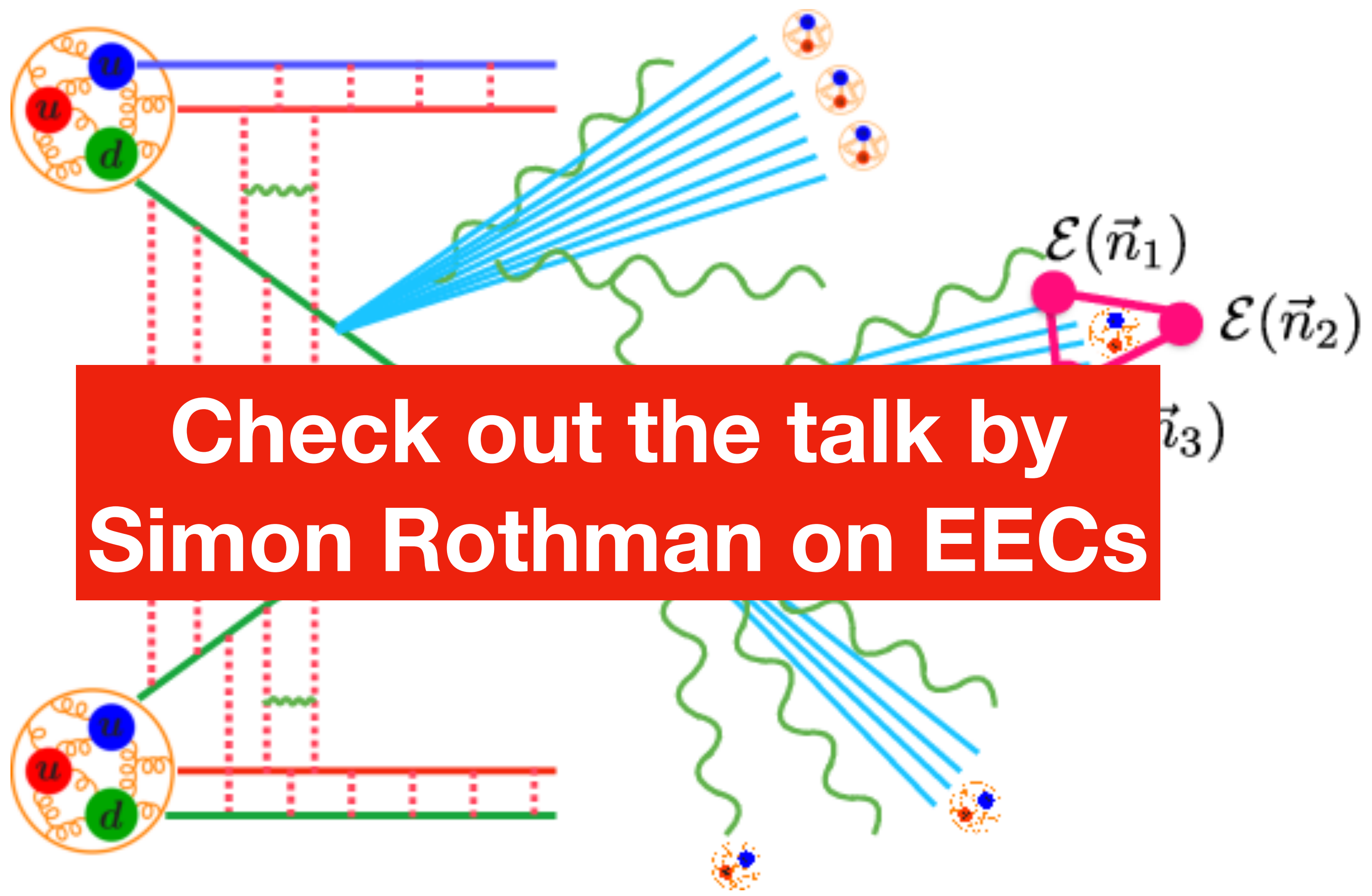

Check out the talk by Simon Rothman on EECs

H Chen, I Moult, XY Zhang, HX Zhu , 2020

Boosted heavy-flavor jets

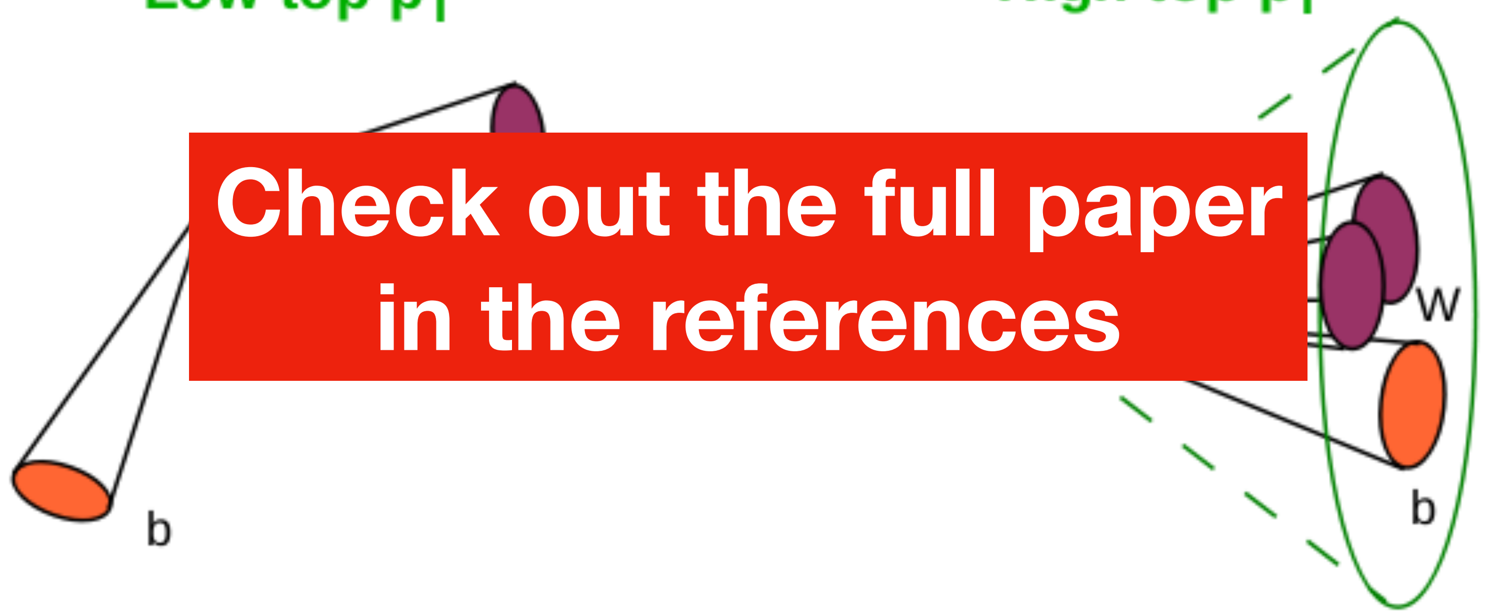

Check out the full paper in the references

Credit: Matthew Anthony

Jet axes from underlying substructure

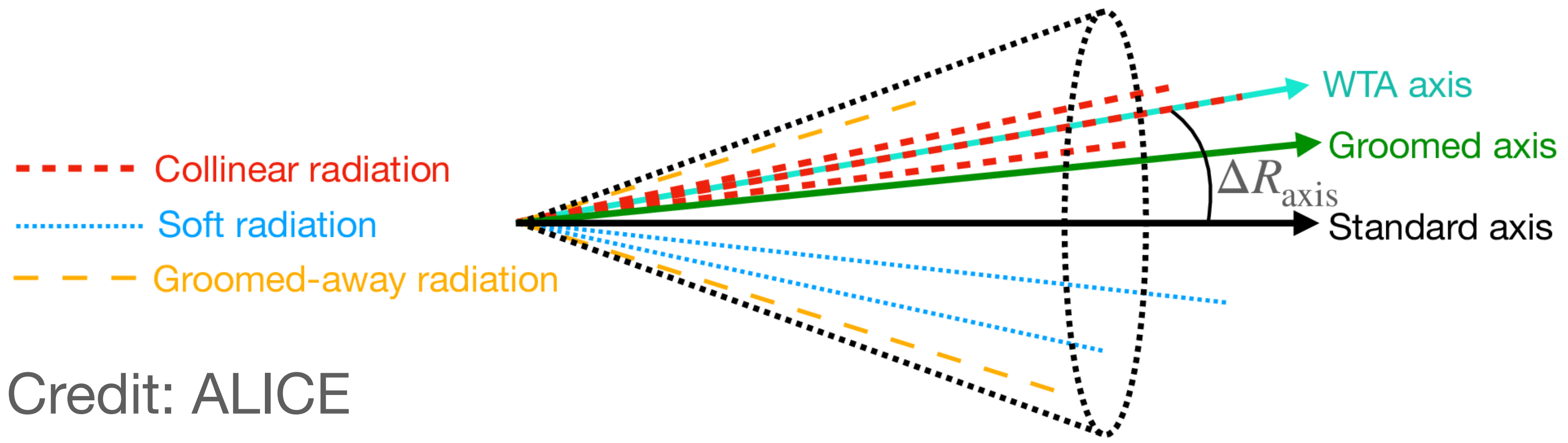

Credit: ALICE

Phase space structure: Lund planes

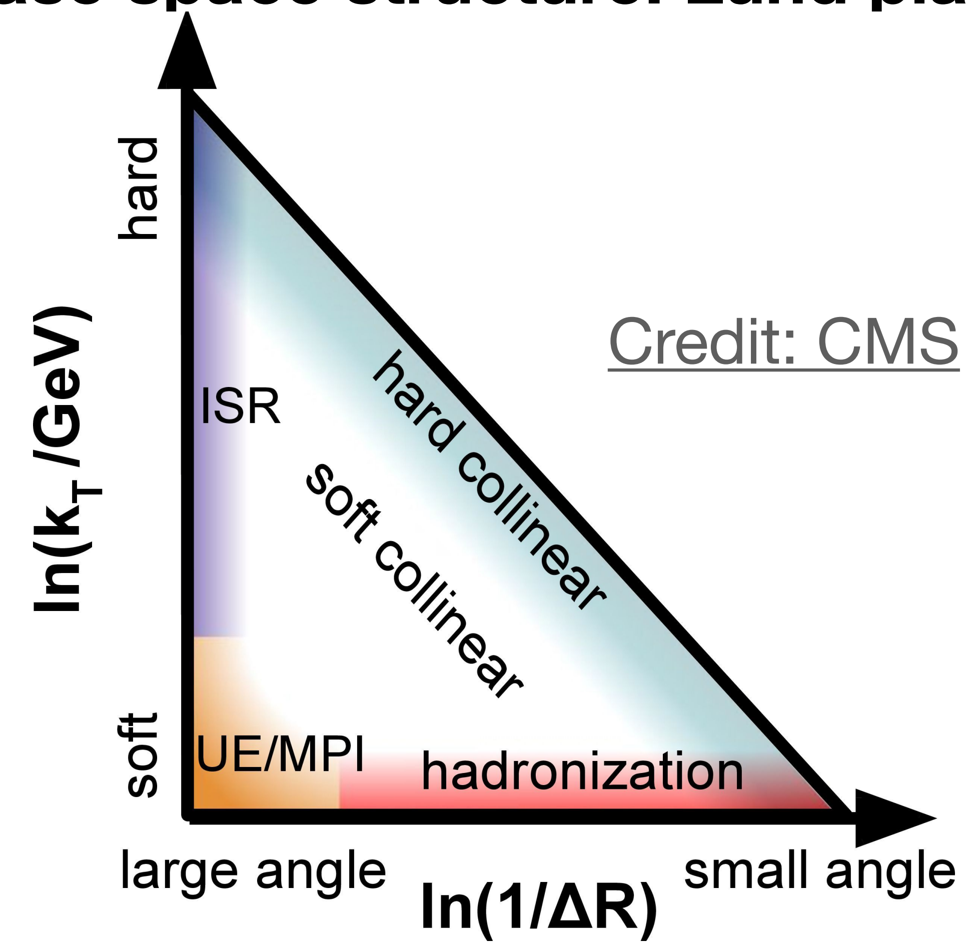

Credit: CMS

Cambridge/Aachen Reclustering

Popular Substructure Technique

- Gluon radiation is ordered from larger to smaller angles throughout the showering

$$\theta_1 > \theta_2 > \ldots > \theta_n$$

- The C/A algorithm clusters jets based on smallest angles first

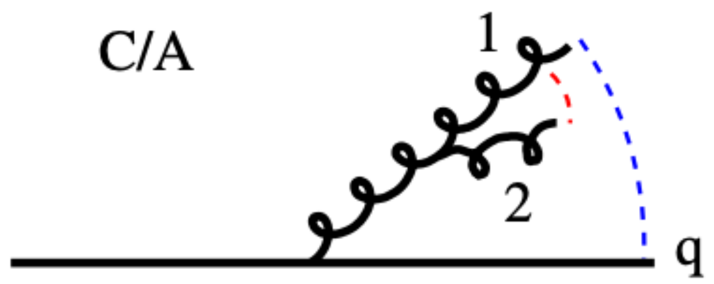

Credit: Lund plane

C/A gives us access to the splitting history of the jet

Inclusive

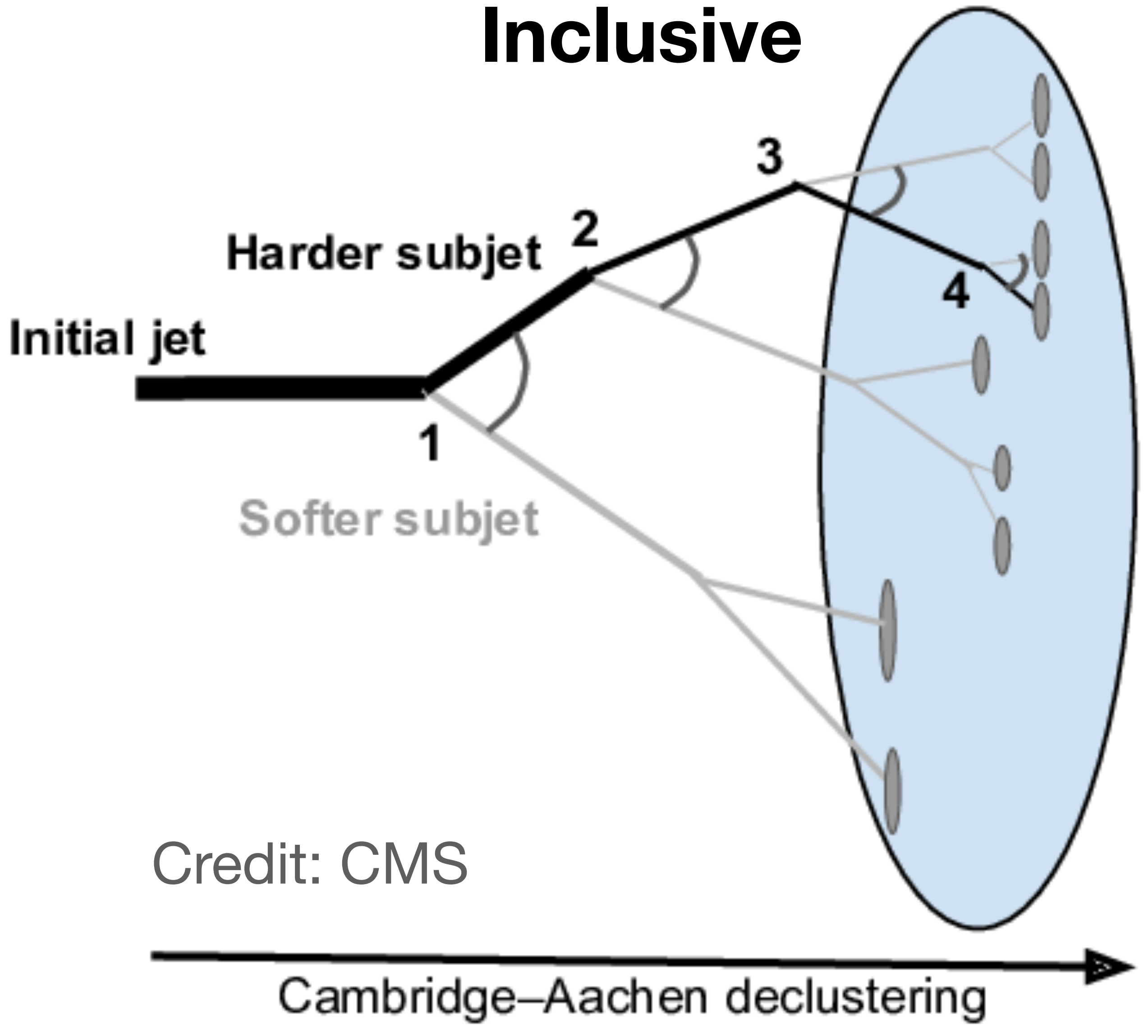

Credit: CMS

Heavy flavor

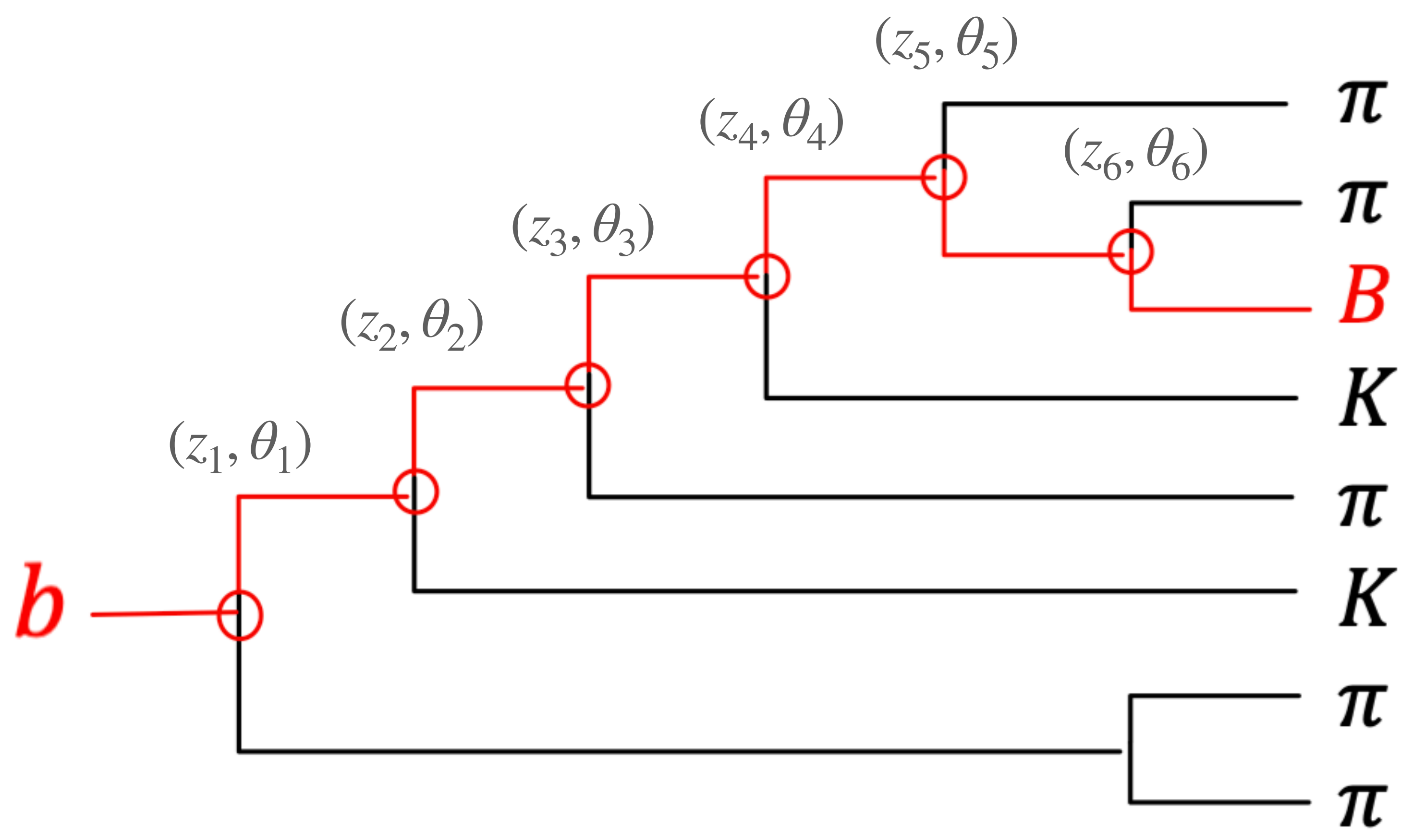

Soft-drop Grooming

Momentum fraction z_g and angular distance R_g

- The soft-drop (SD) procedure was designed to remove wide-angle soft radiation
- An emission is removed if it does not satisfy the soft-drop condition:

$$\frac{\min(p_{T1}, p_{T2})}{p_{T1} + p_{T2}} > z_{\text{cut}} \left(\frac{\Delta R_{12}}{R_0} \right)^{\beta}$$

- The first emission satisfying the SD condition is given a subscript z_g and R_g
- The parameter choice of $z_{cut} = 0.1$ and $\beta = 0$ gives access to the QCD splitting function at high energies via z_g

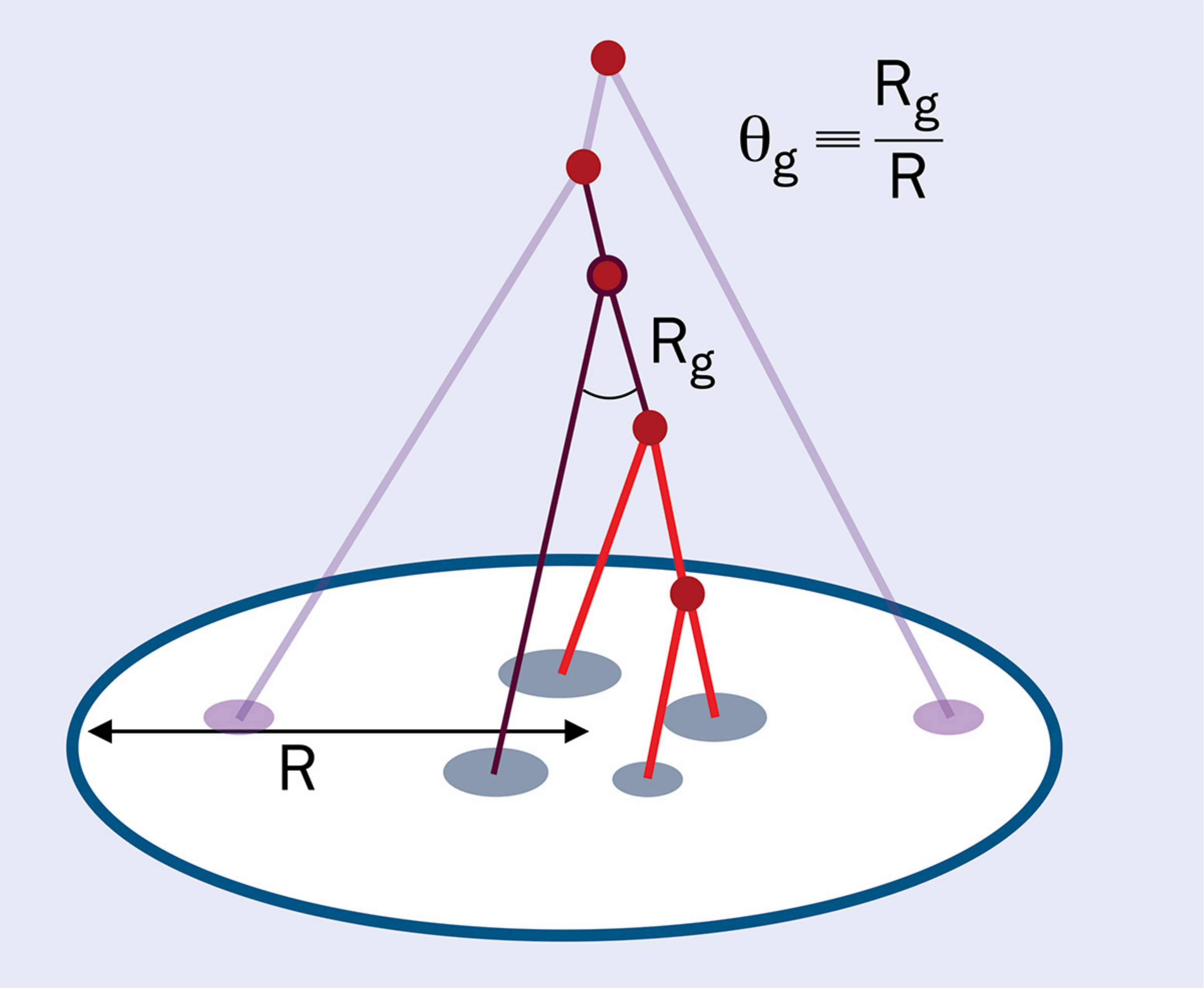

Credit: CERN

$$\bar{P}_q(z) \simeq \bar{P}_g(z) \simeq \frac{1-z}{z} + \frac{z}{1-z} + \frac{1}{2}$$

$$P_{Q \to Qg}(z) = \frac{1-z}{z} + \frac{z}{2} - 2\mu^2_{Qg}$$

$$\mu^2_{Qg} = \frac{m_Q^2}{m^2_{Qg} - m_Q^2}$$

Larkoski, Marzani, Soyez, Thaler, J. High Energy Phys. 05 (2014) 146.

Larkoski, Marzani, Thaler, Tripathee, Xue, , Phys. Rev. Lett. 119, 132003 (2017)

Ilten, Rodd, Thaler, Williams 2017

Charm splitting function

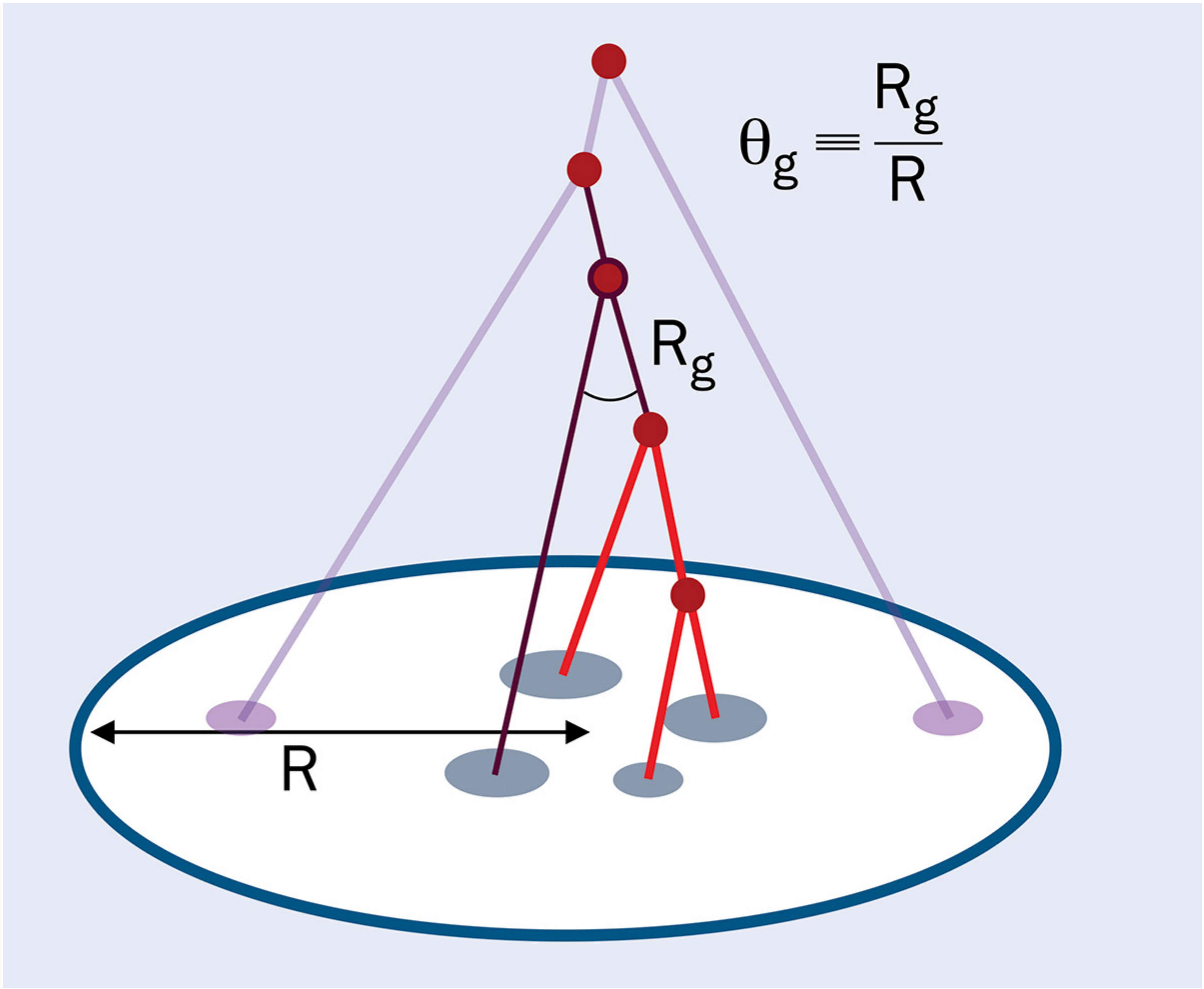

Credit: CERN

Charm quark splitting function

ALICE Collaboration

PHYSICAL REVIEW LETTERS 131, 192301 (2023)

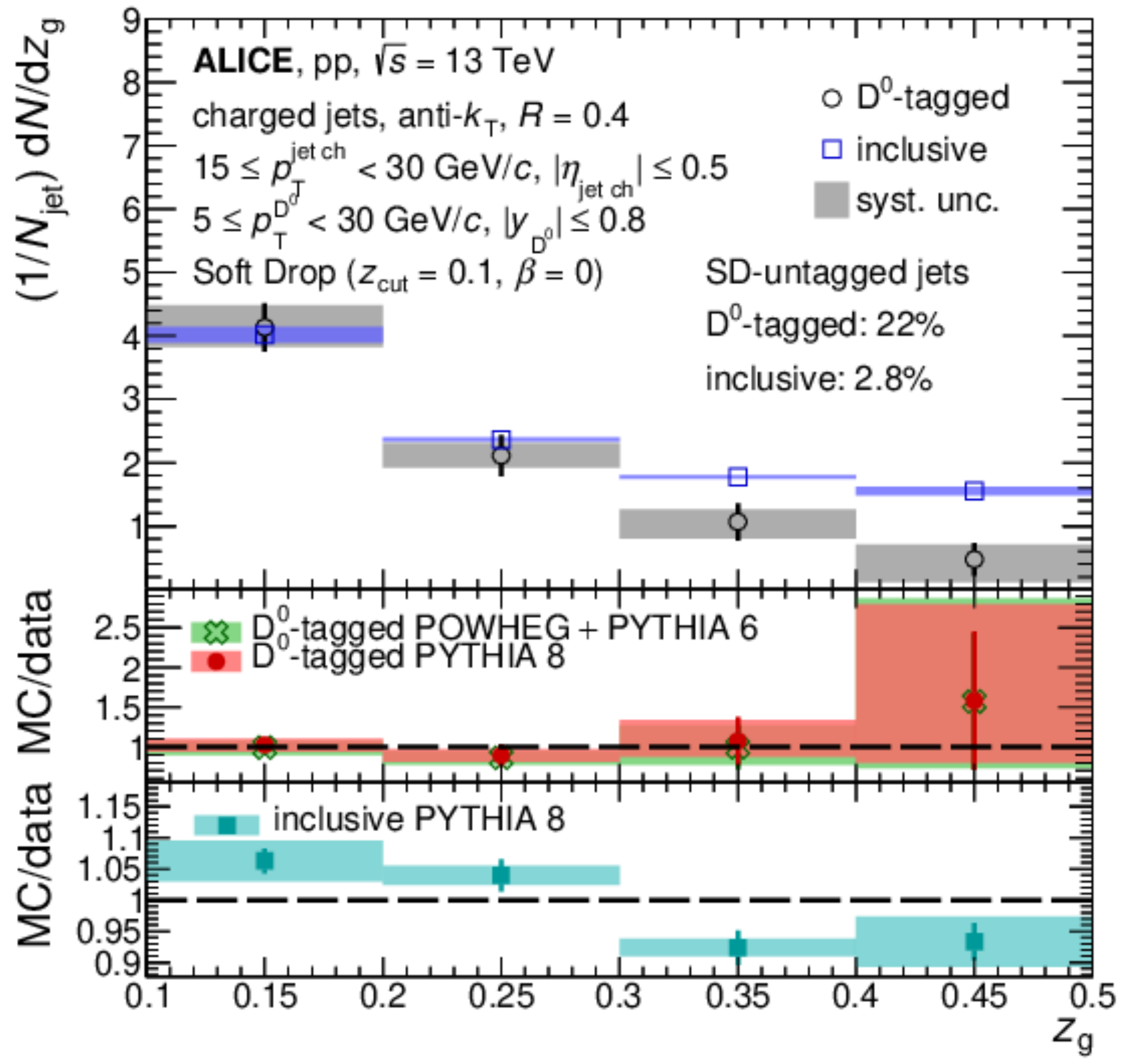

- Charm splittings are significantly less likely to share energy (large z_g) compared to the inclusive case

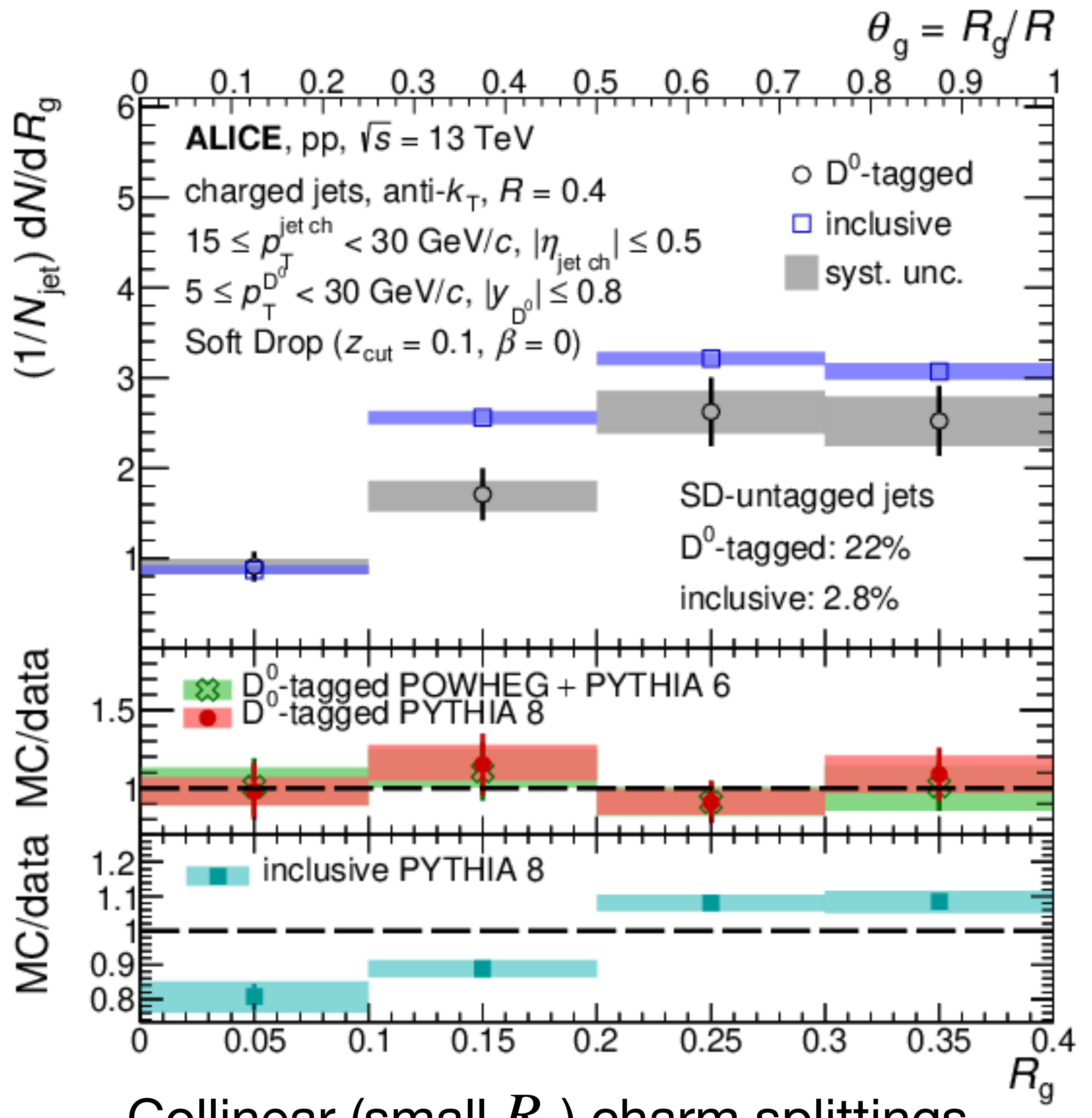

- Collinear (small R_g) charm splittings happen as often as in the gluon-dominated inclusive sample. This does not contradict the expectation from the dead cone since the reduction of collinear splittings in the charm quark can be balanced by wide-radiation gluon jets

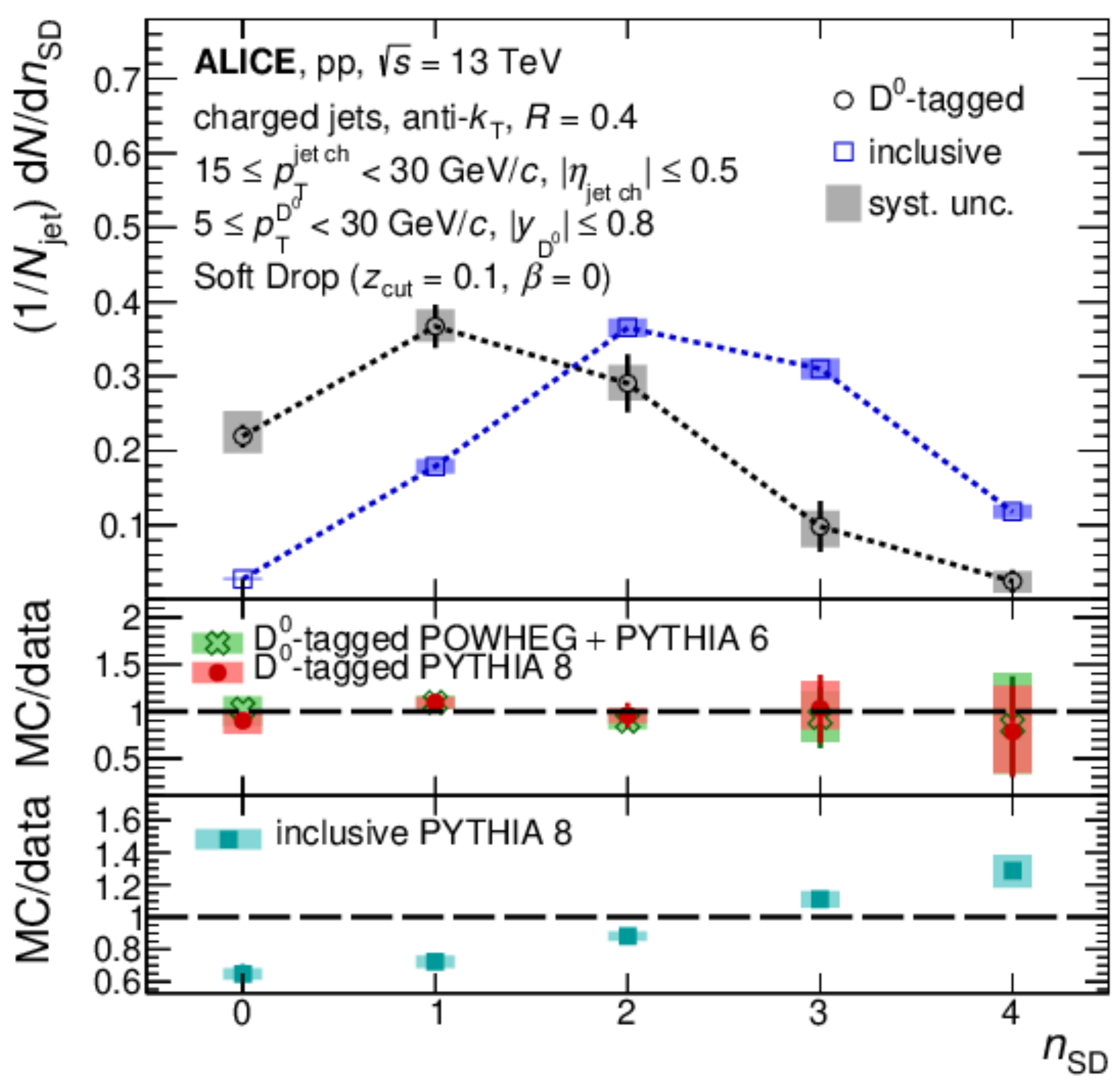

- Charm splittings are less likely to pass the SD condition. This is consistent with the dead-cone effect which limits hard collinear radiation

Angle between jet axes

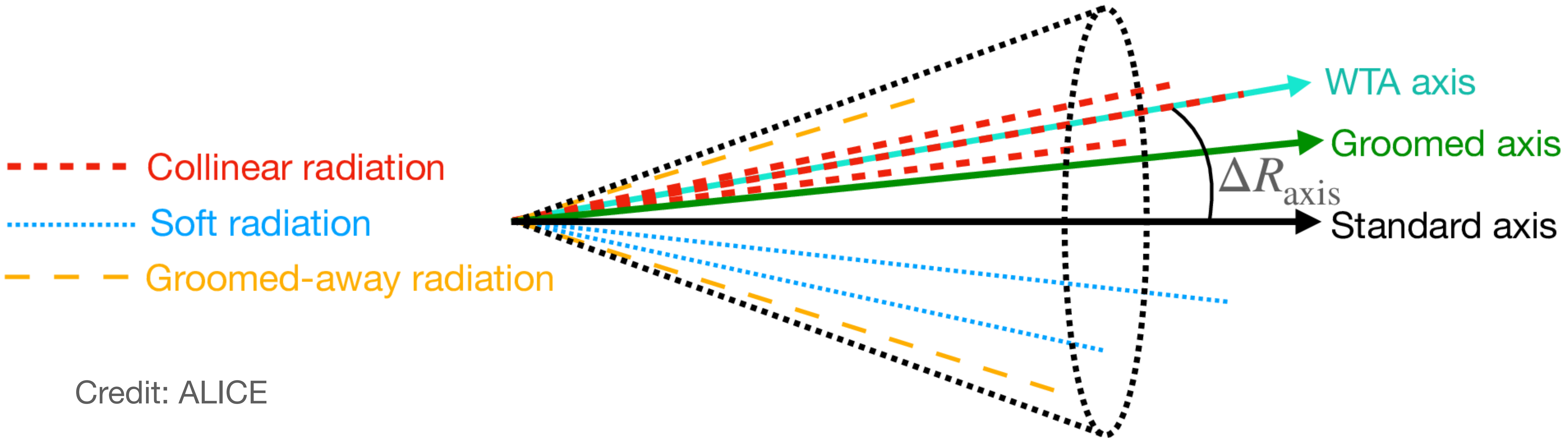

Credit: ALICE

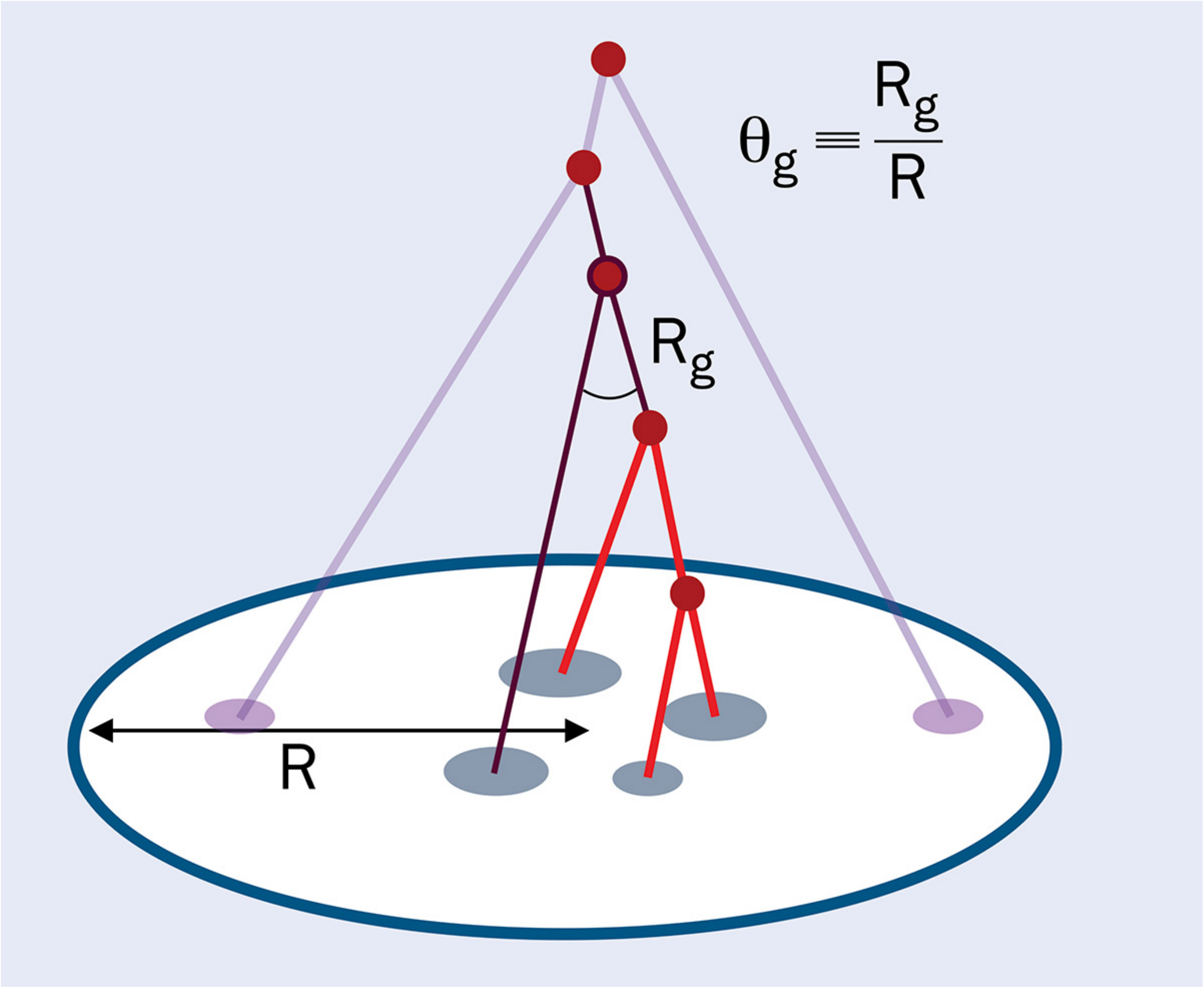

Credit: CERN

Angles between Jet Axes

ALICE Collaboration

JHEP 2307 (2023) 201

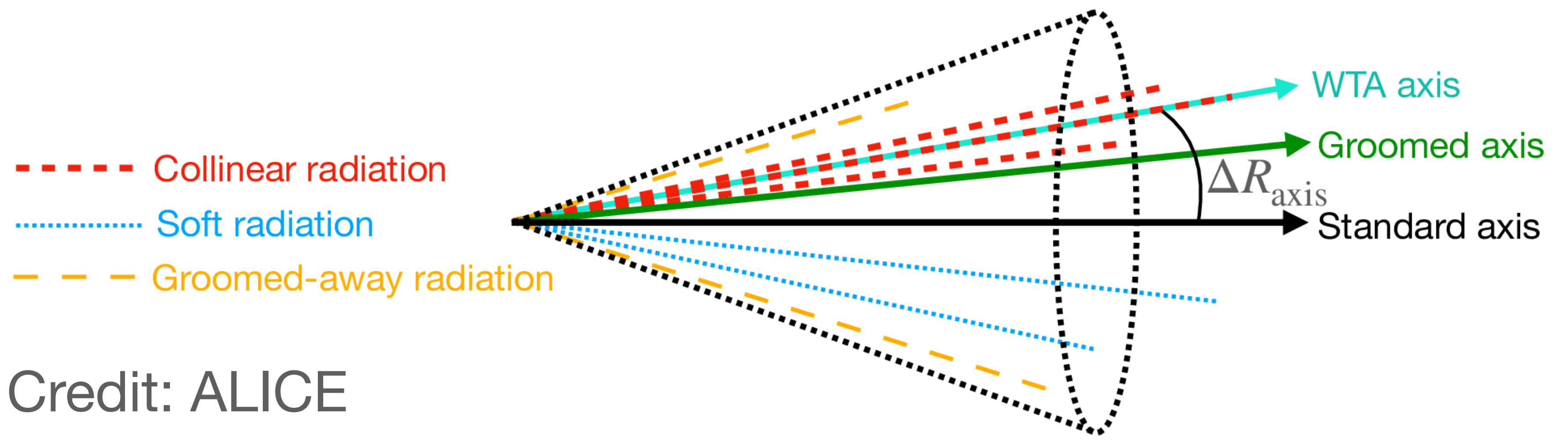

Credit: ALICE

Experimental Setup and Jet Reconstruction:

- $\sqrt{s} = 5.02$ **TeV**
- **Charged-particle jets**
- **Anti-kt jets with R = 0.2 or 0.4**
- $|\eta_{jet}| < 0.9$
- $p_T^{jet} \in [20,100]$ **GeV**

$$\Delta R_{WTA-SD}, \Delta R_{WTA-Standard}, \Delta R_{SD-Standard}$$

Sensitive to Transverse Momentum Dependent Distributions (TMDs)

Groomed Axis

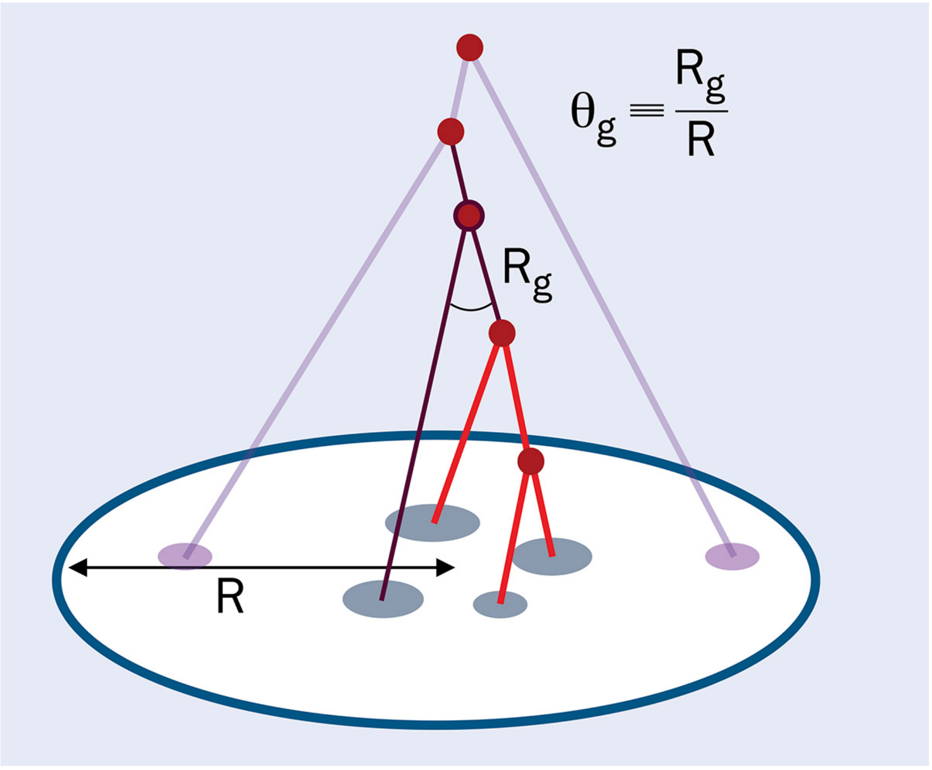

Credit: CERN

Winner-Take-All Axis

$$p_{TJ} = p_{Ti} + p_{Tj}$$

$$\phi_J = \begin{cases} \phi_i, & p_{Ti} > p_{Tj} \\ \phi_j, & p_{Tj} > p_{Ti} \end{cases}$$

$$\eta_J = \begin{cases} \eta_i, & p_{Ti} > p_{Tj} \\ \eta_j, & p_{Tj} > p_{Ti} \end{cases}$$

Angles between Jet Axes

ALICE Collaboration

JHEP 2307 (2023) 201

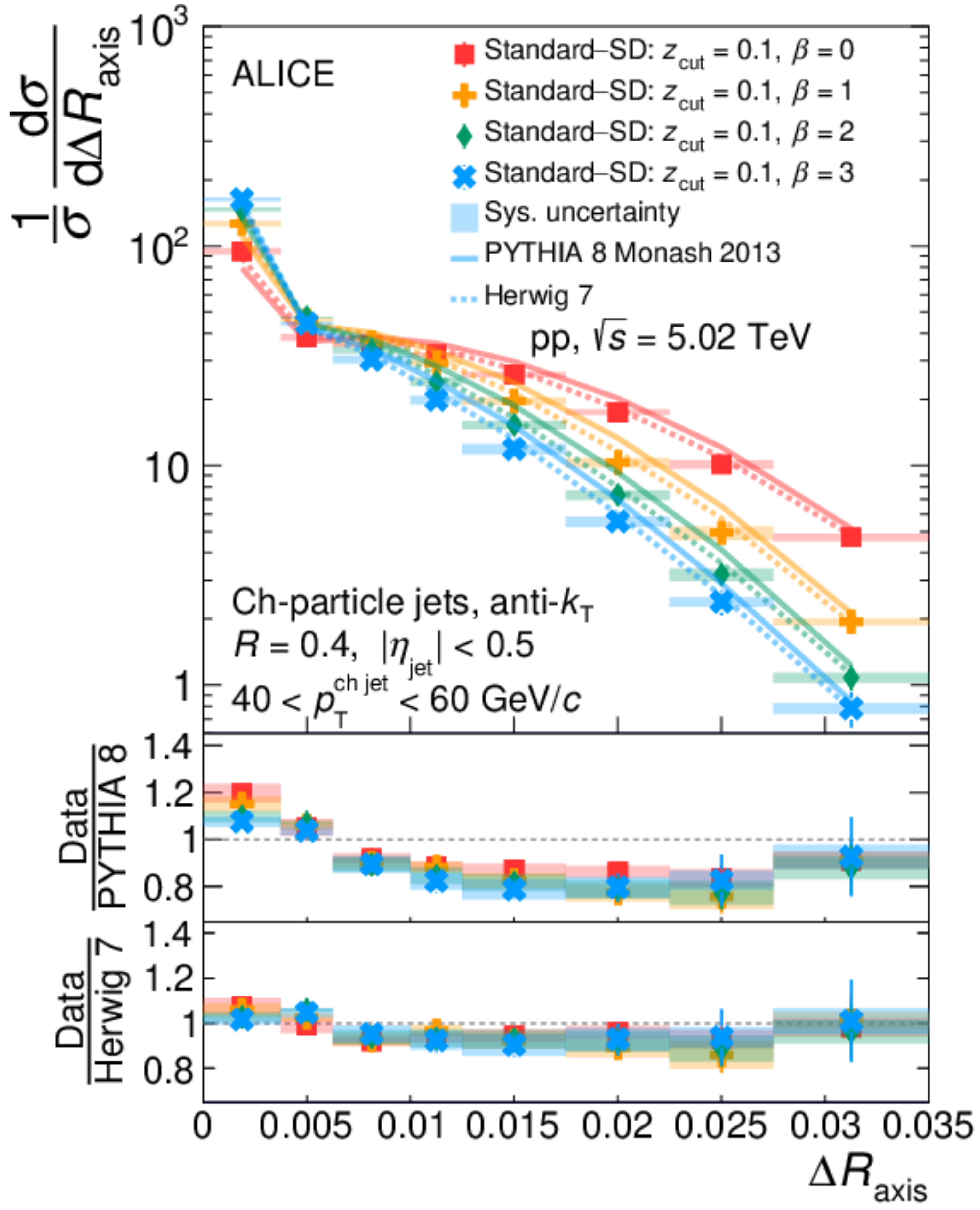

- SD and standard jet axes are mostly aligned
- Grooming does have a big impact
- Aggressive grooming (lower β) has the most impact on the jet direction

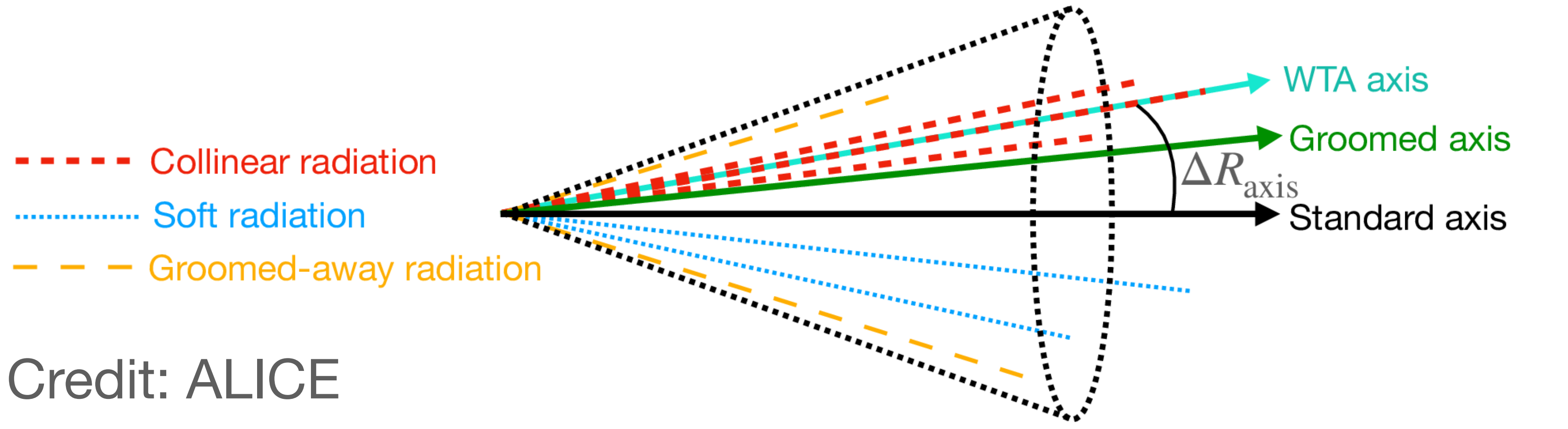

Credit: ALICE

Groomed Axis

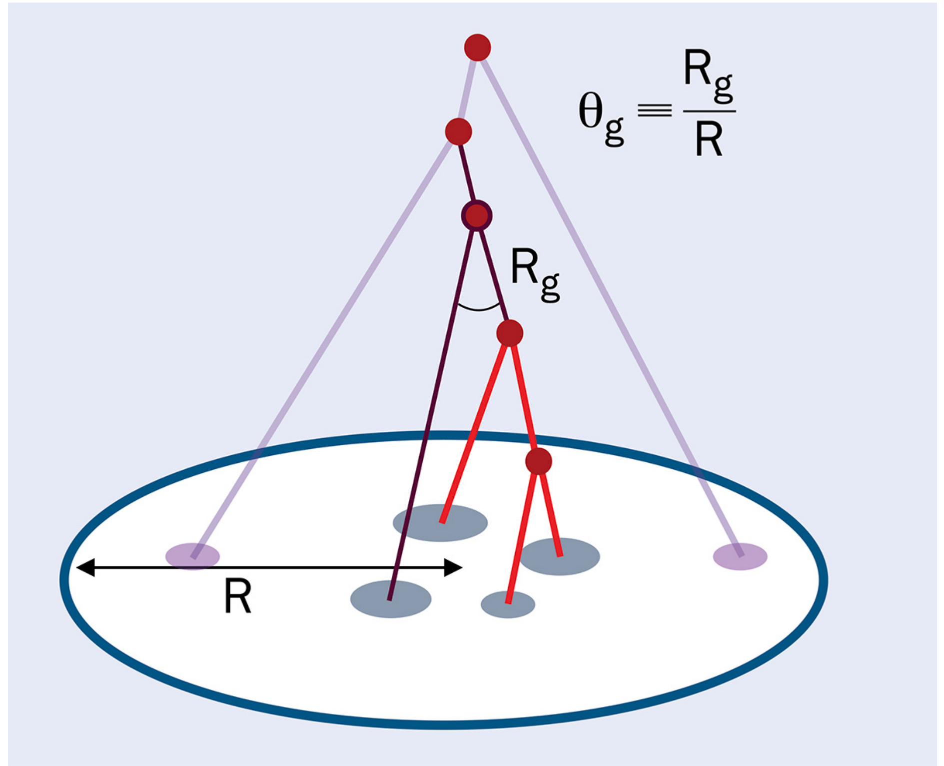

Credit: CERN

Winner-Take-All Axis

$$p_{TJ} = p_{Ti} + p_{Tj}$$

$$\phi_J = \begin{cases} \phi_i, & p_{Ti} > p_{Tj} \\ \phi_j, & p_{Tj} > p_{Ti} \end{cases}$$

$$\eta_J = \begin{cases} \eta_i, & p_{Ti} > p_{Tj} \\ \eta_j, & p_{Tj} > p_{Ti} \end{cases}$$

Angles between Jet Axes

ALICE Collaboration

JHEP 2307 (2023) 201

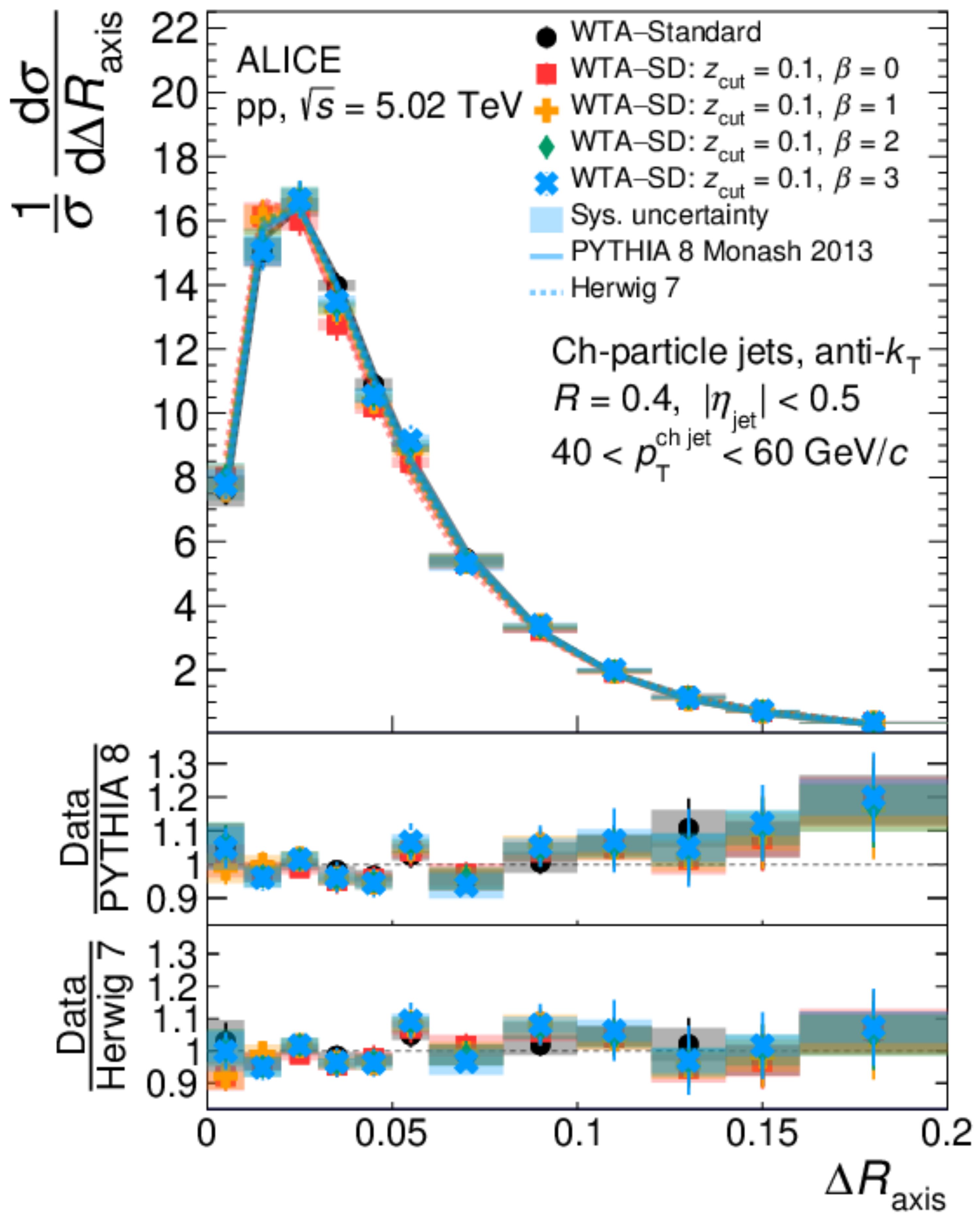

- Significant deviation between WTA and standard jet axes
- MC generators (Herwig 7 and PYTHIA 8) are mostly consistent with the data

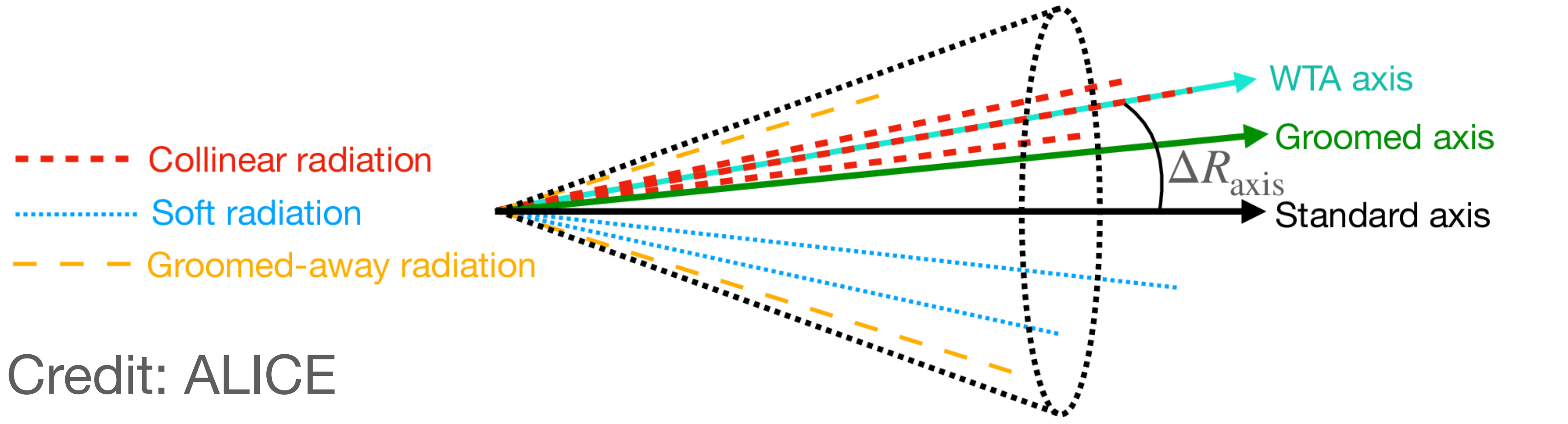

Credit: ALICE

Groomed Axis

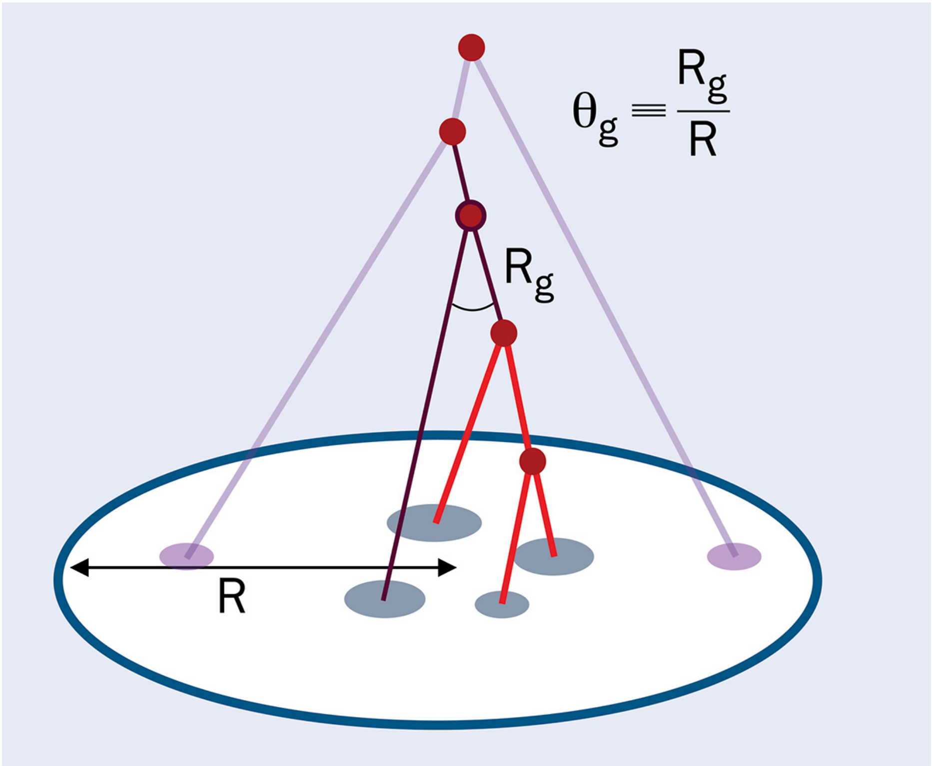

Credit: CERN

Winner-Take-All Axis

$$p_{TJ} = p_{Ti} + p_{Tj}$$

$$\phi_J = \begin{cases} \phi_i, & p_{Ti} > p_{Tj} \\ \phi_j, & p_{Tj} > p_{Ti} \end{cases}$$

$$\eta_J = \begin{cases} \eta_i, & p_{Ti} > p_{Tj} \\ \eta_j, & p_{Tj} > p_{Ti} \end{cases}$$

Angles between Jet Axes

ALICE Collaboration

JHEP 2307 (2023) 201

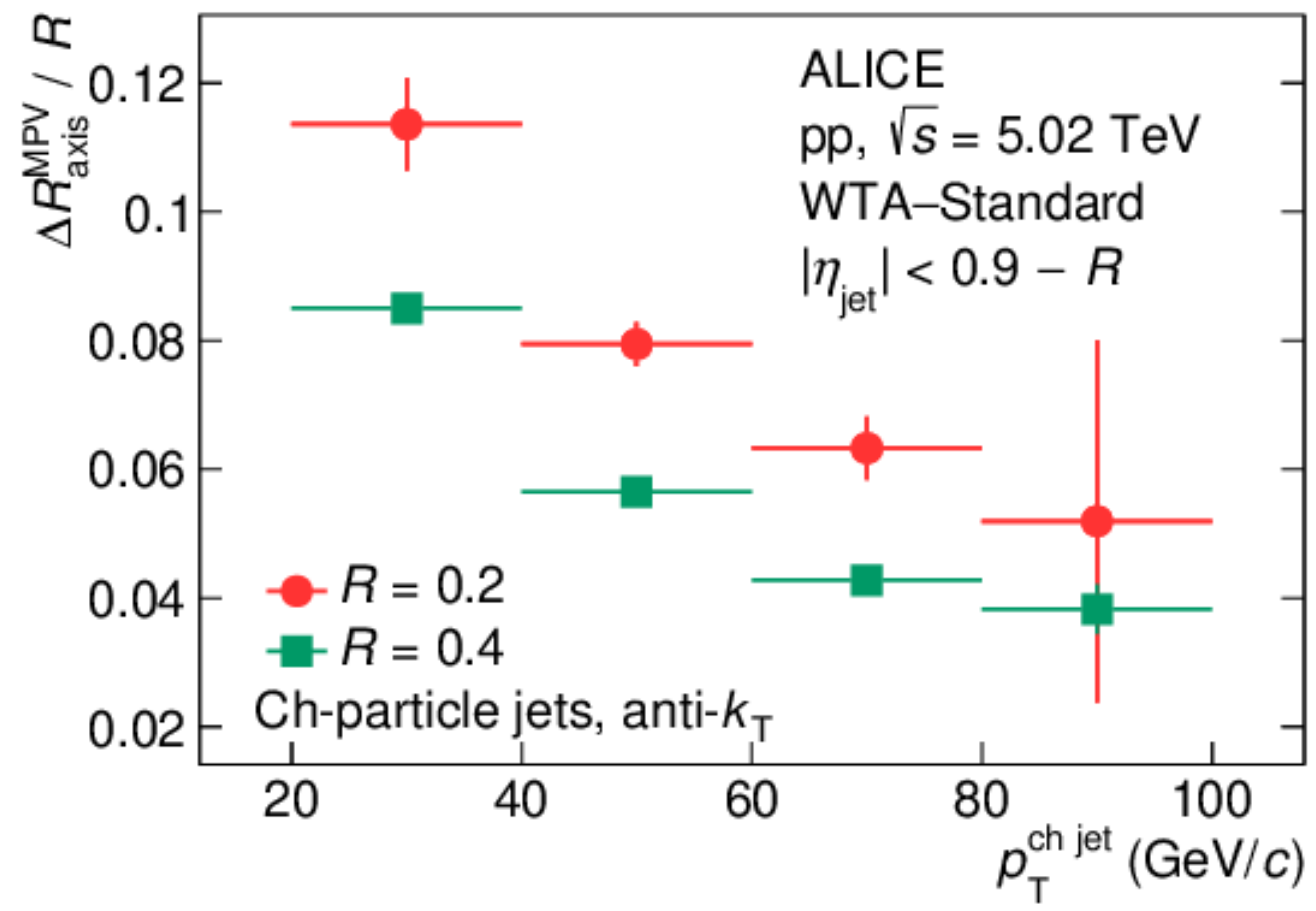

- The peak location of $\Delta R_{WTA-Standard}$ shifts towards lower values at larger jet transverse momentum for both jet radii

ALICE

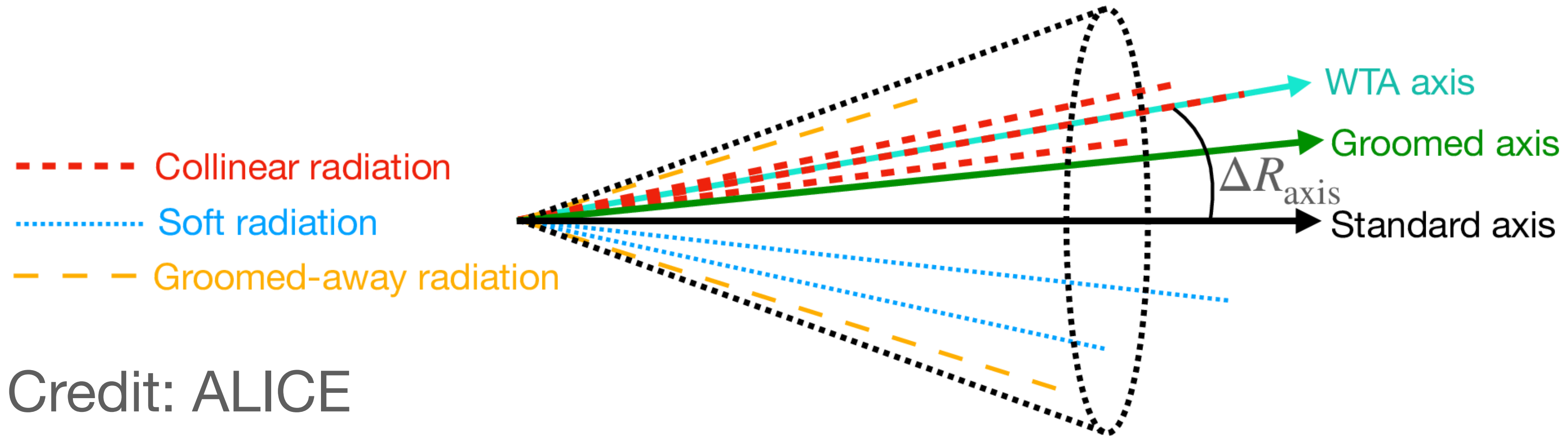

Credit: ALICE

Groomed Axis

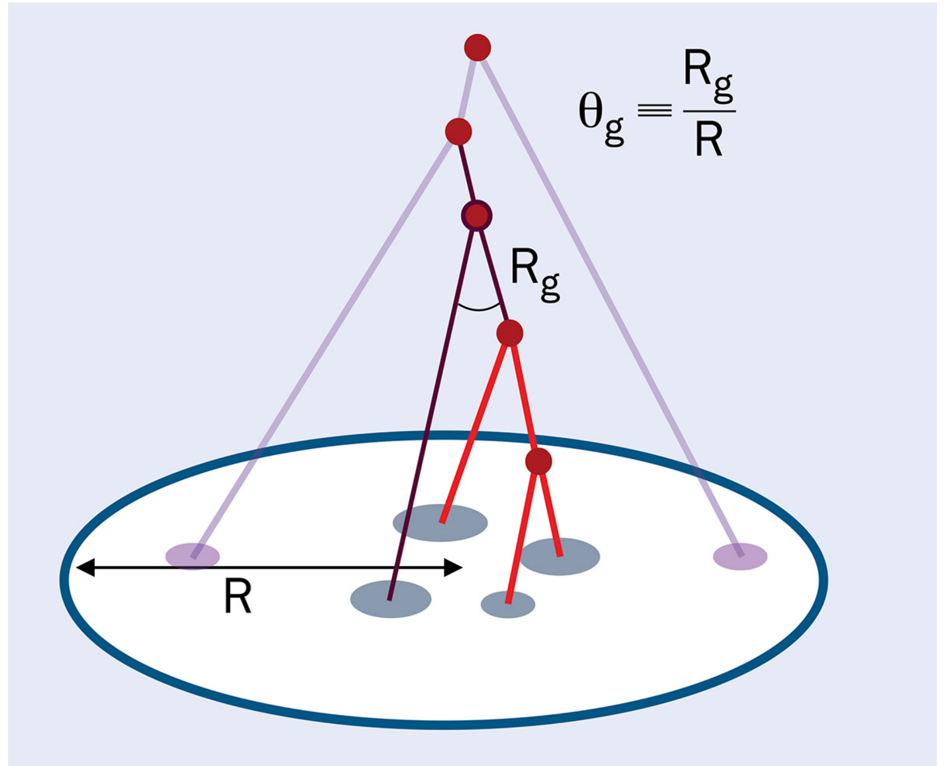

Credit: CERN

Winner-Take-All Axis

$$p_{TJ} = p_{Ti} + p_{Tj}$$

$$\phi_J = \begin{cases} \phi_i, & p_{Ti} > p_{Tj} \\ \phi_j, & p_{Tj} > p_{Ti} \end{cases}$$

$$\eta_J = \begin{cases} \eta_i, & p_{Ti} > p_{Tj} \\ \eta_j, & p_{Tj} > p_{Ti} \end{cases}$$

Lund jet Plane

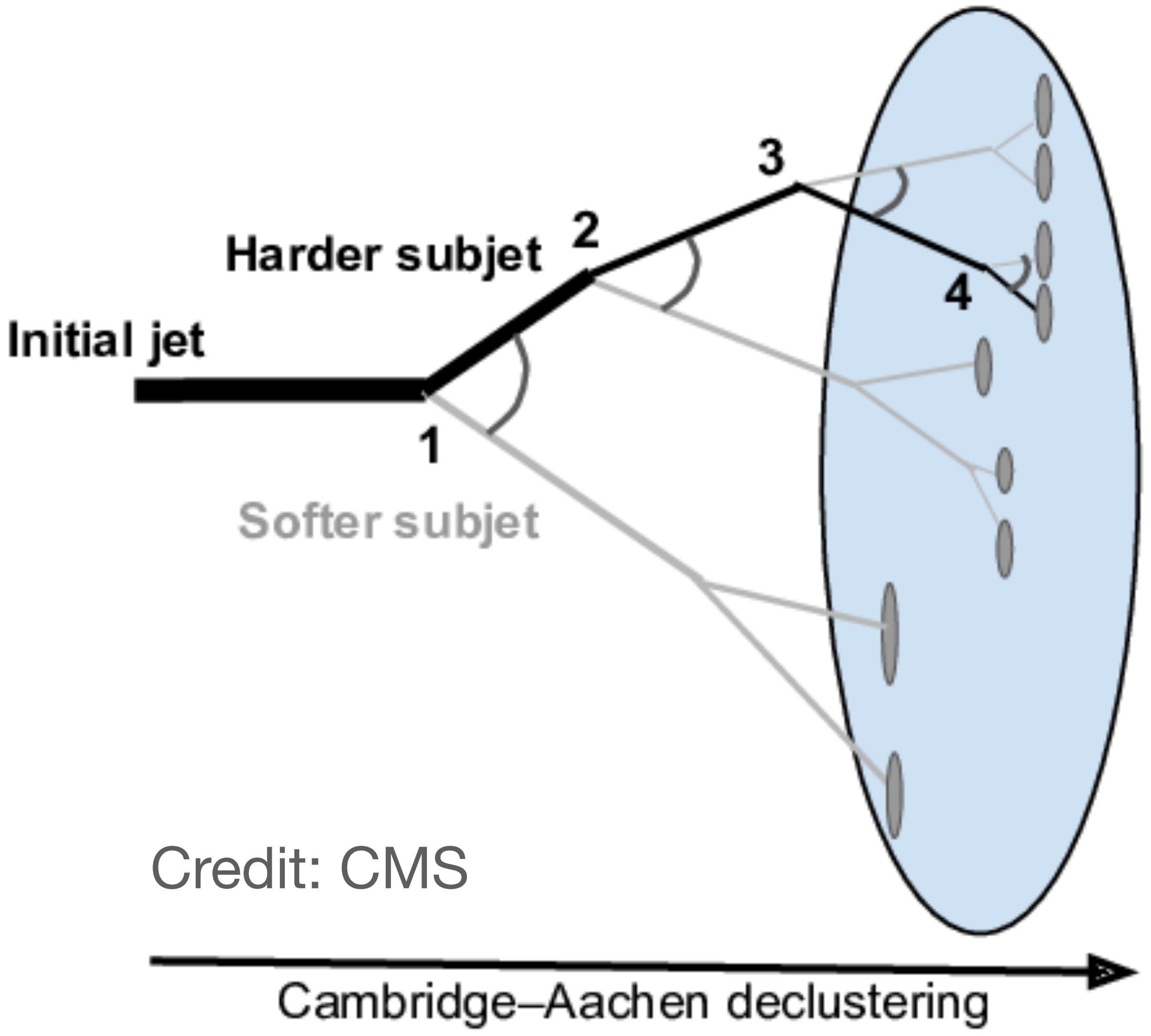

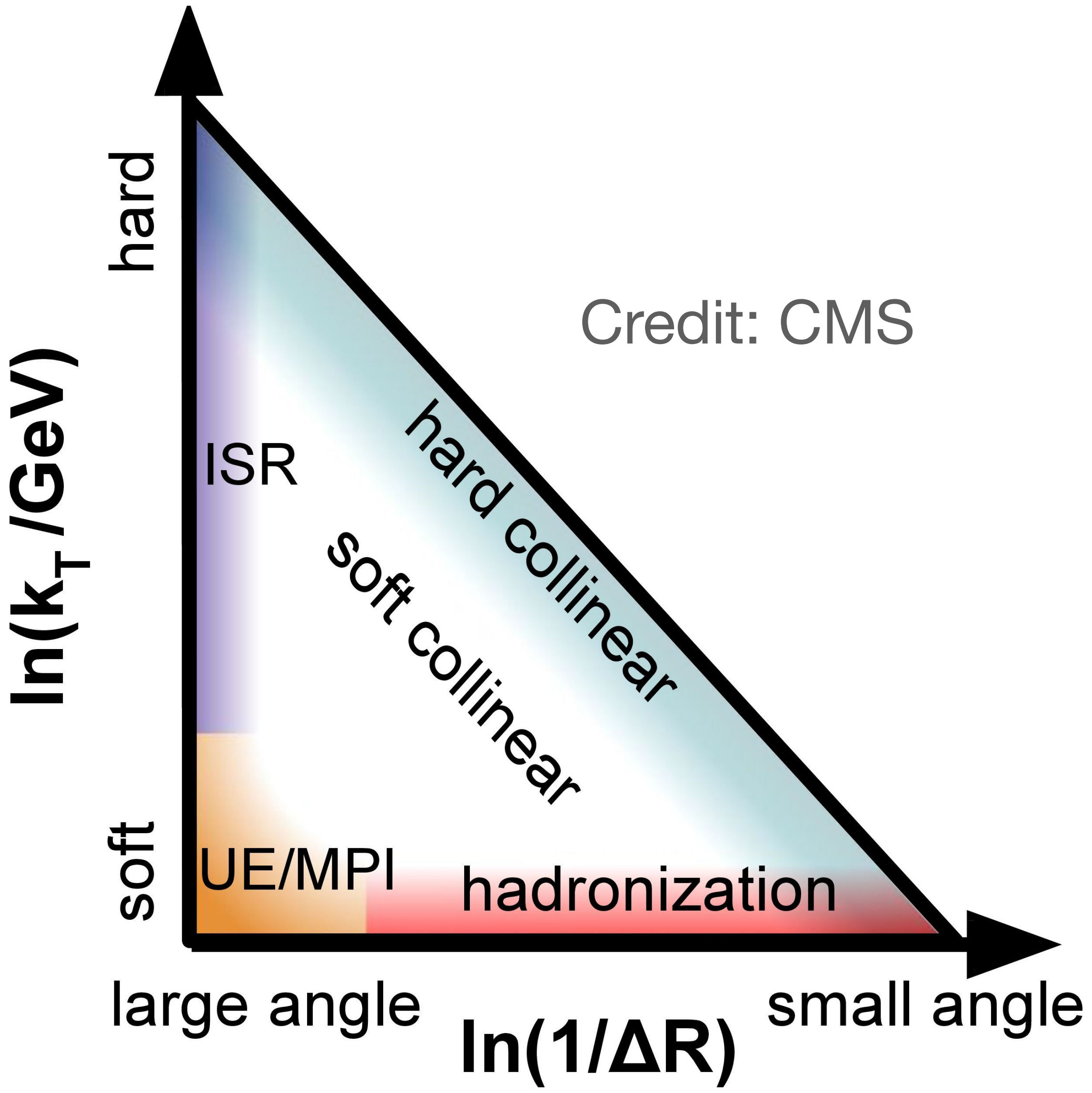

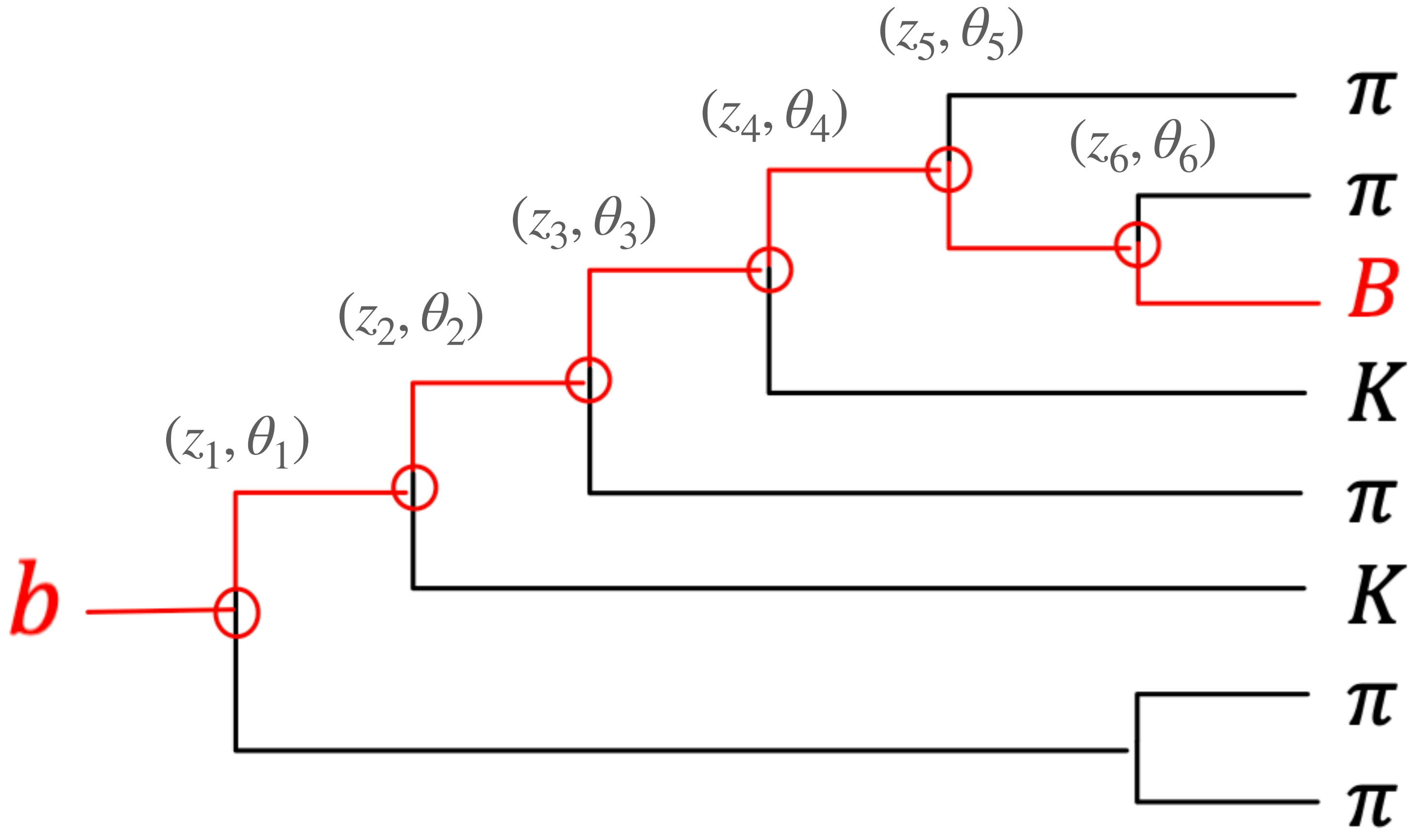

Primary Lund jet plane

CMS Collaboration

arXiv:2312.16343

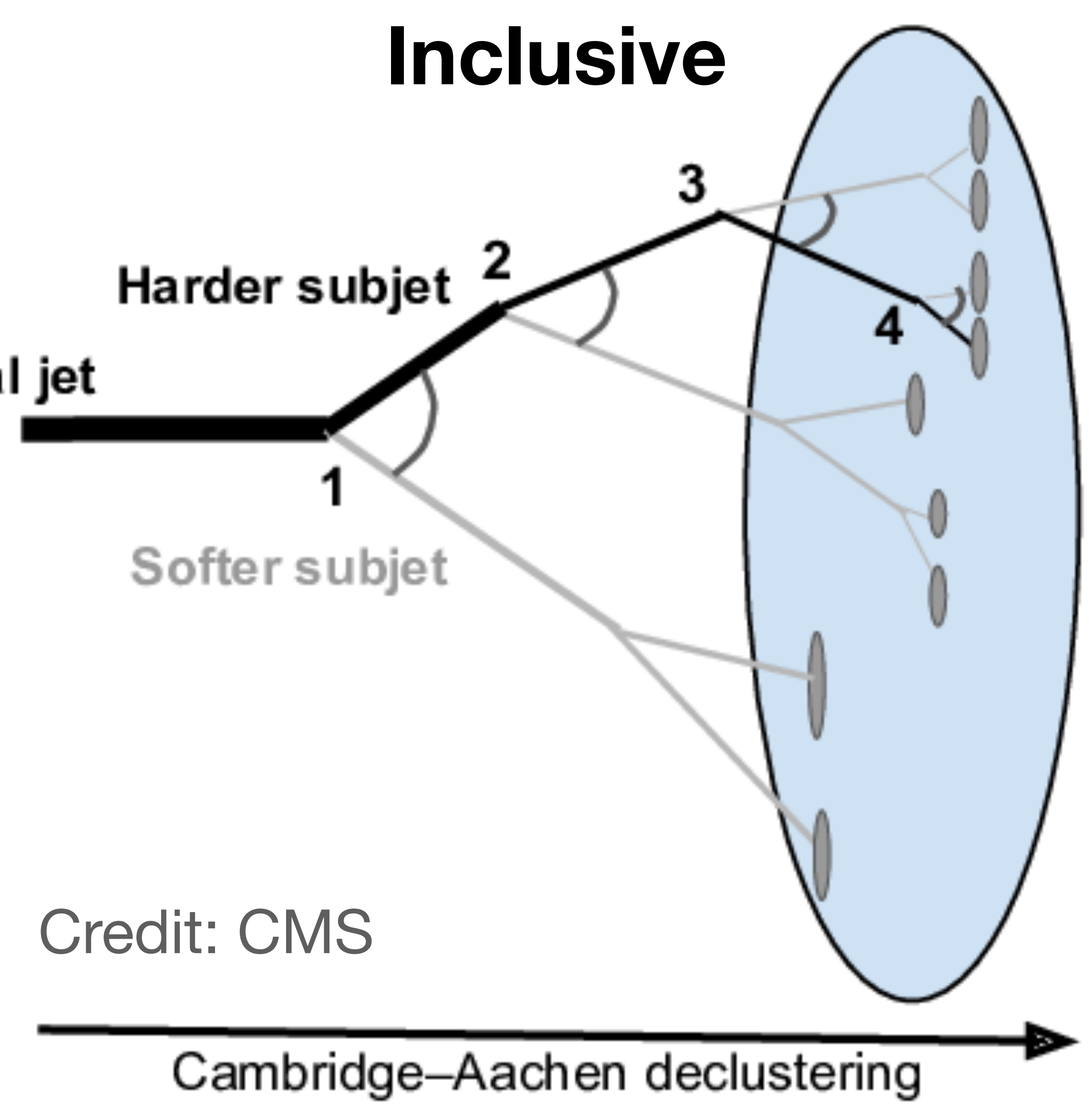

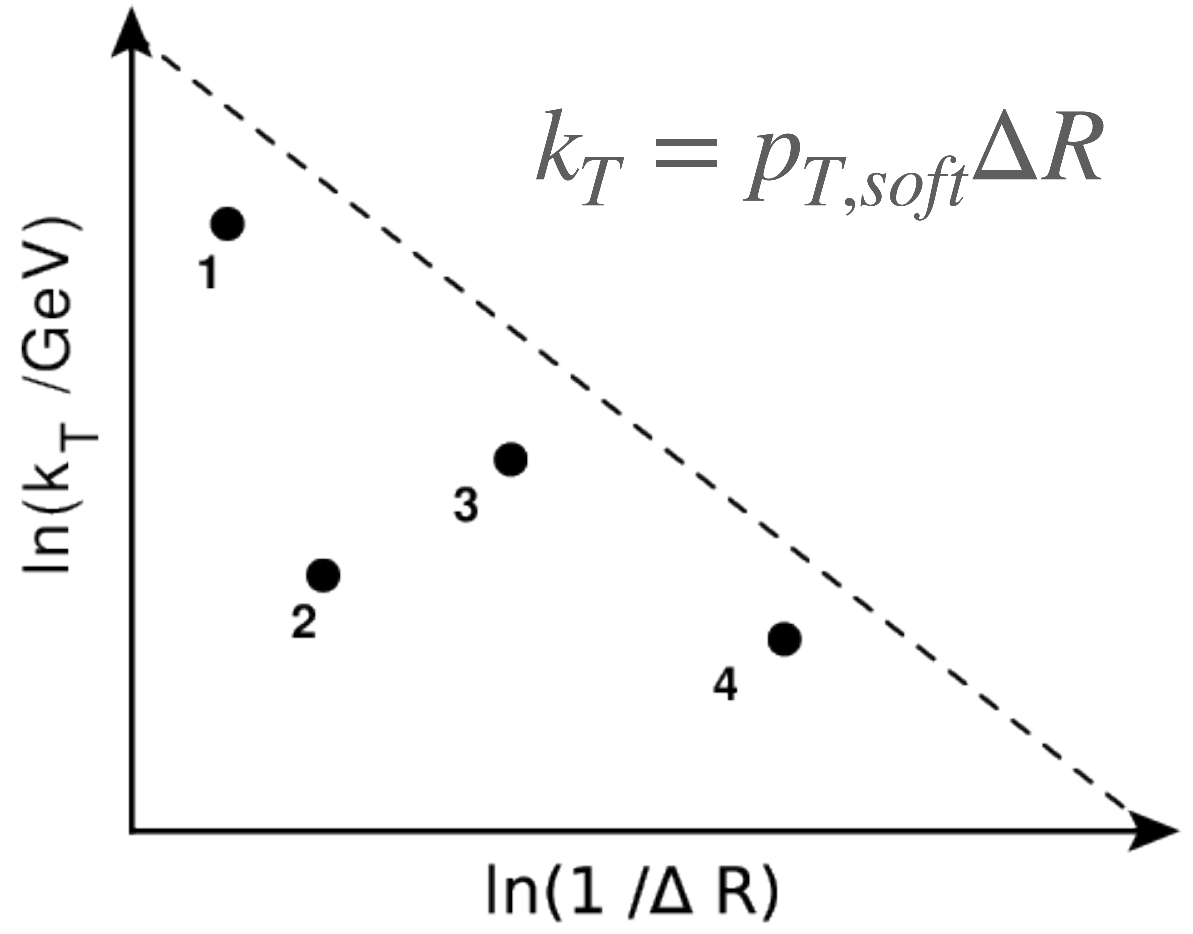

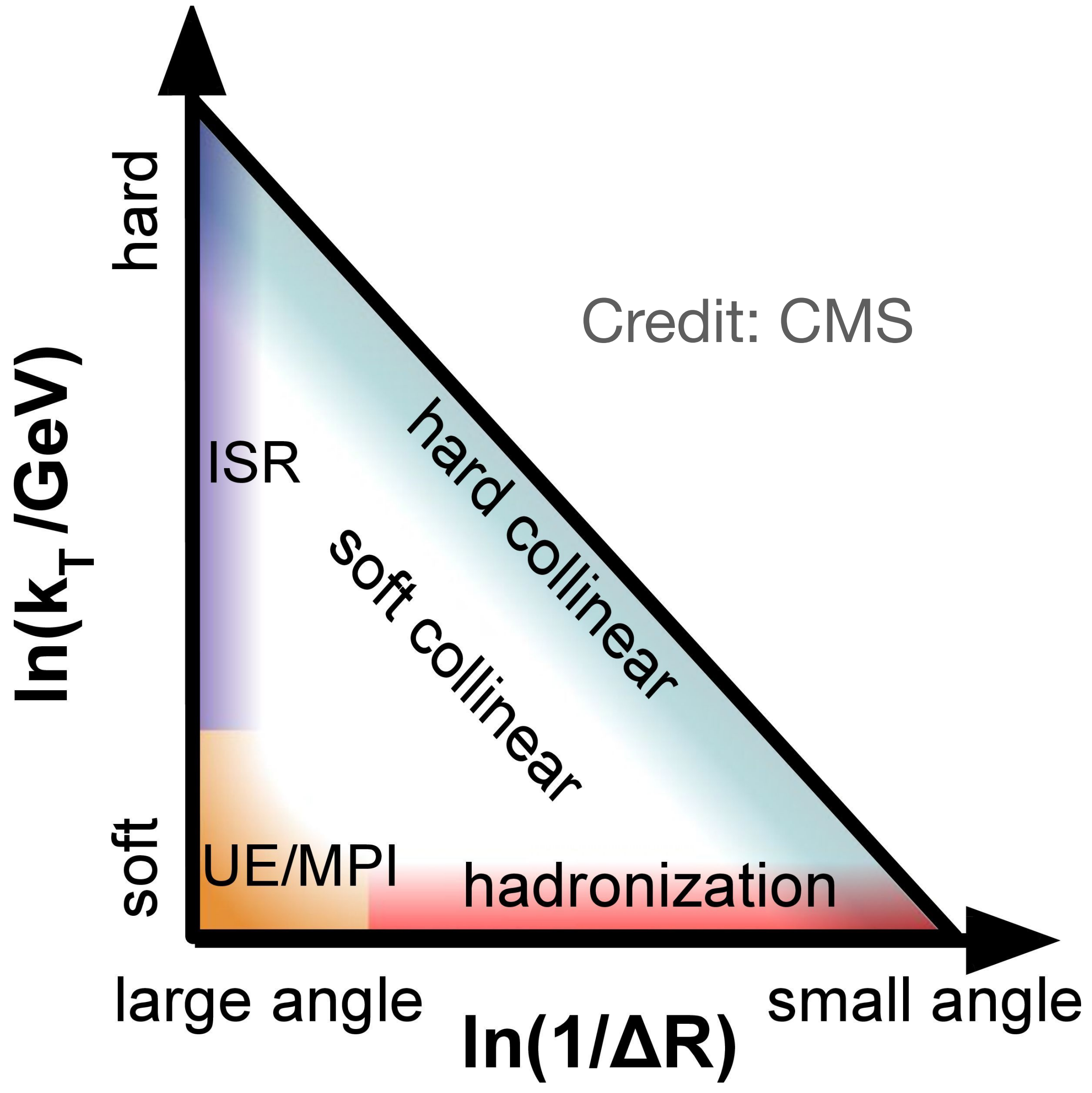

Experimental Setup and Jet Reconstruction:

- $\sqrt{s} = 13$ **TeV (Run 2)**
- **Full jet reconstruction, track reclustering**
- **Anti-kt jets with R = 0.4 or 0.8**
- $|y_{jet}| < 1.7$
- $p_T^{jet} > 700$ **GeV**

- Follow the hardest branch in the C/A reclustered tree
- Populate the Lund plane with the properties of the emission

Primary Lund jet plane

CMS Collaboration

arXiv:2312.16343

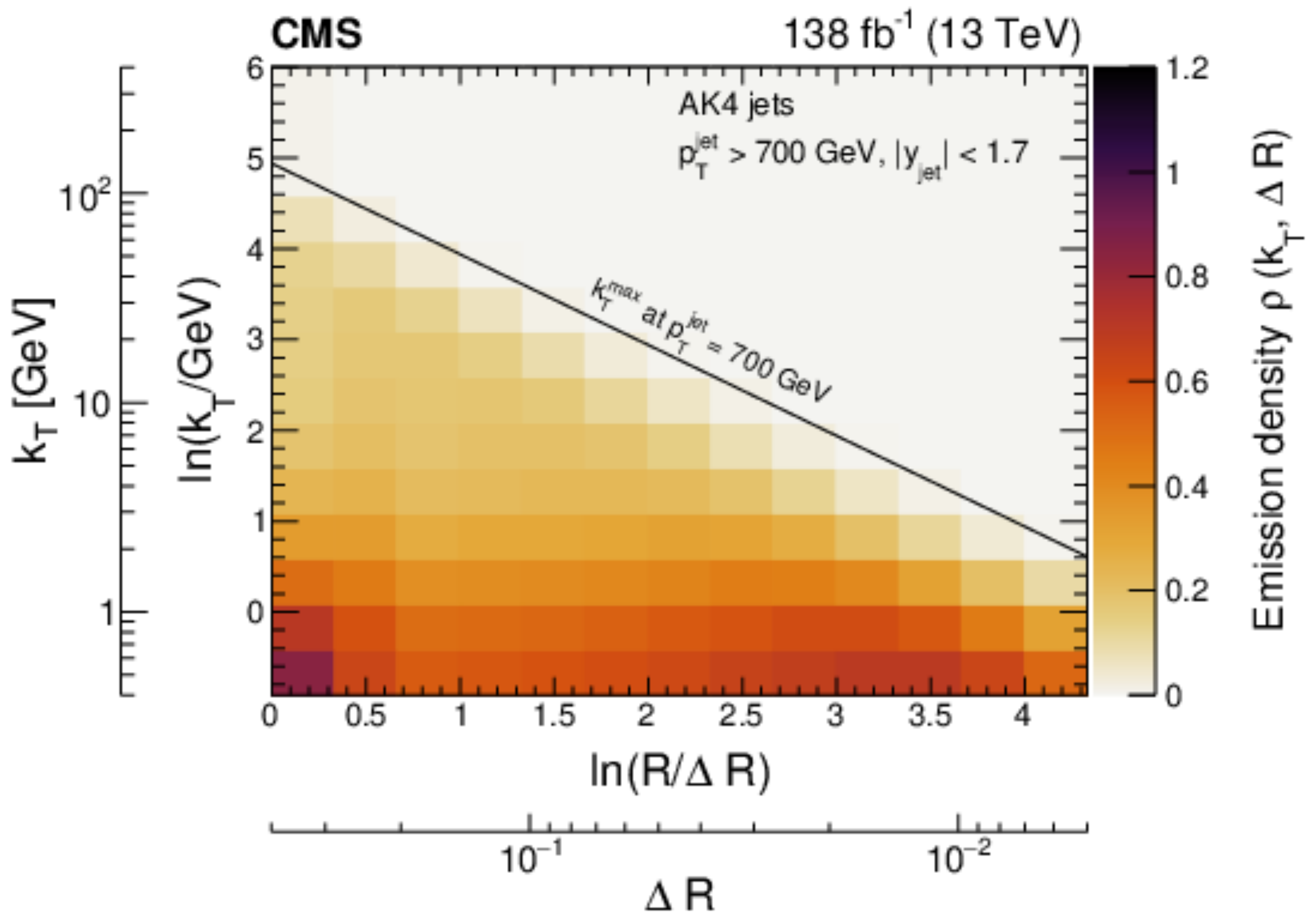

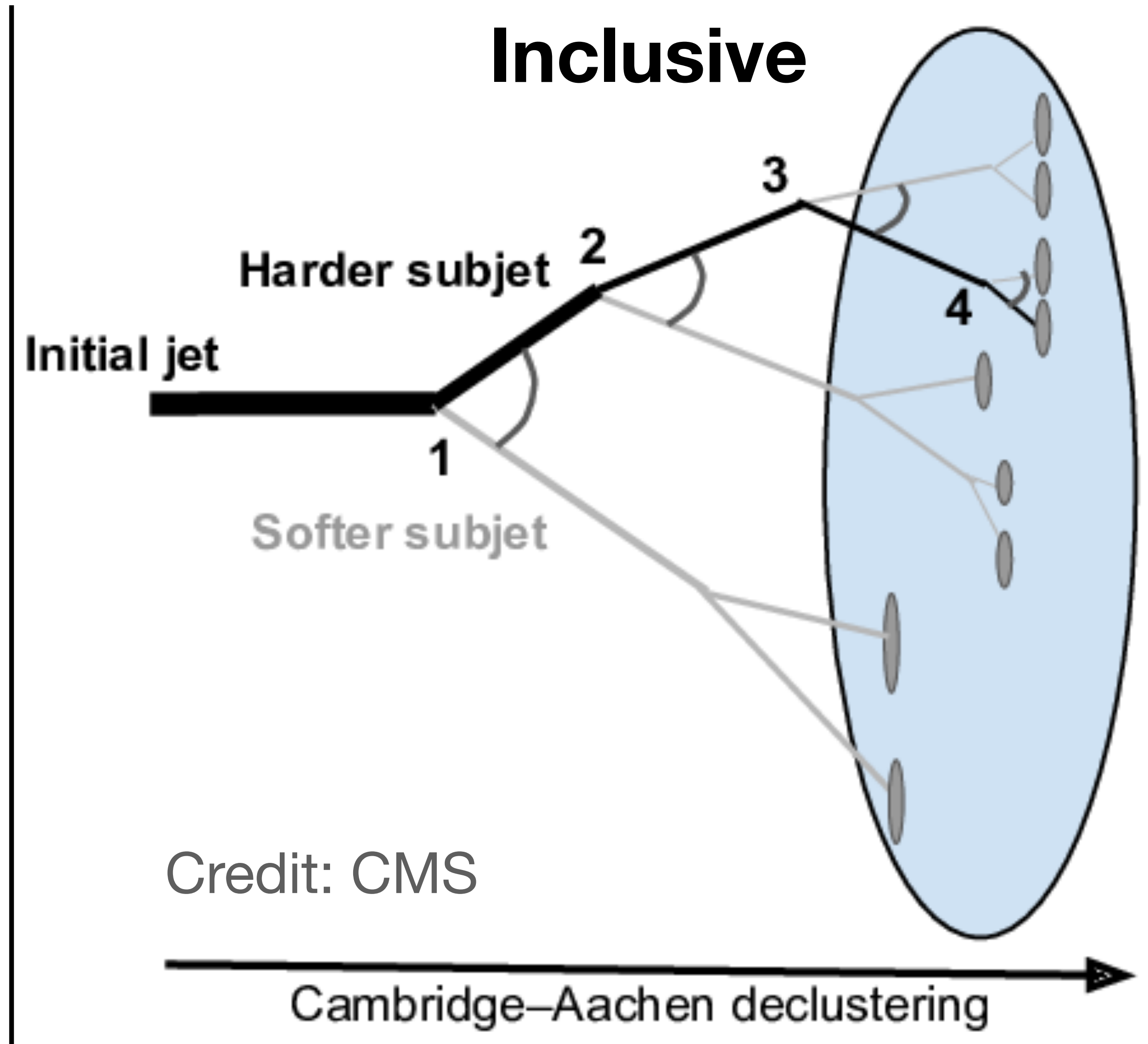

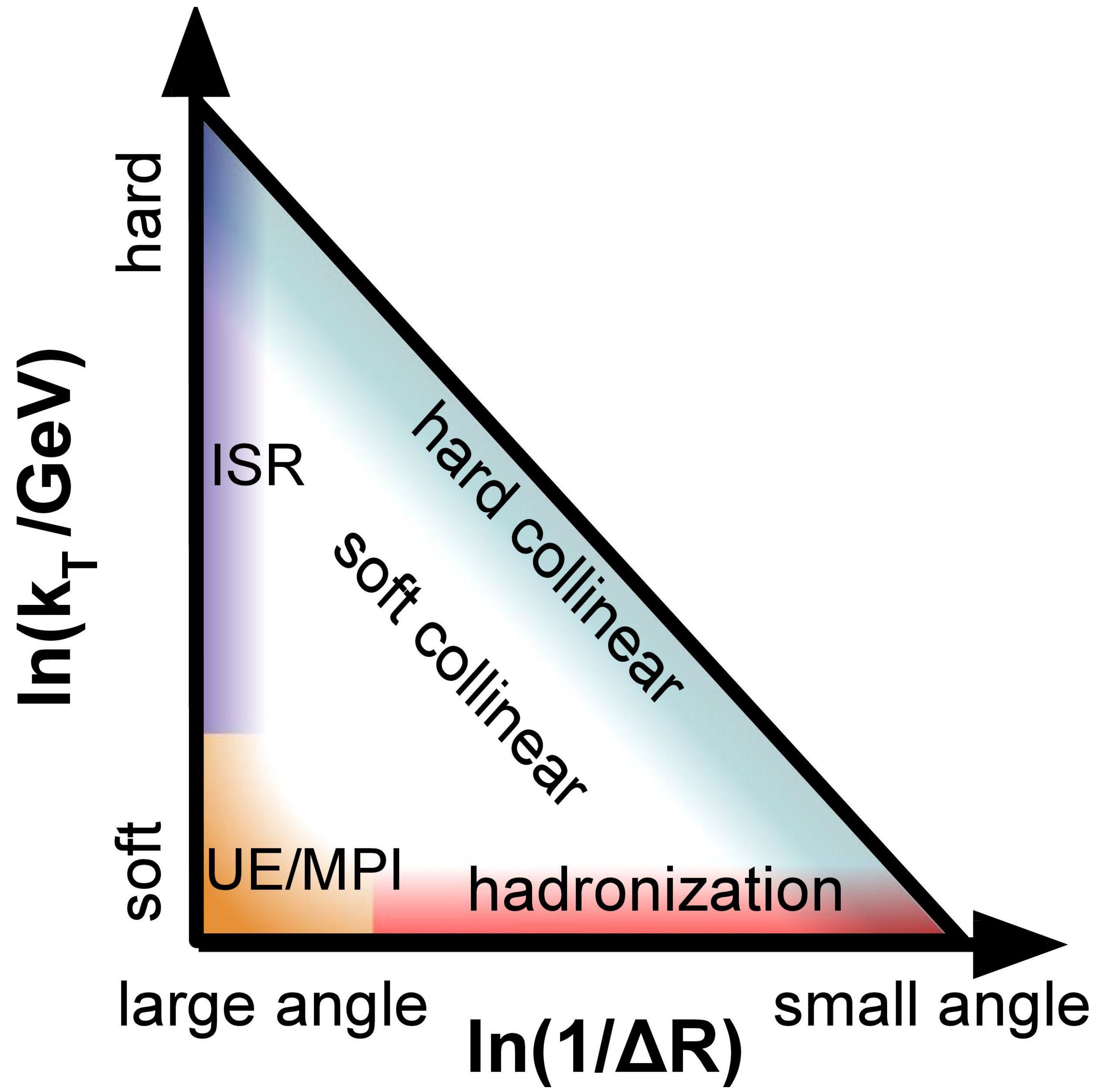

- Emission density plateaus at large k_T as α_S plateaus, while the density is increasing towards lower k_T where α_S is rising

Primary Lund jet plane

CMS Collaboration

arXiv:2312.16343

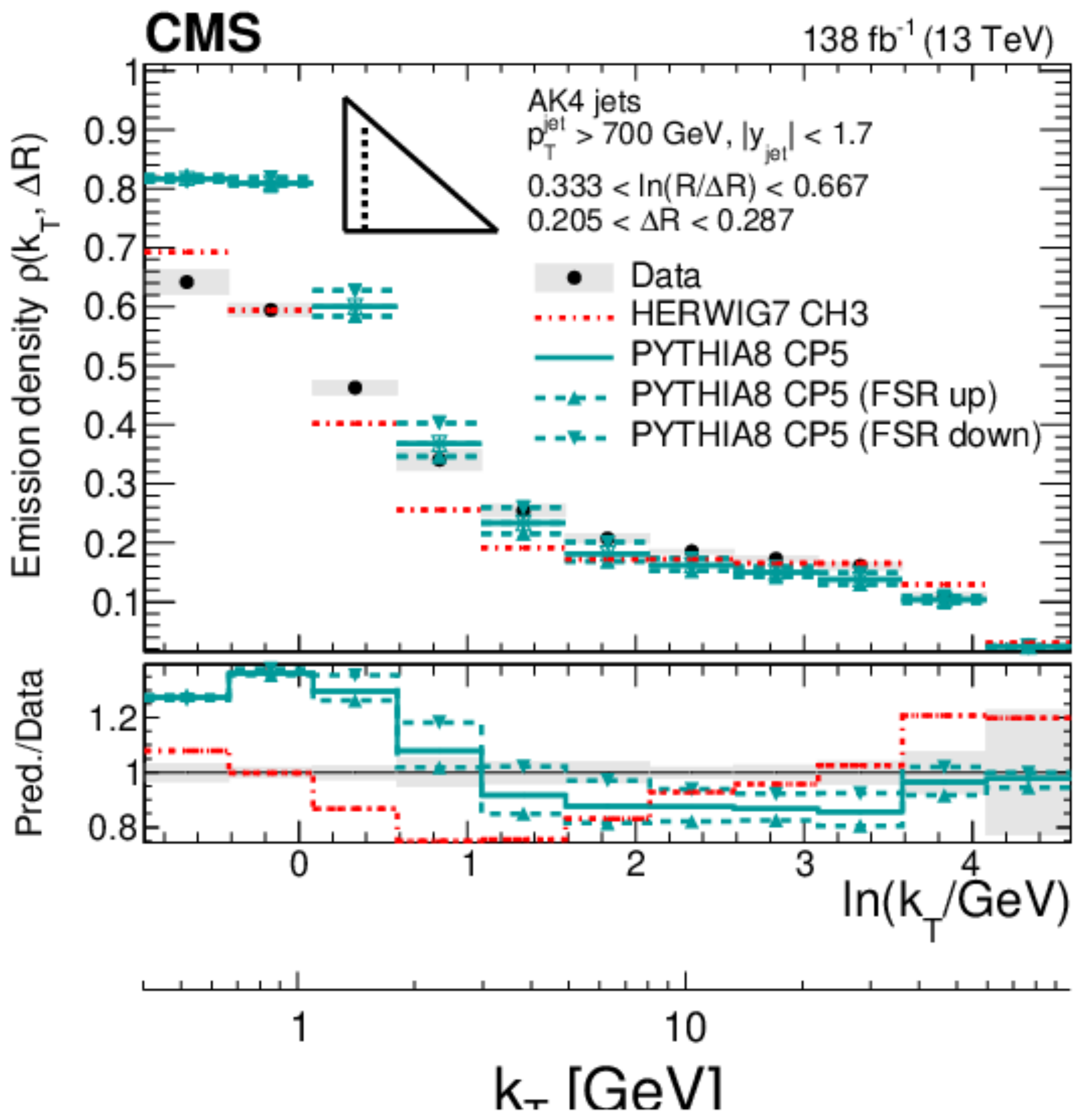

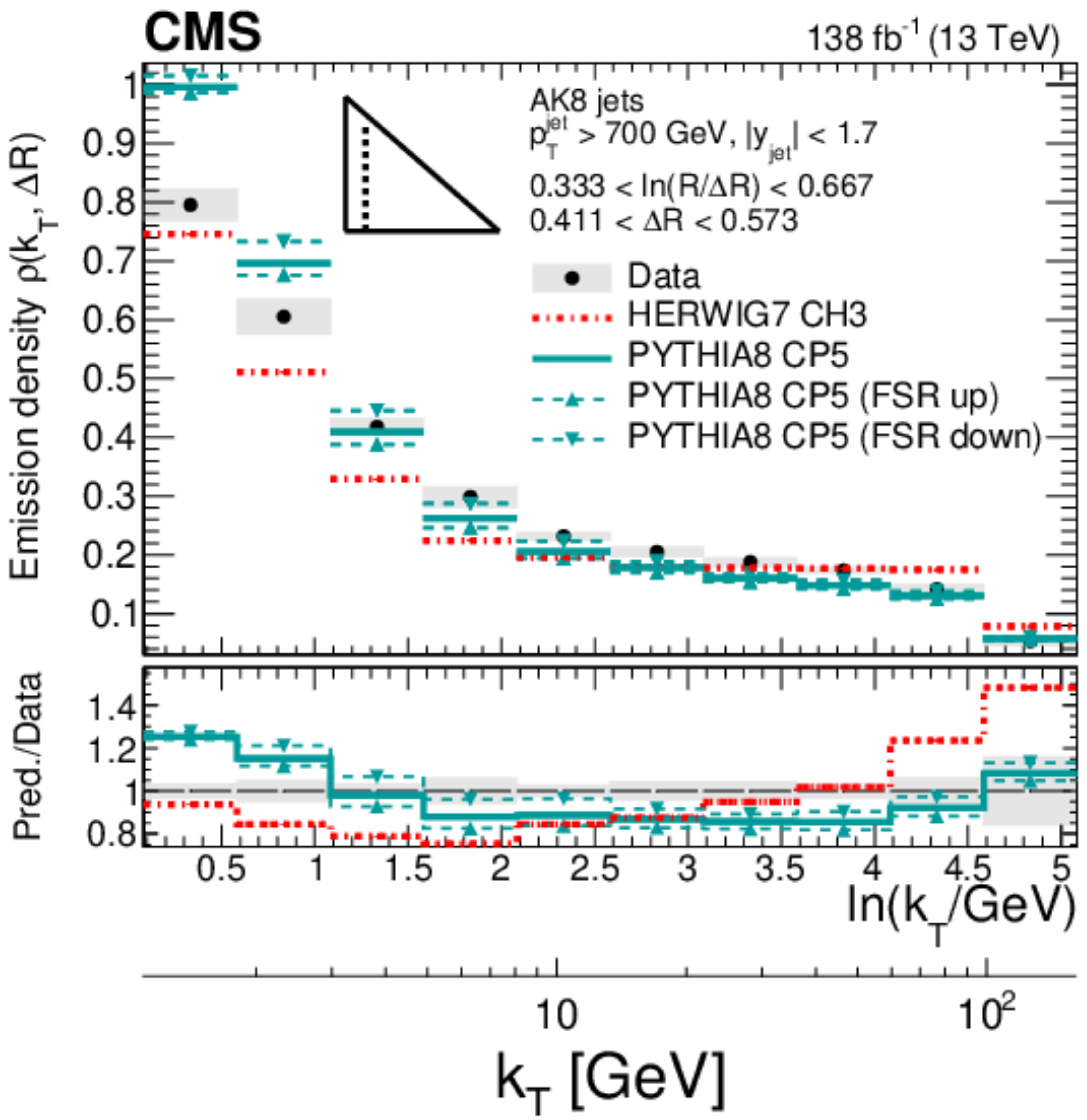

- Take slices of the LJP at fixed ΔR to see the running of $\alpha_S(k_T)$
- Event generators can be tuned from the primary LJP data

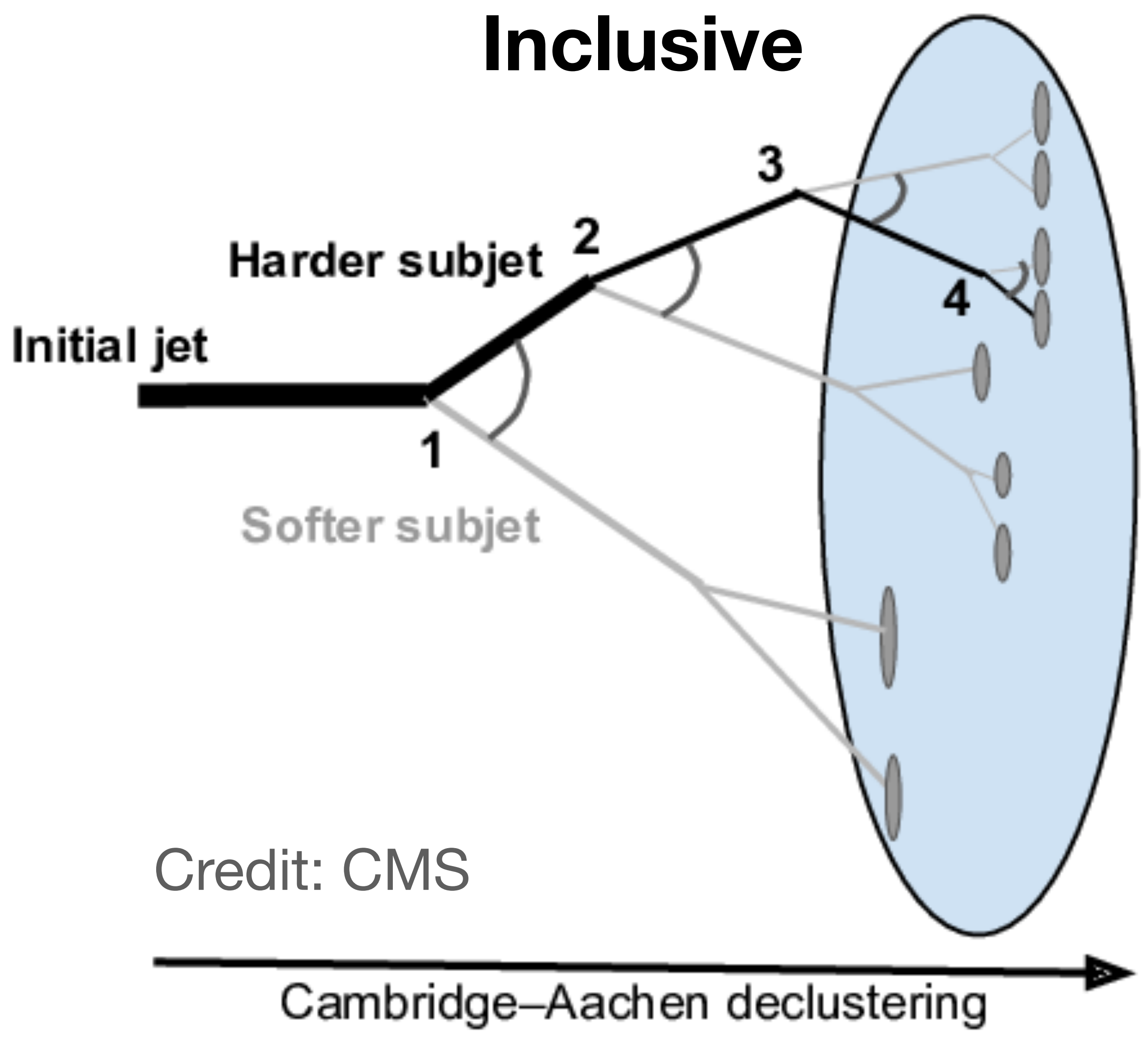

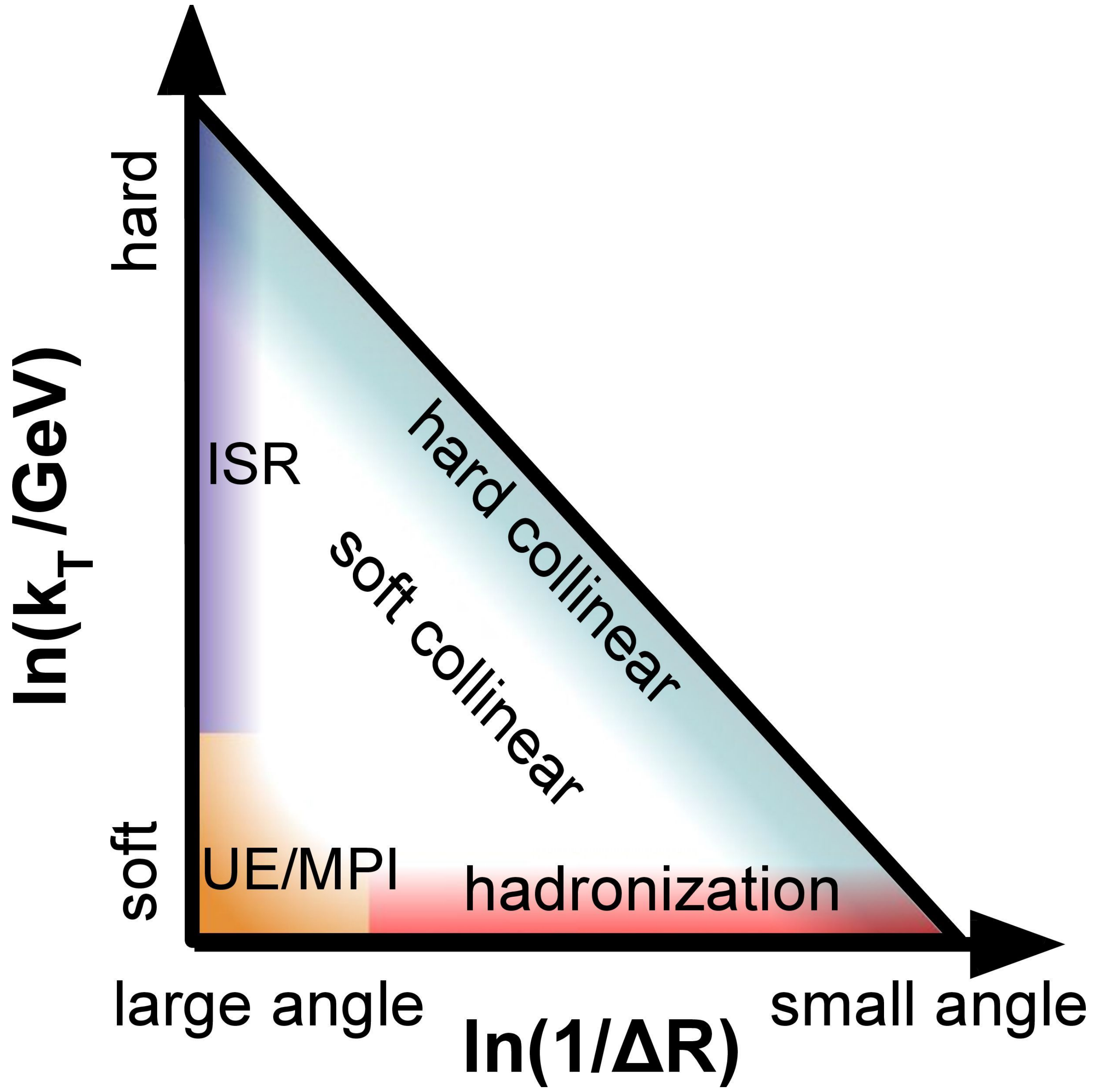

Primary Lund jet plane

CMS Collaboration

arXiv:2312.16343

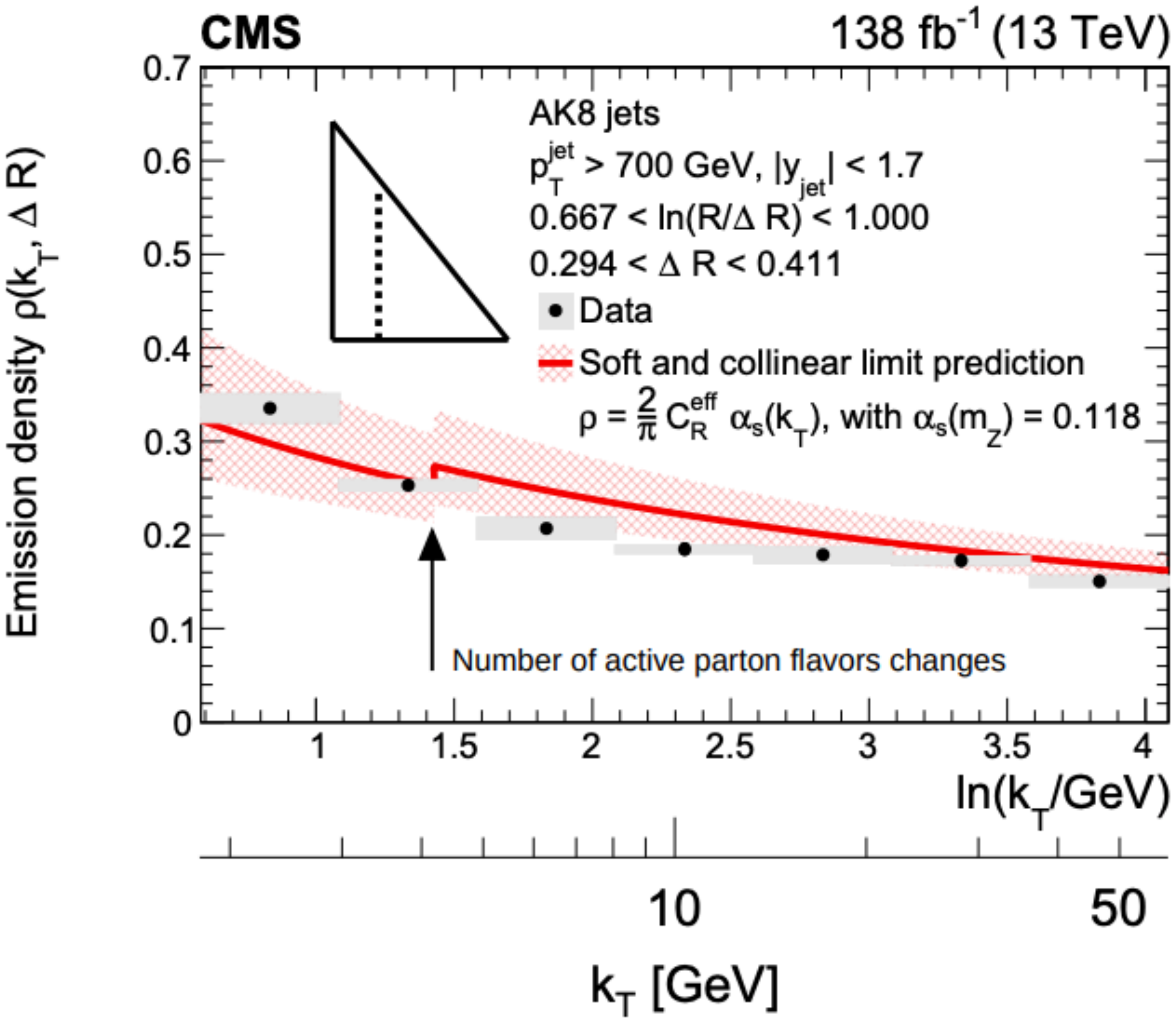

- The soft and collinear limit is directly proportional to $\alpha_S\left(k_T\right)$ through $\rho = \frac{2}{\pi} C_R^{eff} \alpha_S(k_T)$
- Qualitative agreement between the data and the soft-collinear prediction

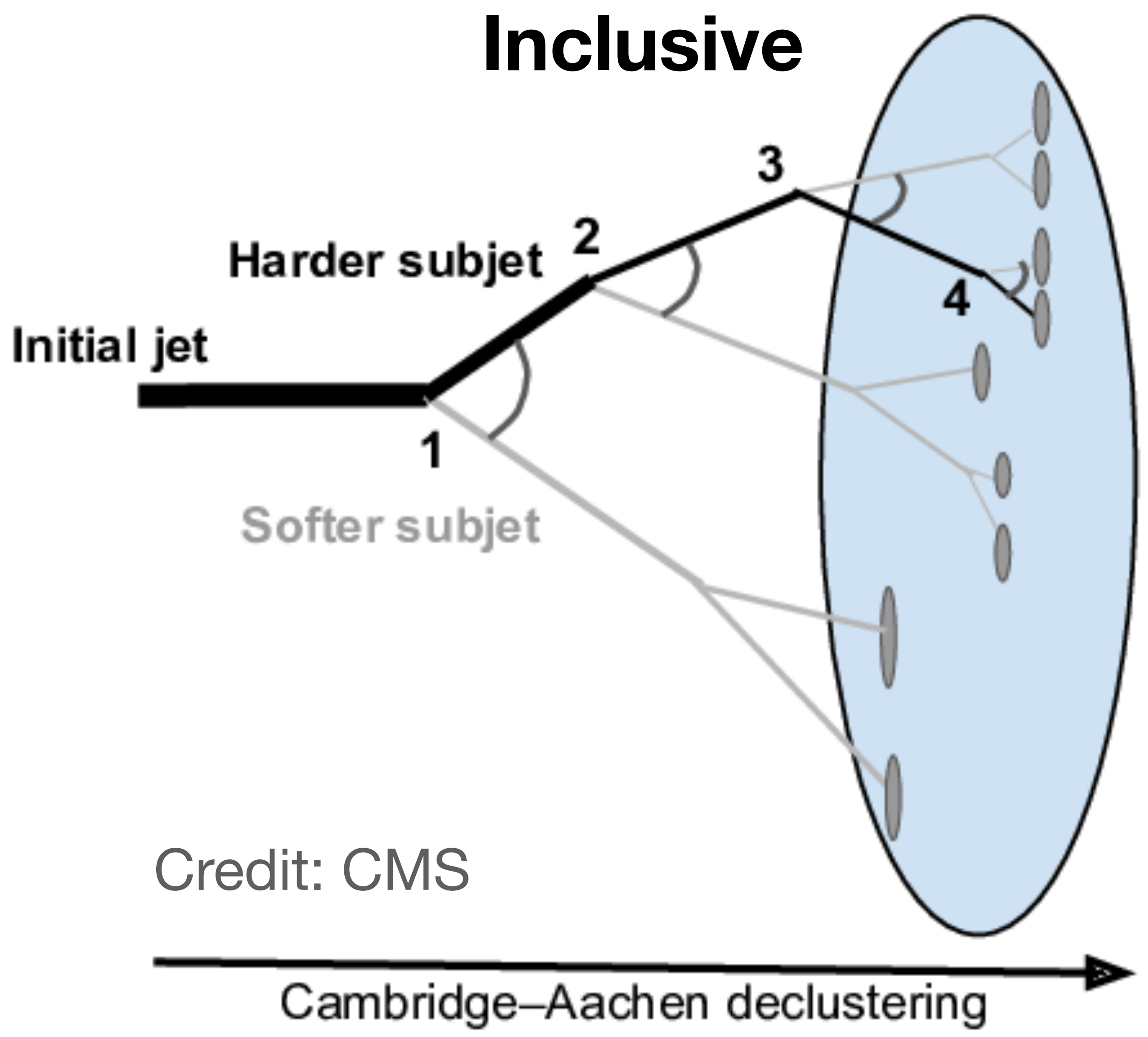

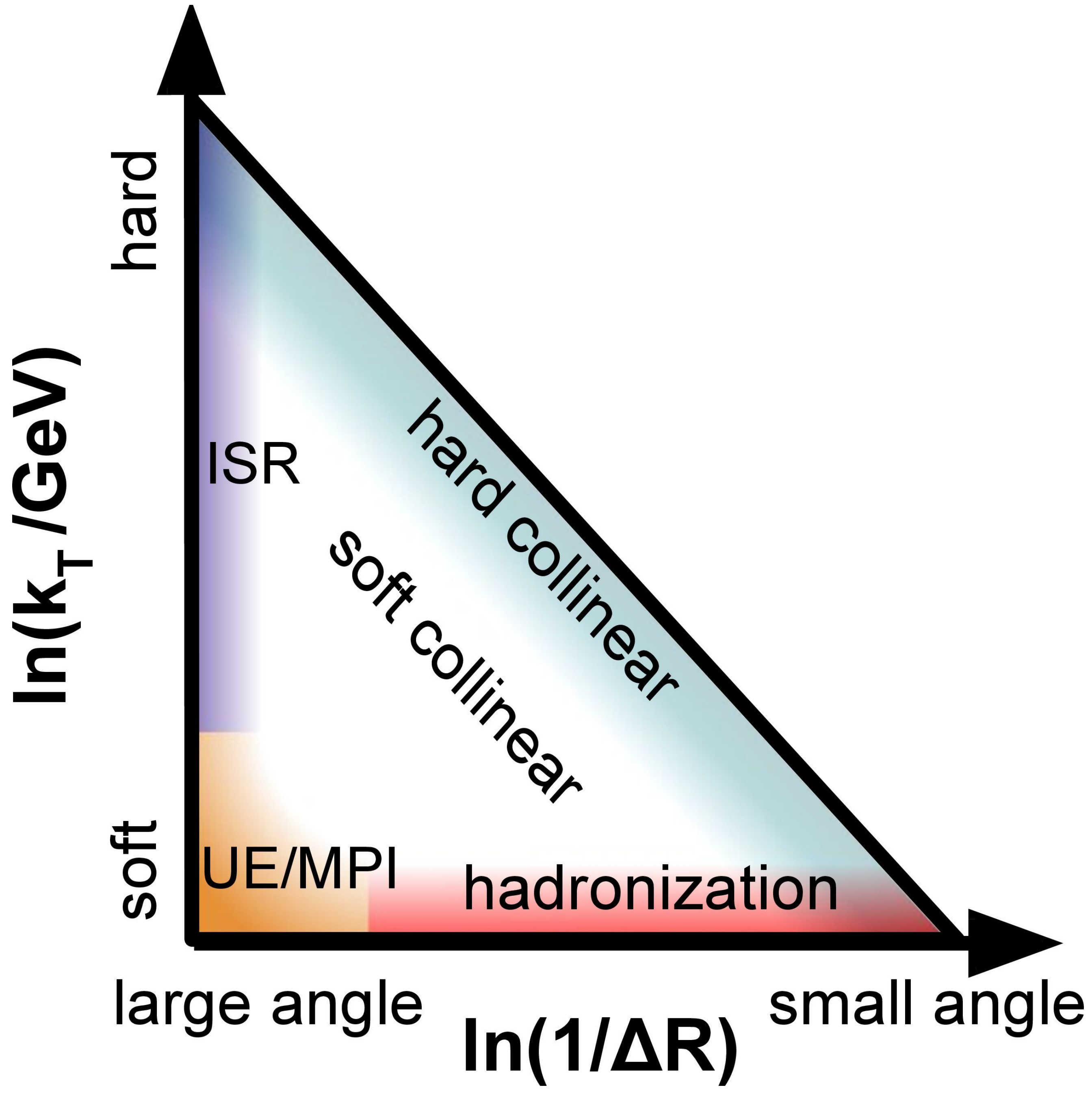

Primary Lund jet plane

ALICE, CMS, and ATLAS. LHCb is on the way!

ALICE

arXiv:2111.00020v1

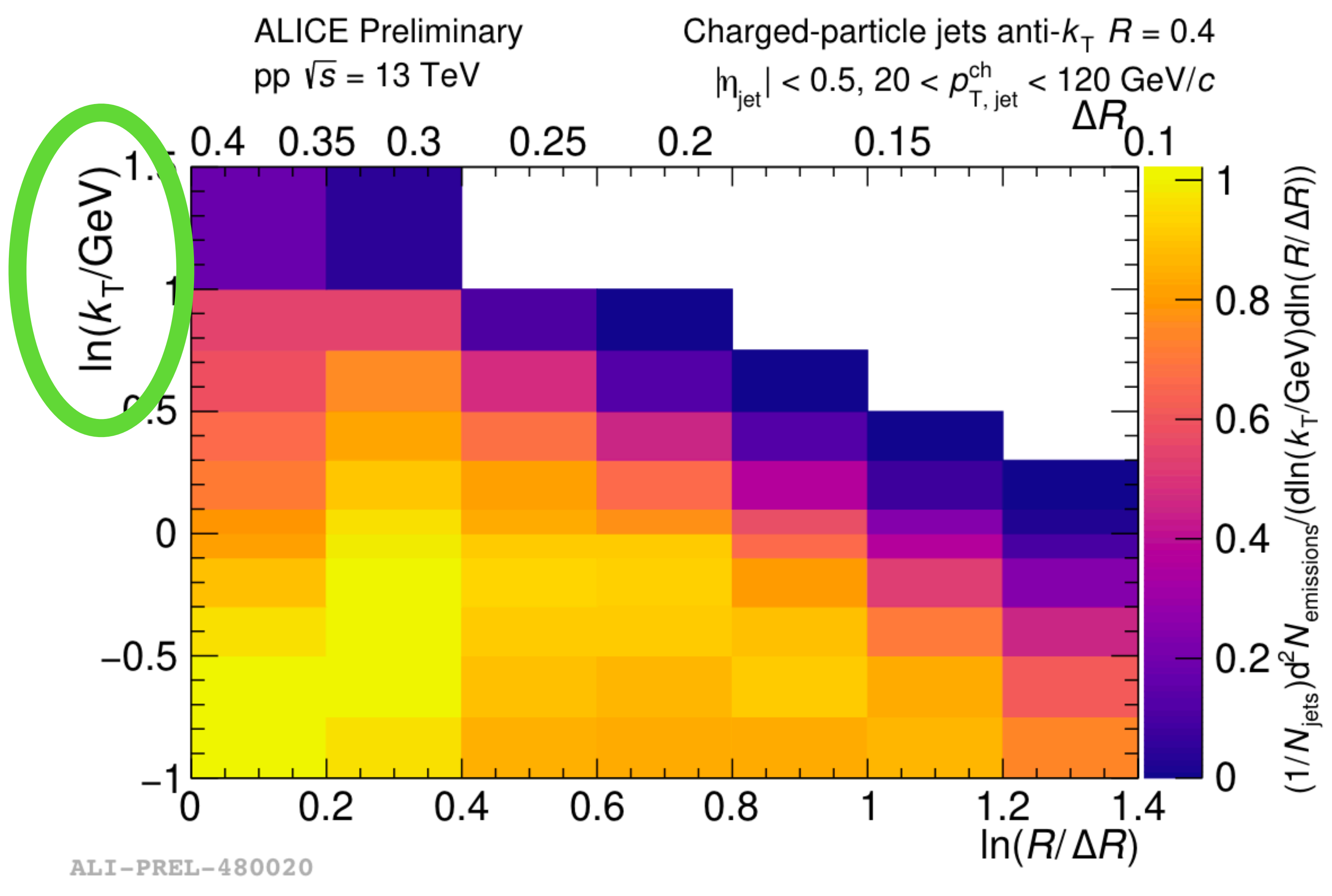

Figure 3: Fully corrected primary Lund plane density.

CMS

arXiv:2312.16343

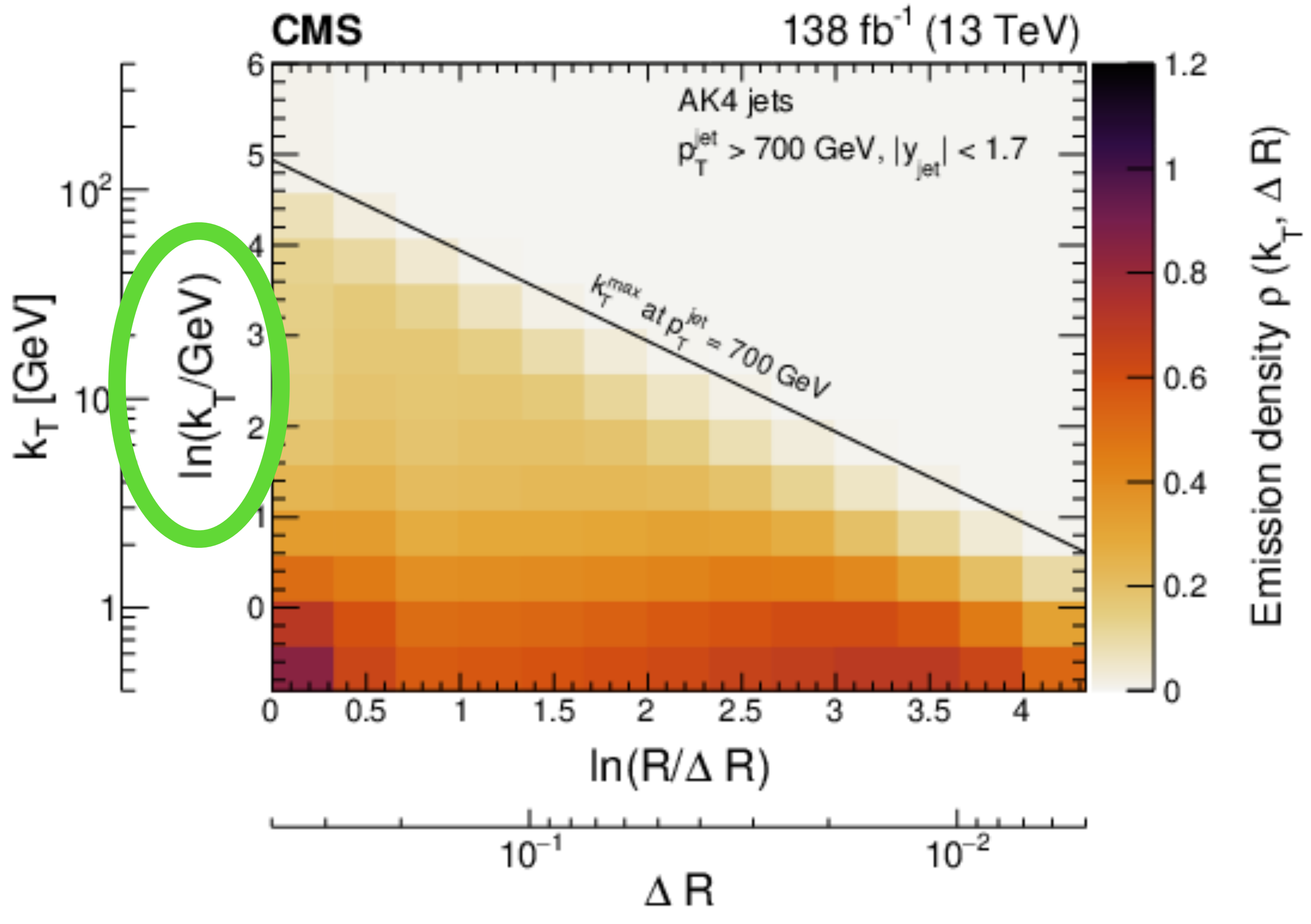

ATLAS

PRL 124.22 (2020): 222002

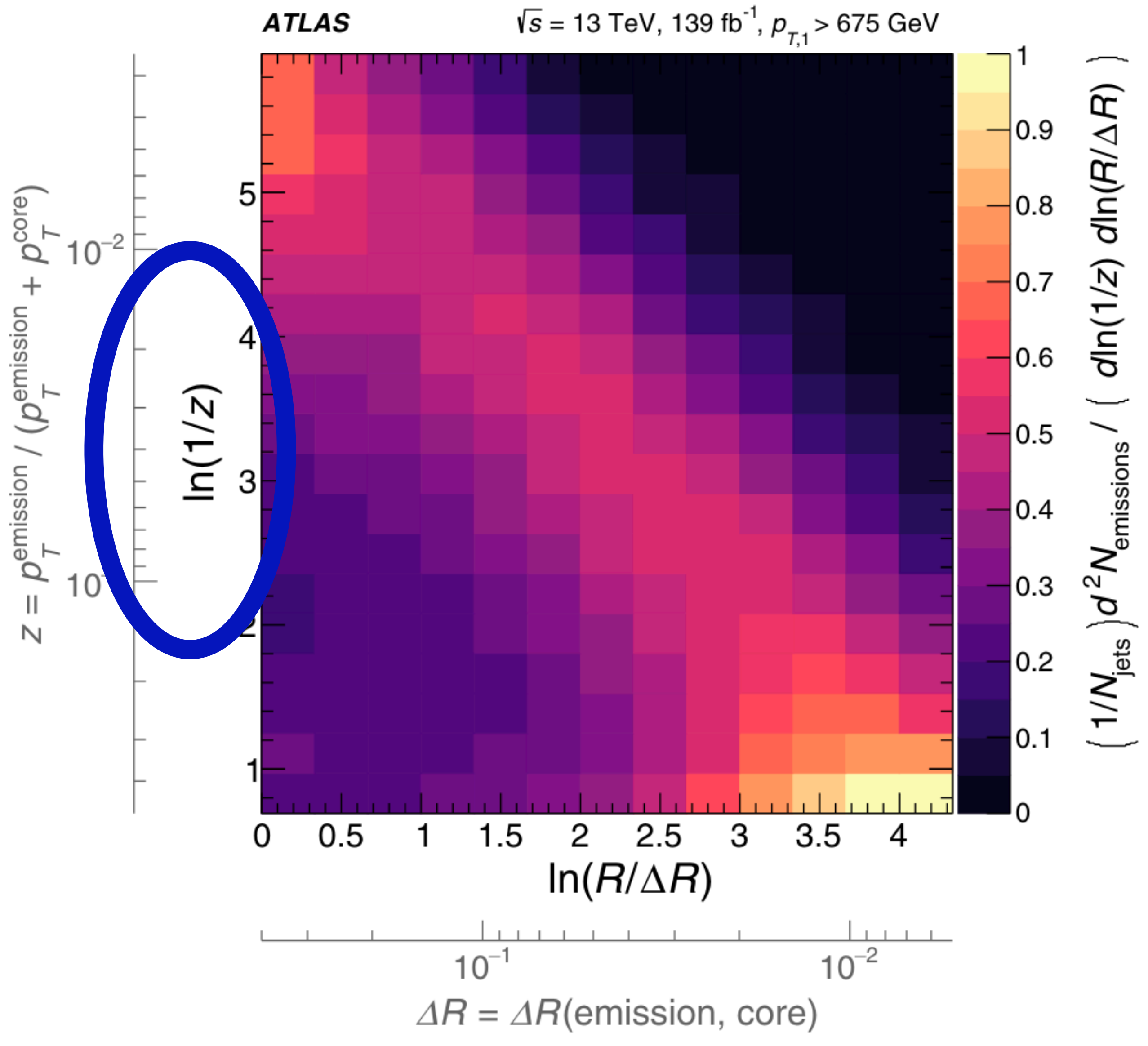

FIG. 2. The LJP measured using jets in 13 TeV pp collision data, corrected to particle level. The inner set of axes indicates the coordinates of the LJP itself, while the outer set indicates corresponding values of z and ΔR.

Lund subjet multiplicity

ATLAS Collaboration

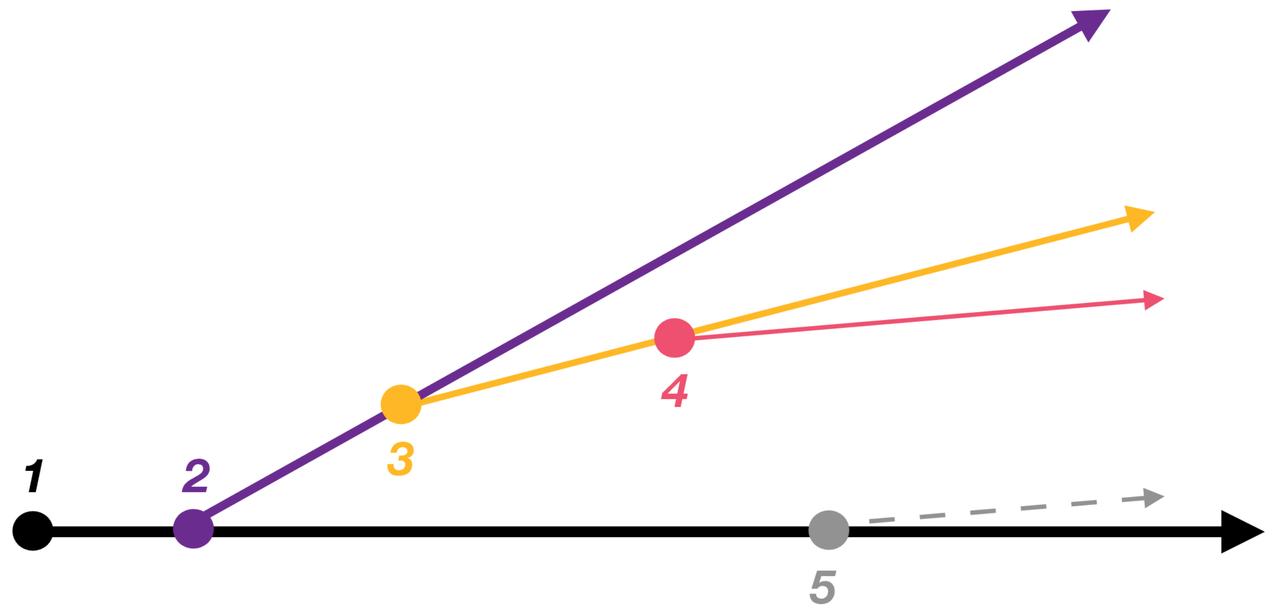

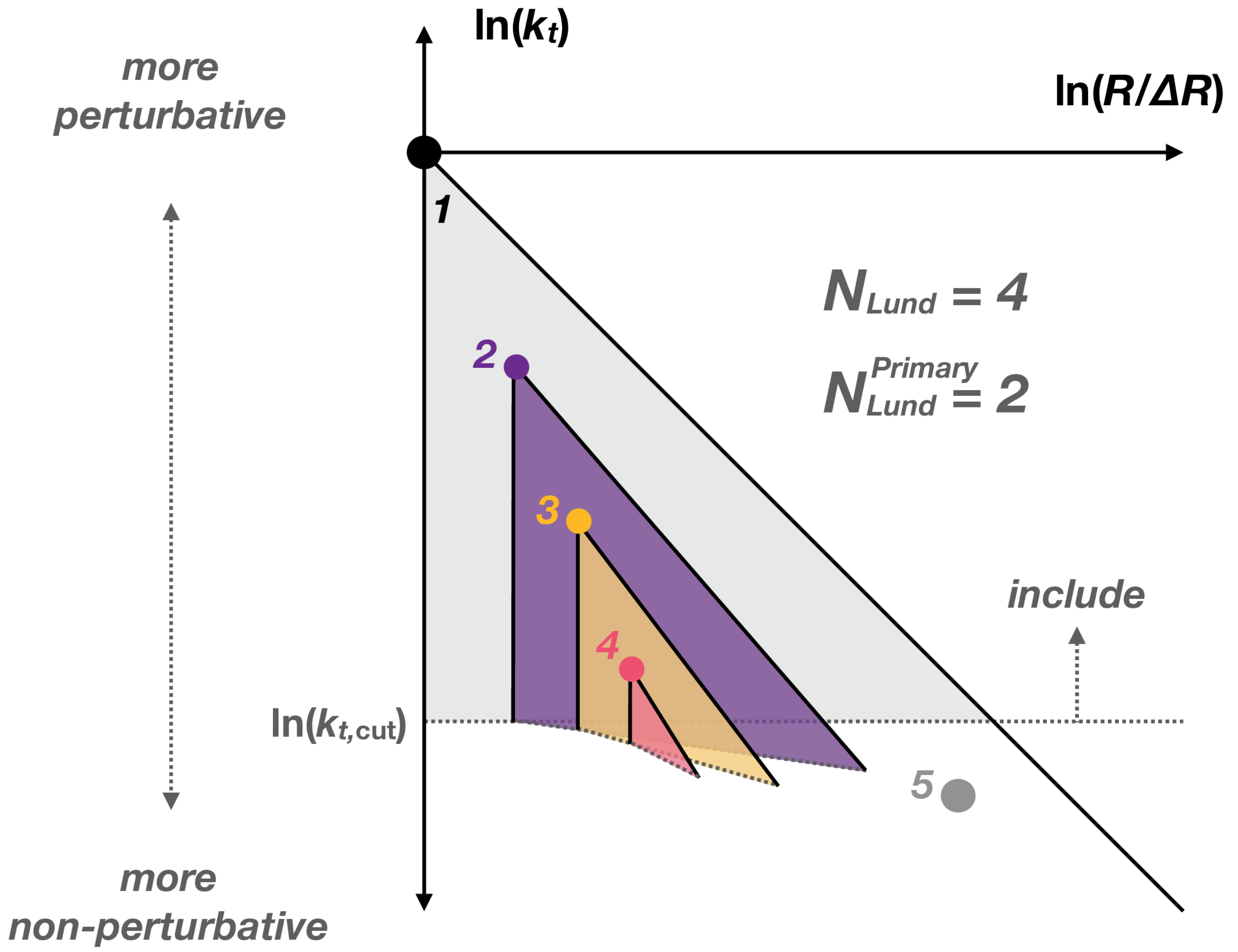

Experimental Setup and Jet Reconstruction:

- $\sqrt{s} = 13$ **TeV (Run 2)**
- **Full jet reconstruction, tracks reclustering**
- **Anti-kt jets with R = 0.4**
- $|y_{jet}| < 2.1$
- $p_T^{jet} > 120$ **GeV**

- The number of emissions in successive Lund planes with $k_t > k_{t,cut}$ is denoted by N_{Lund}
- The number of emissions on the hardest branch is denoted by $N_{Lund}^{Primary}$
- Constrains and tests Parton Shower Monte Carlo (PSMC) through double-soft splittings

Lund subjet multiplicity

ATLAS Collaboration

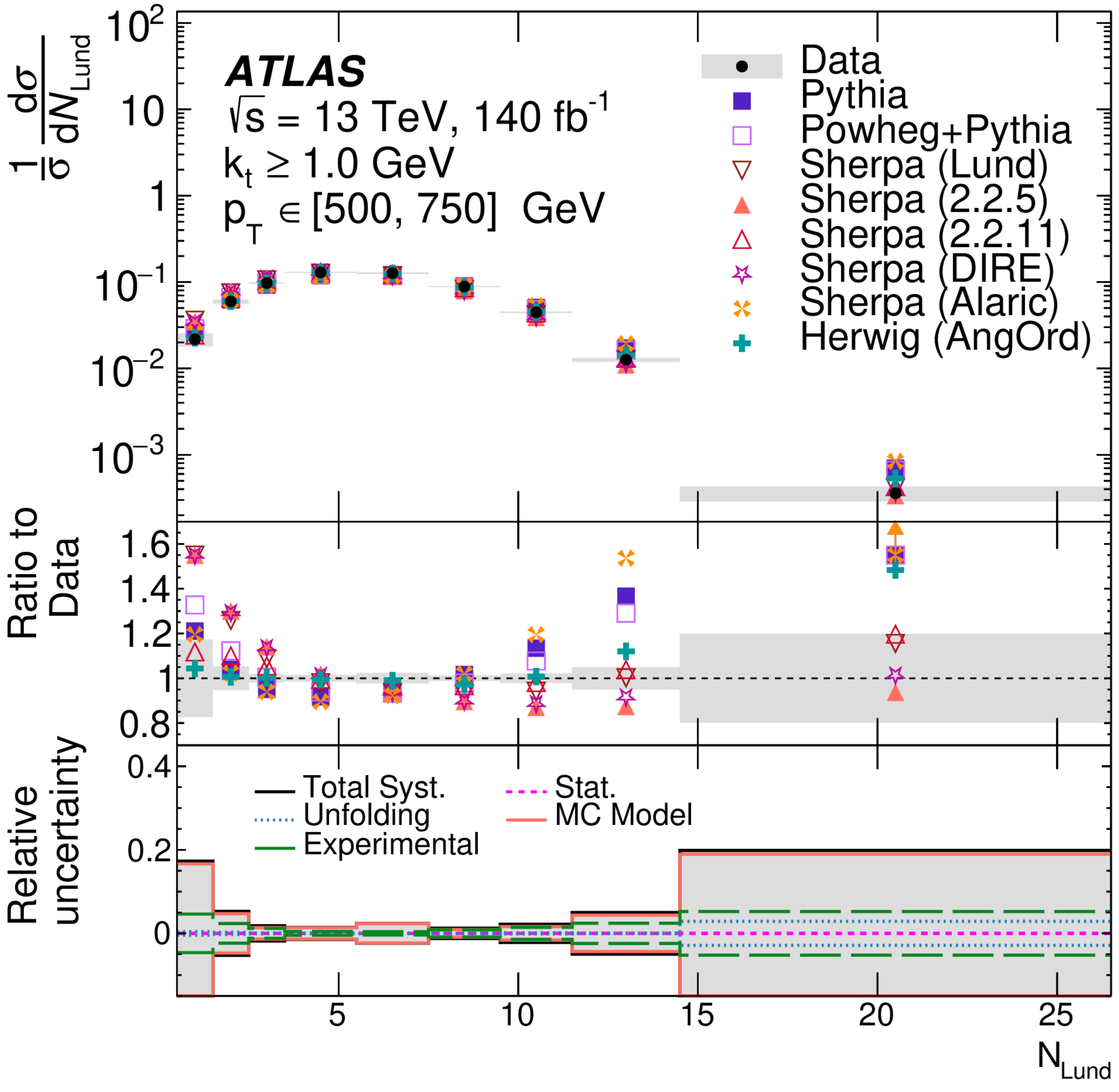

- Multiplicity distribution for $k_{t,cut} > 1$ GeV
- Large disagreement between data and MC at low and high multiplicities
- Herwig (AngOrd) performs best compared to the other models considered

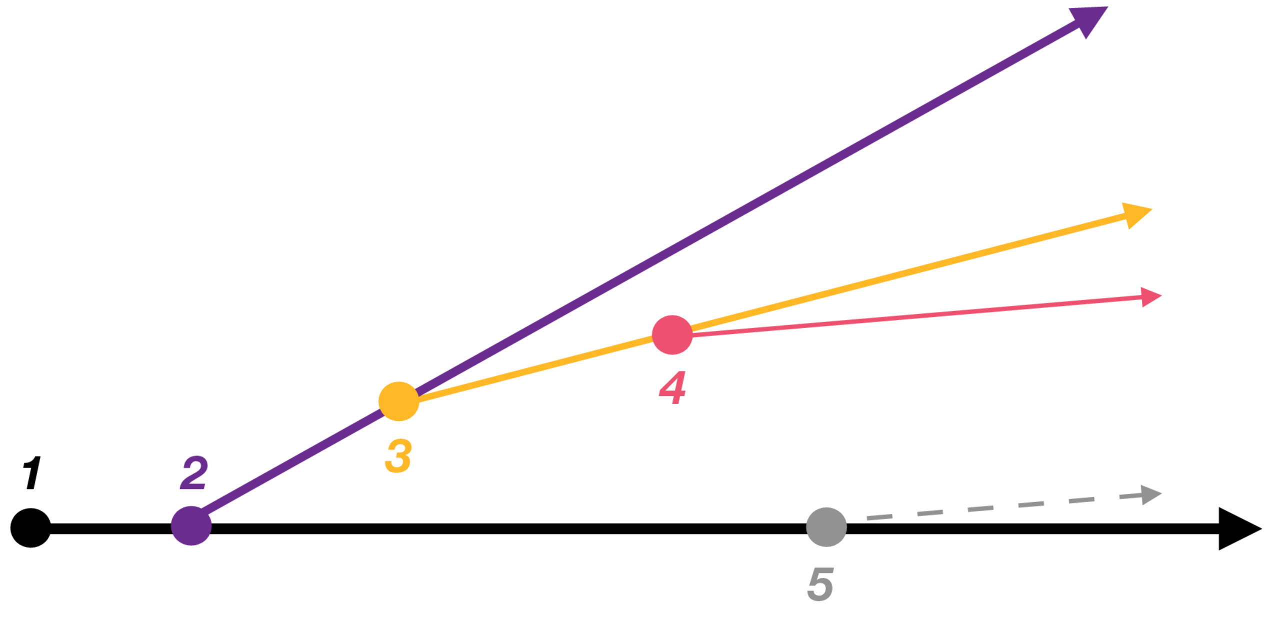

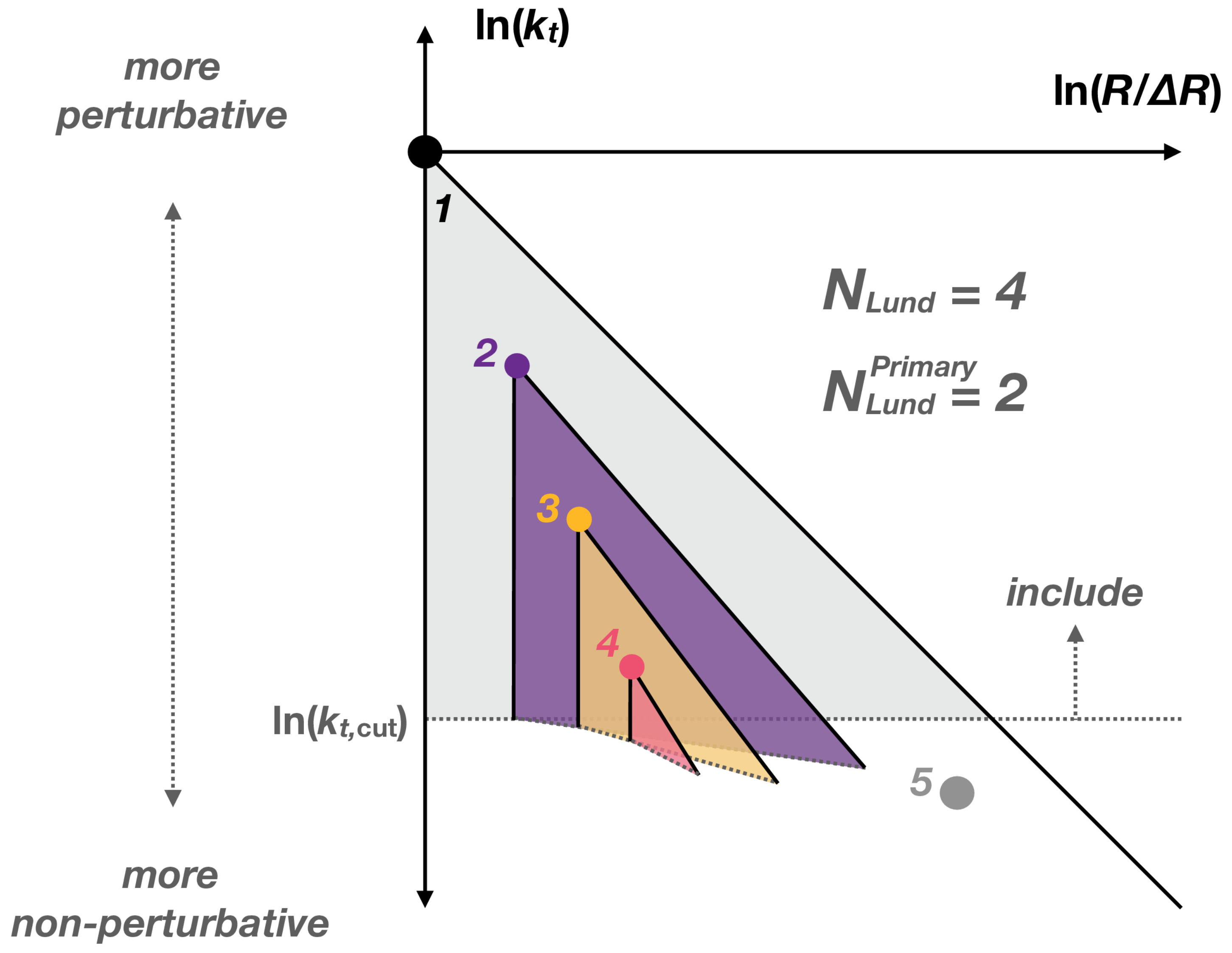

- The number of emissions in successive Lund planes with $k_t > k_{t,cut}$ is denoted by N_{Lund}
- The number of emissions on the hardest branch is denoted by $N_{Lund}^{Primary}$
- Constrains and tests Parton Shower Monte Carlo (PSMC) through double-soft splittings

Lund subjet multiplicity

ATLAS Collaboration

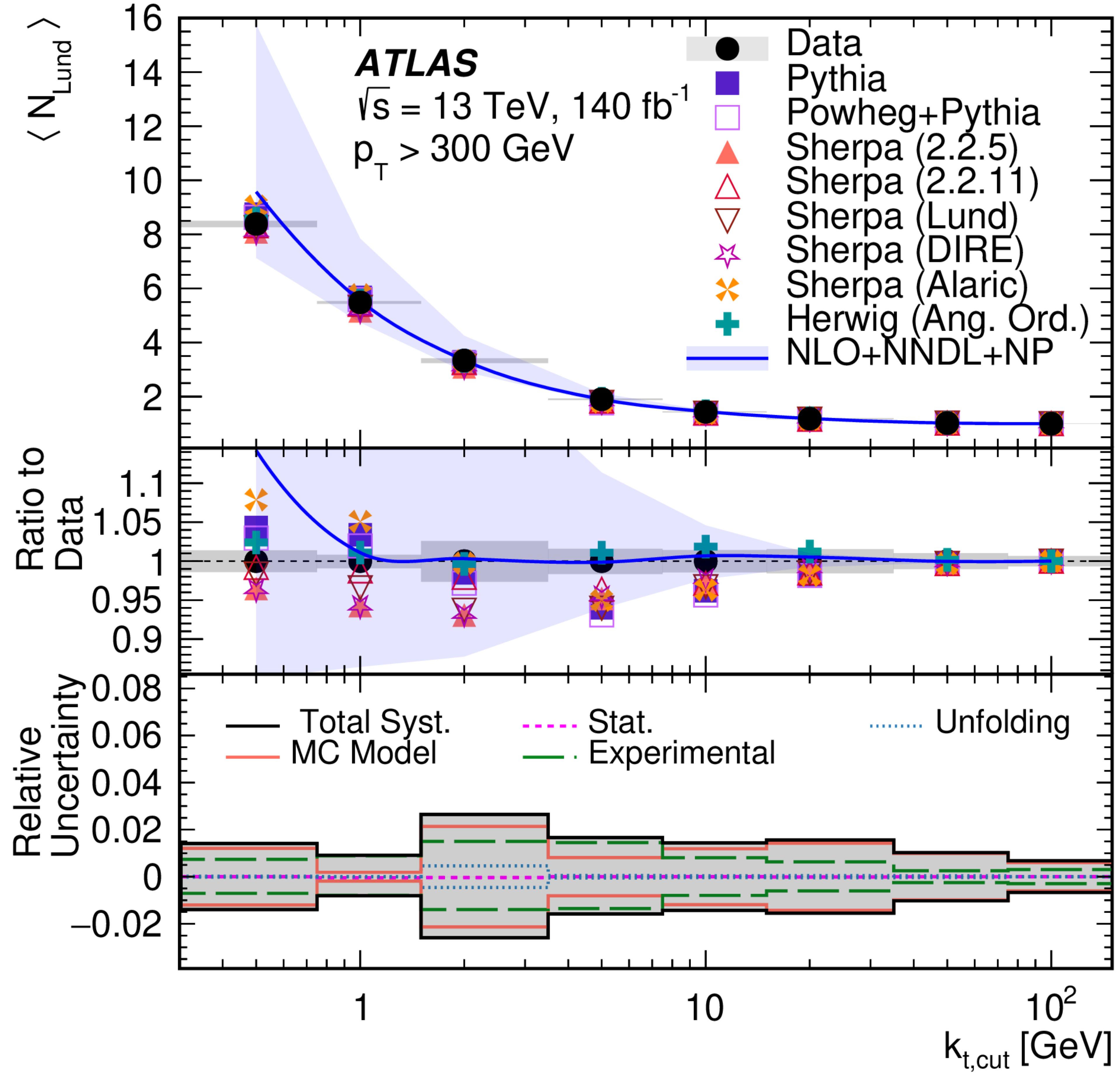

- Average subjet multiplicity $\langle N_{Lund} \rangle$ as a function of $k_{t,cut}$
- Theoretical predictions at NLO matched to NNDL resummation in good agreement in the perturbative region ($k_{t,cut} > 5$ GeV)
- Nonperturbative corrections to theoretical prediction derived from MC simulations

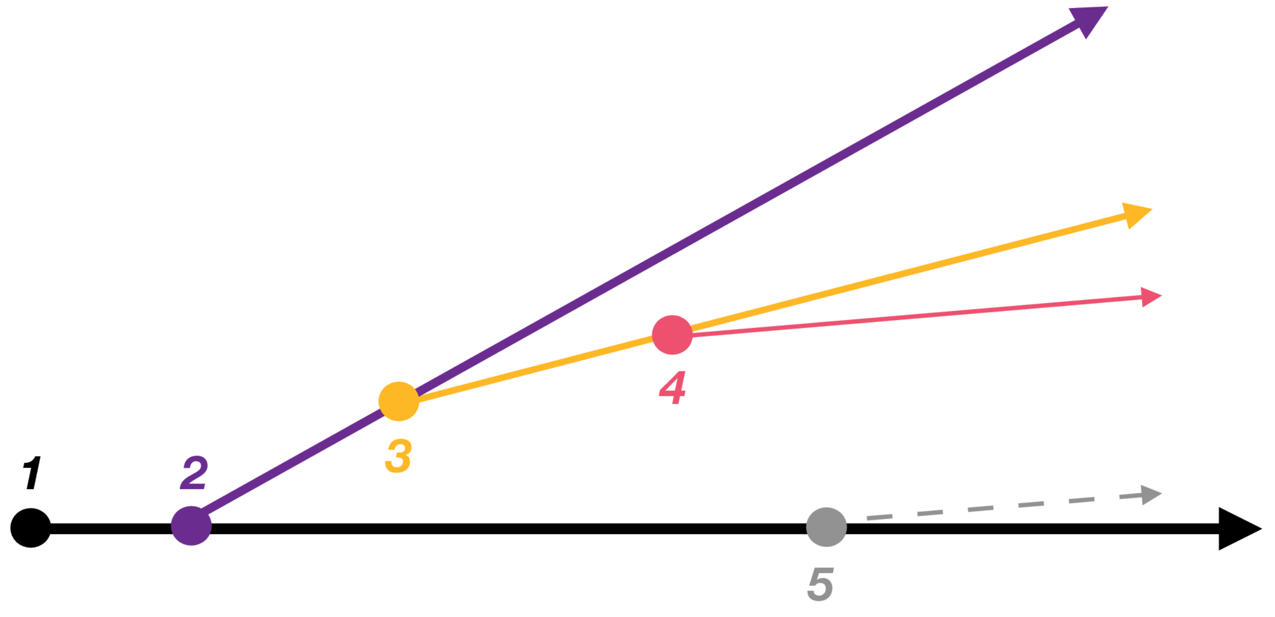

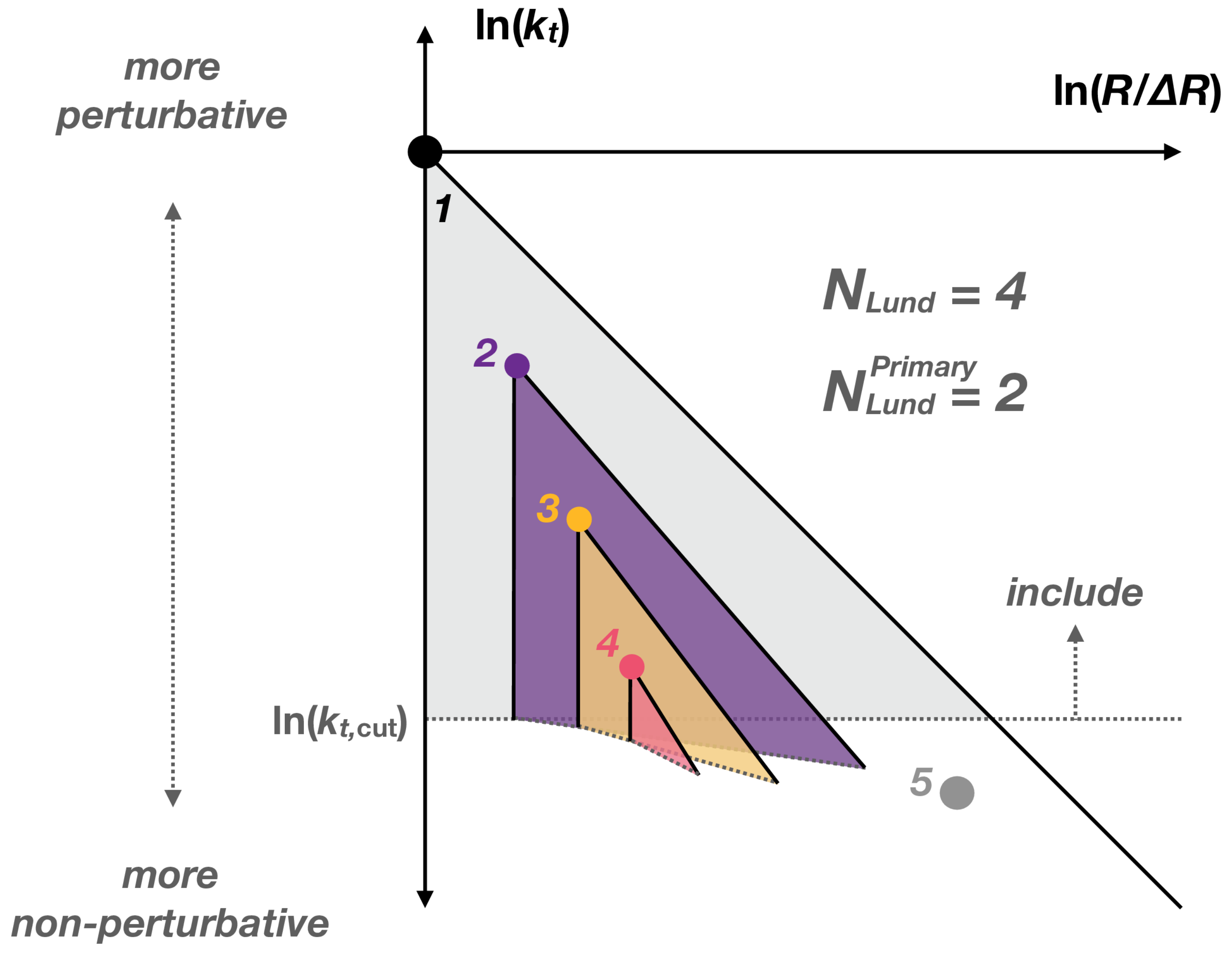

- The number of emissions in successive Lund planes with $k_t > k_{t,cut}$ is denoted by N_{Lund}
- The number of emissions on the hardest branch is denoted by $N_{Lund}^{Primary}$
- Constrains and tests Parton Shower Monte Carlo (PSMC) through double-soft splittings

Lund subjet multiplicity

ATLAS Collaboration

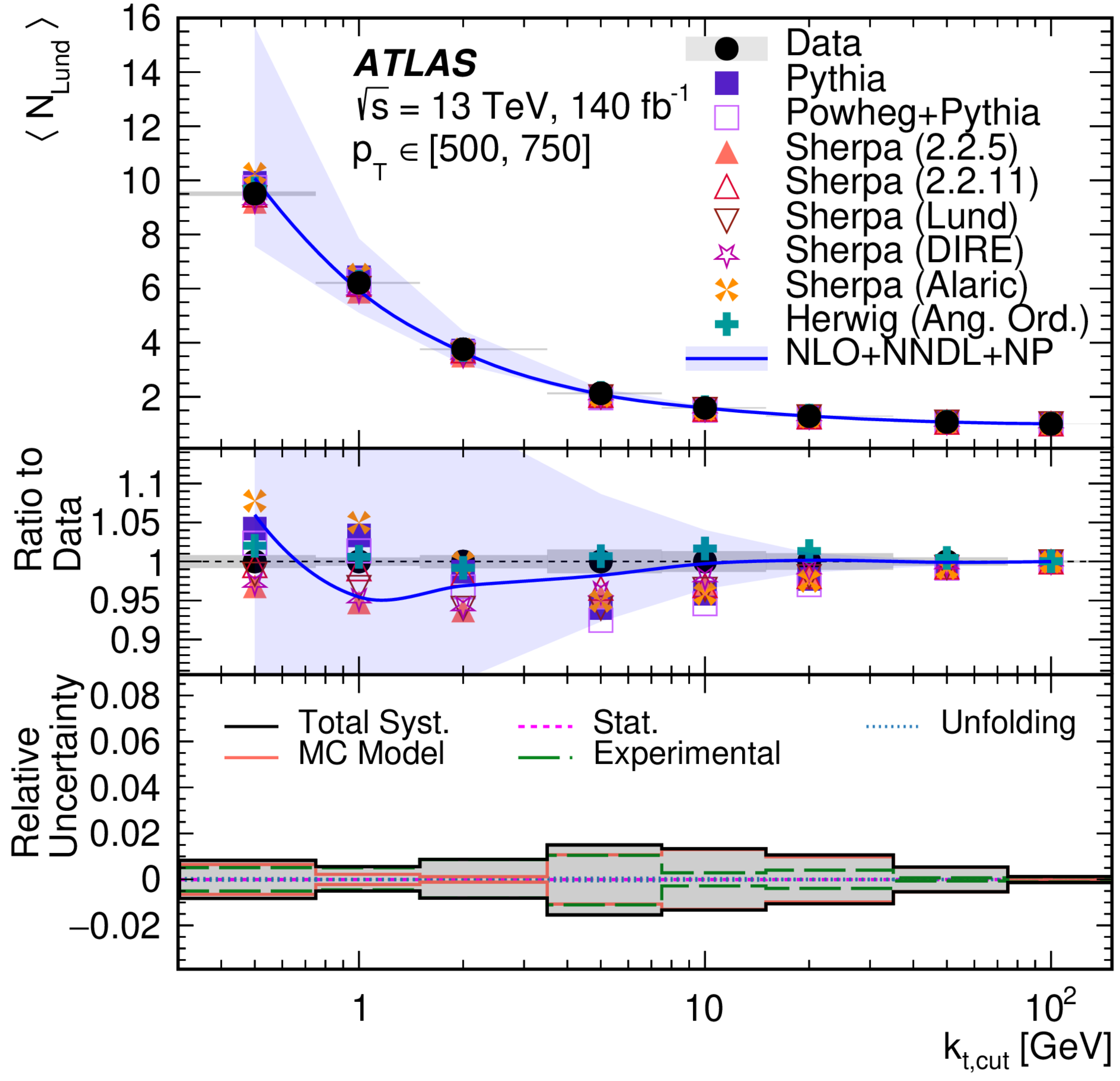

- Average subjet multiplicity $\langle N_{Lund} \rangle$ as a function of $k_{t,cut}$
- For higher jet p_T, the theoretical prediction begins to underestimate the average multiplicity

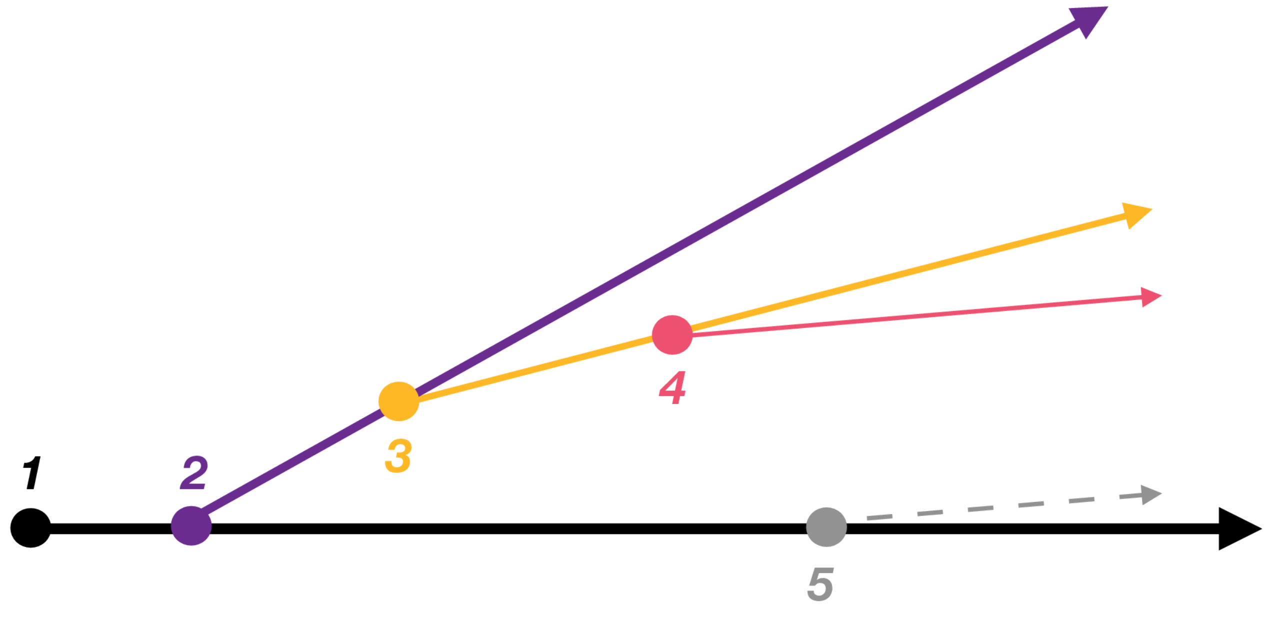

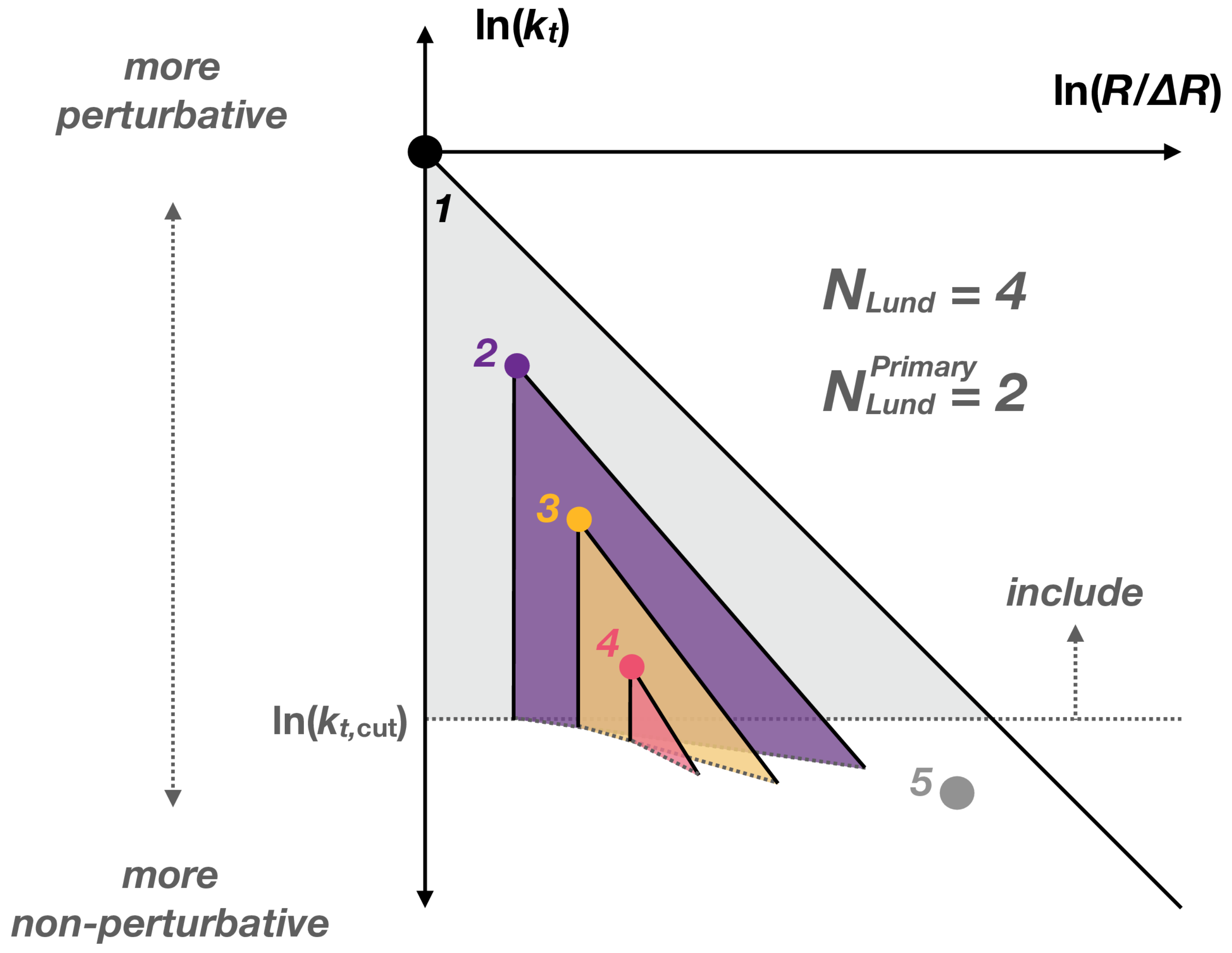

- The number of emissions in successive Lund planes with $k_t > k_{t,cut}$ is denoted by N_{Lund}
- The number of emissions on the hardest branch is denoted by $N_{Lund}^{Primary}$
- Constrains and tests Parton Shower Monte Carlo (PSMC) through double-soft splittings

Lund subjet multiplicity

ATLAS Collaboration

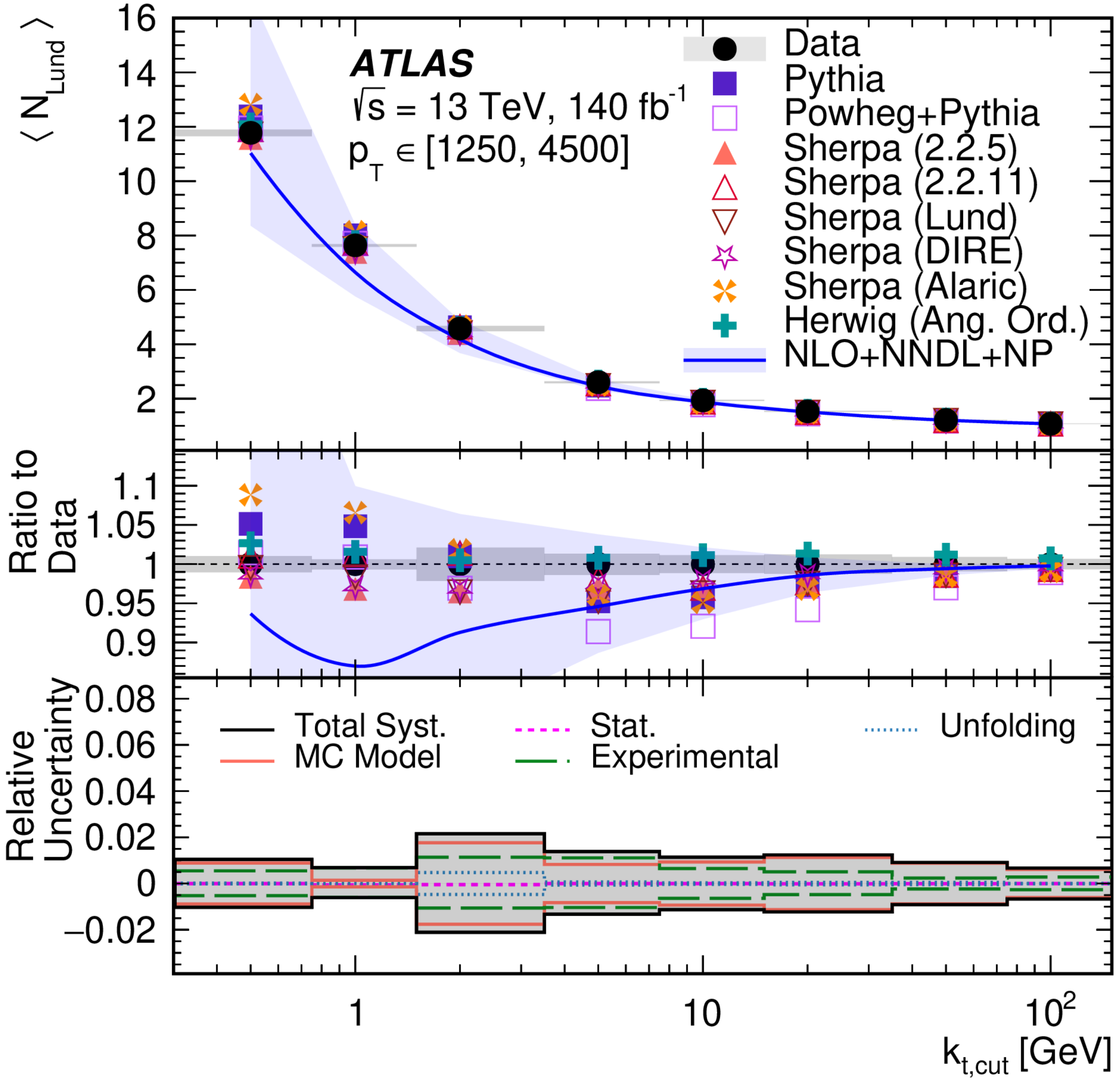

- Average subjet multiplicity $\langle N_{Lund} \rangle$ as a function of $k_{t,cut}$
- For even higher jet p_T, the theoretical prediction significantly underestimates the average multiplicity
- PSMC outperform the theoretical prediction at higher jet p_T

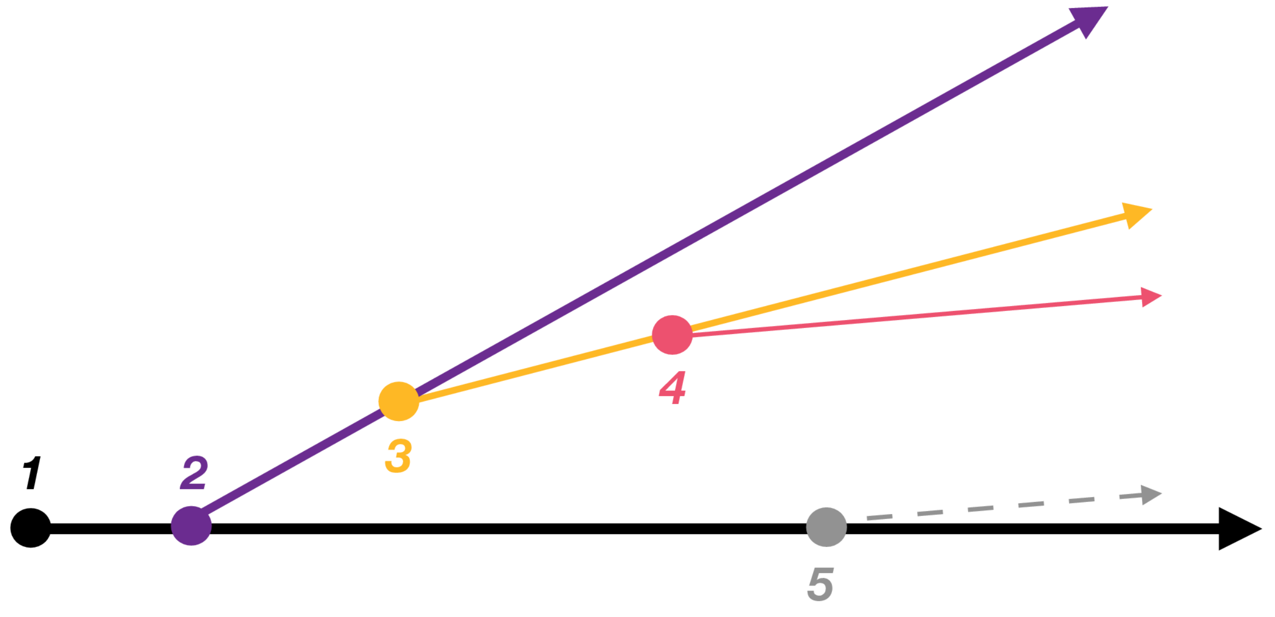

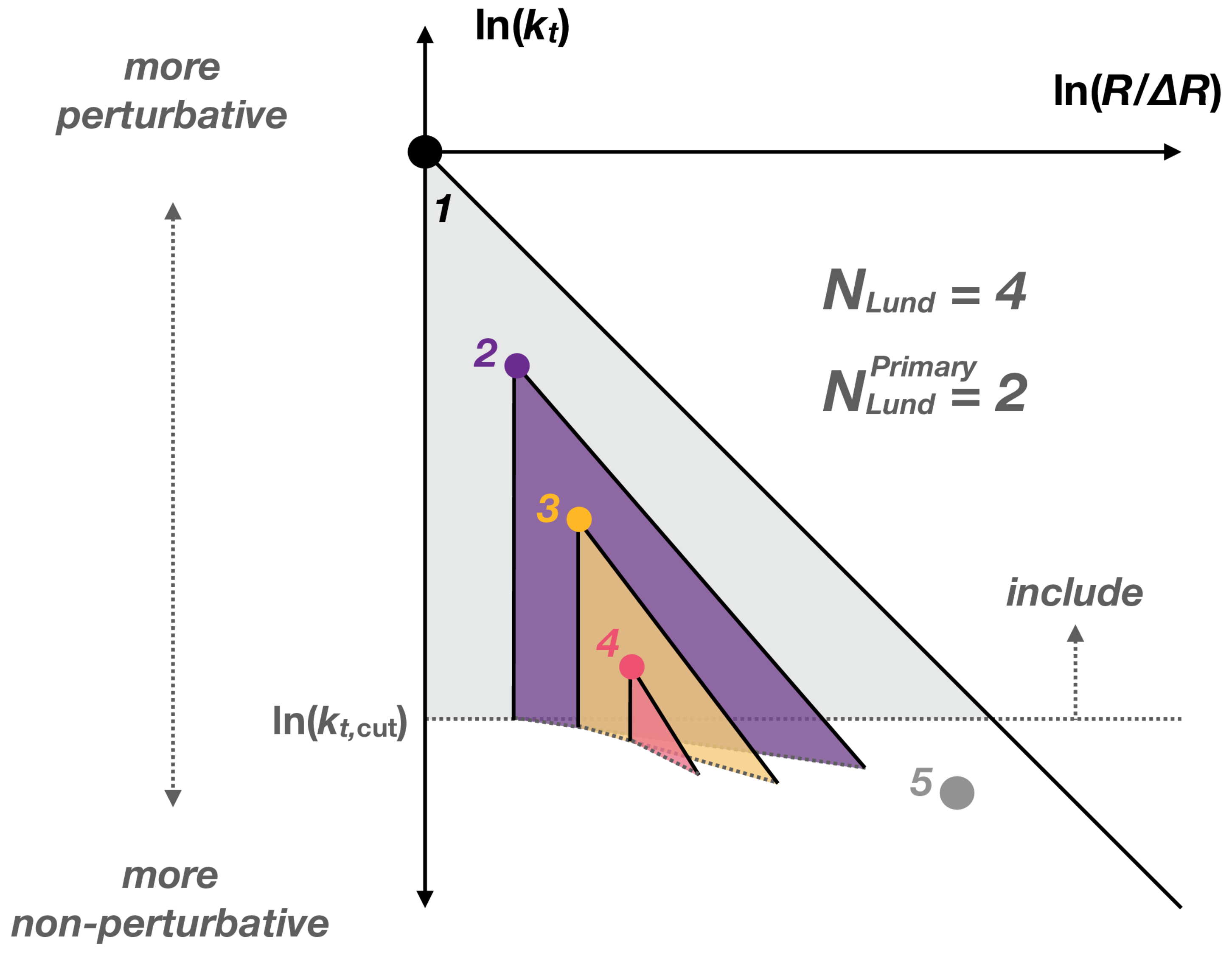

- The number of emissions in successive Lund planes with $k_t > k_{t,cut}$ is denoted by N_{Lund}
- The number of emissions on the hardest branch is denoted by $N_{Lund}^{Primary}$
- Constrains and tests Parton Shower Monte Carlo (PSMC) through double-soft splittings

Identified charged hadrons in jets

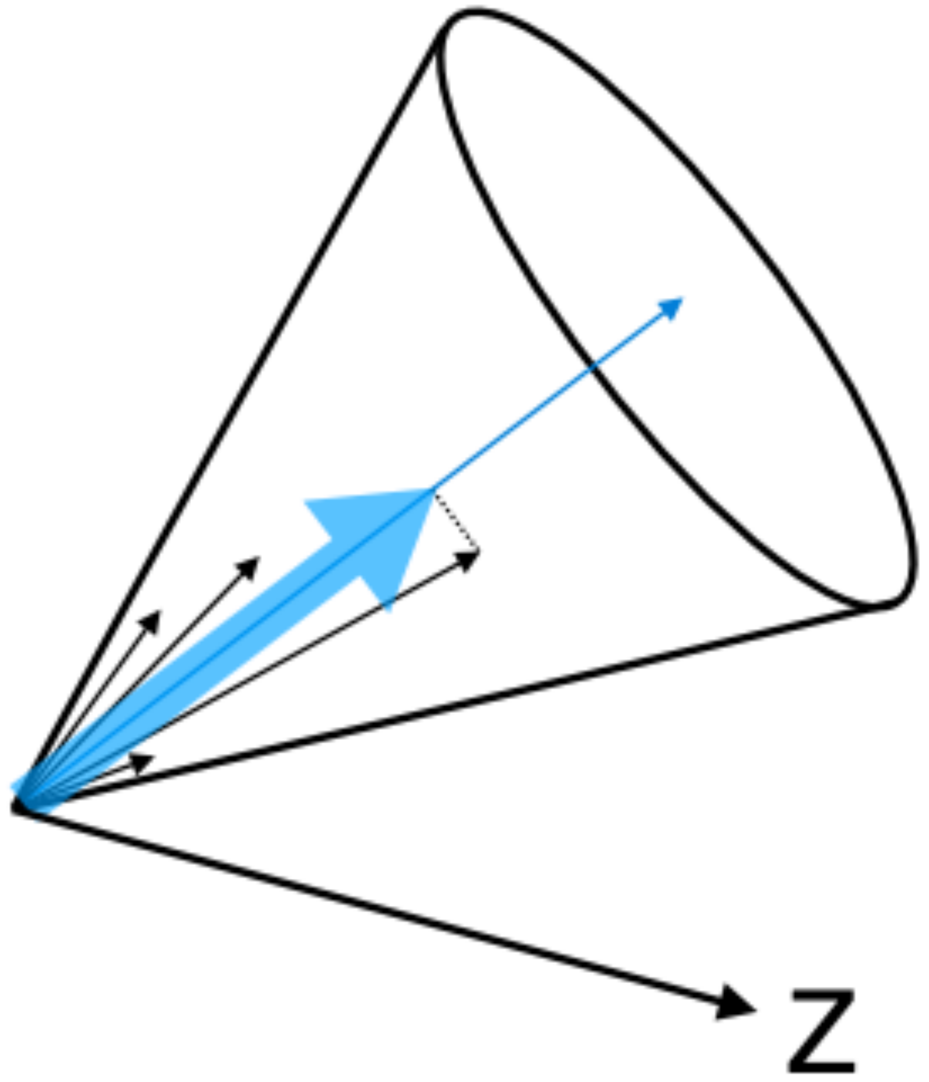

$$z = \frac{\mathbf{p}_{\mathrm{jet}} \cdot \mathbf{p}_{\mathrm{hadron}}}{|\mathbf{p}_{\mathrm{jet}}|^2}$$

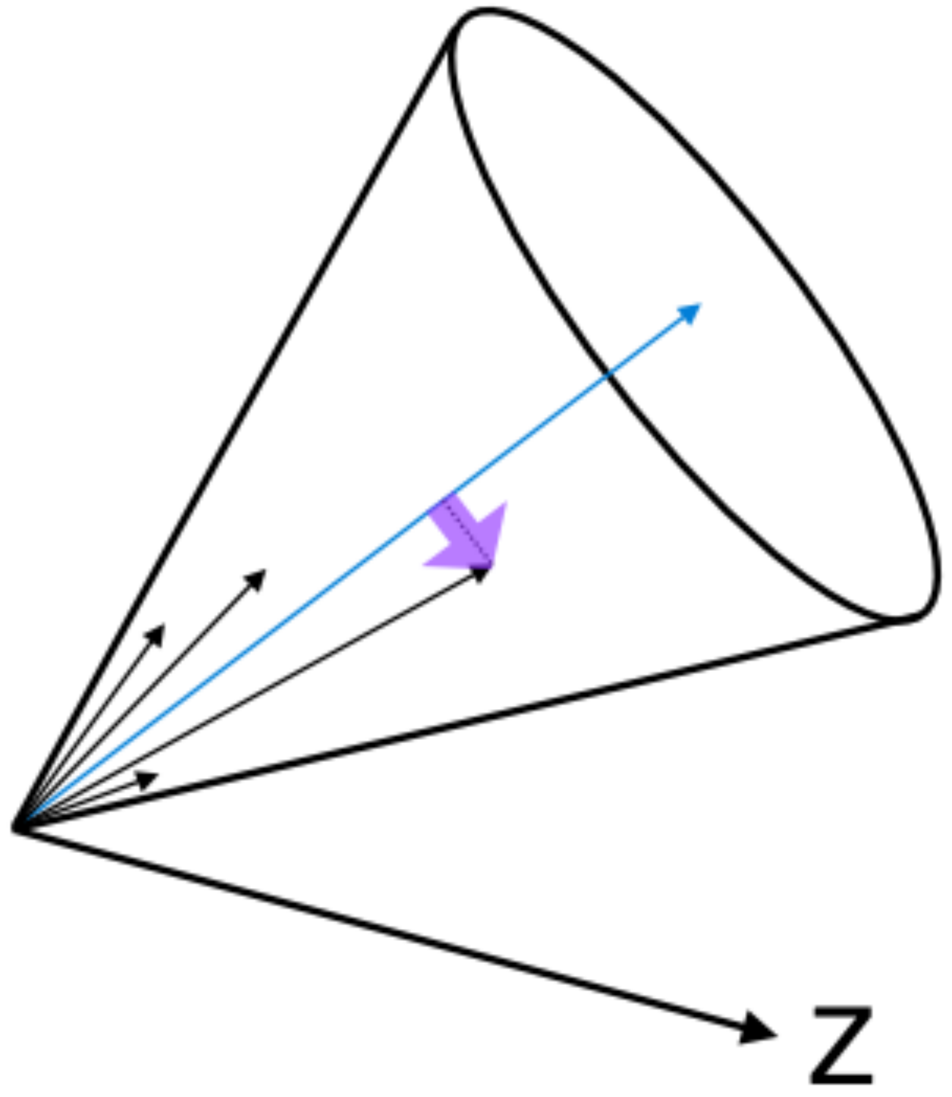

$$j_T = \frac{|\mathbf{p}_{\mathrm{jet}} \times \mathbf{p}_{\mathrm{hadron}}|}{|\mathbf{p}_{\mathrm{jet}}|}$$

Charged Hadrons in Z-tagged Jets

LHCb Collaboration

PHYSICAL REVIEW D 108, L031103 (2023)

Experimental Setup and Jet Reconstruction:

- $\sqrt{s} = 13$ **TeV (Run 2)**
- **Back-to-back Z + jet** $|\Delta\phi| > 2.75$
- **Full jet reconstruction, identified charged hadrons used**
- **Anti-kt jets with R = 0.5**
- $2.5 < \eta_{jet} < 4.0$
- $p_T^{jet} \in [20,100]$ **GeV**

Longitudinal Momentum Fraction

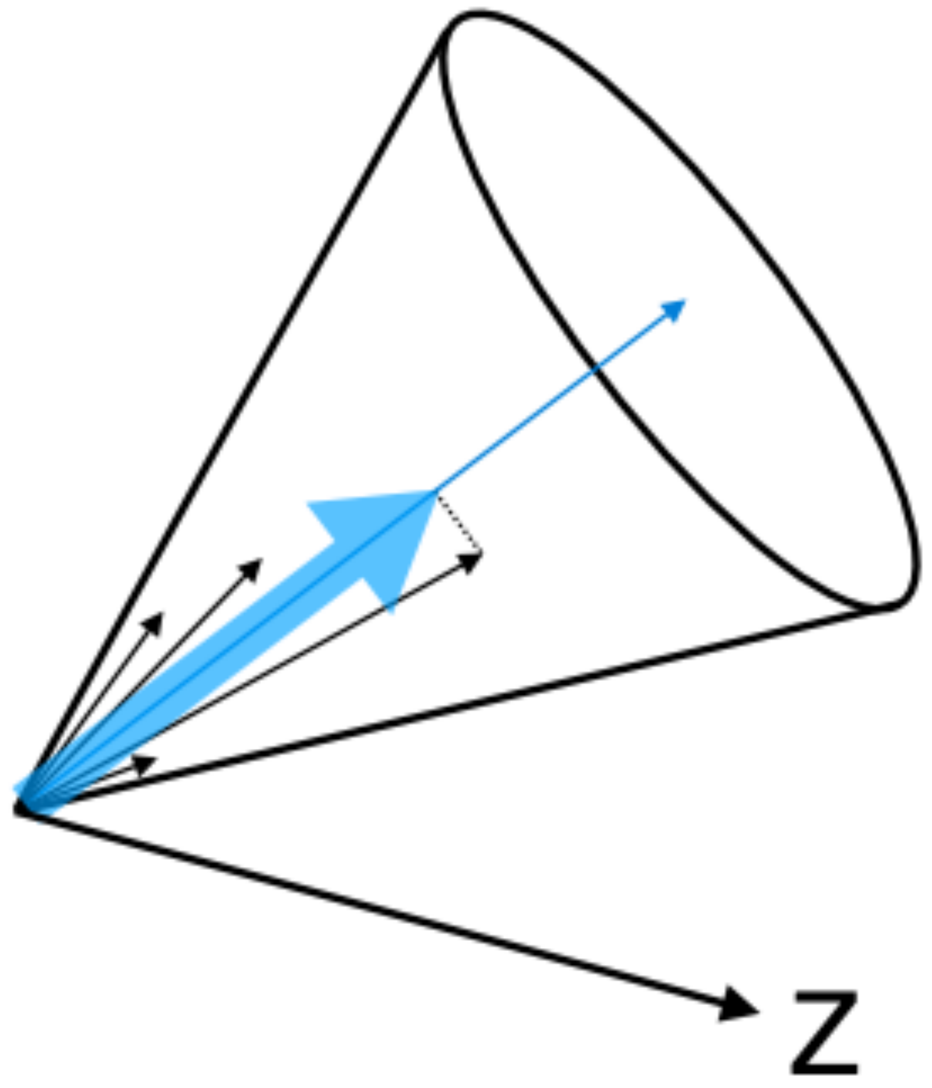

$$z = \frac{\mathbf{p}_{\mathrm{jet}} \cdot \mathbf{p}_{\mathrm{hadron}}}{|\mathbf{p}_{\mathrm{jet}}|^2}$$

Transverse Momentum

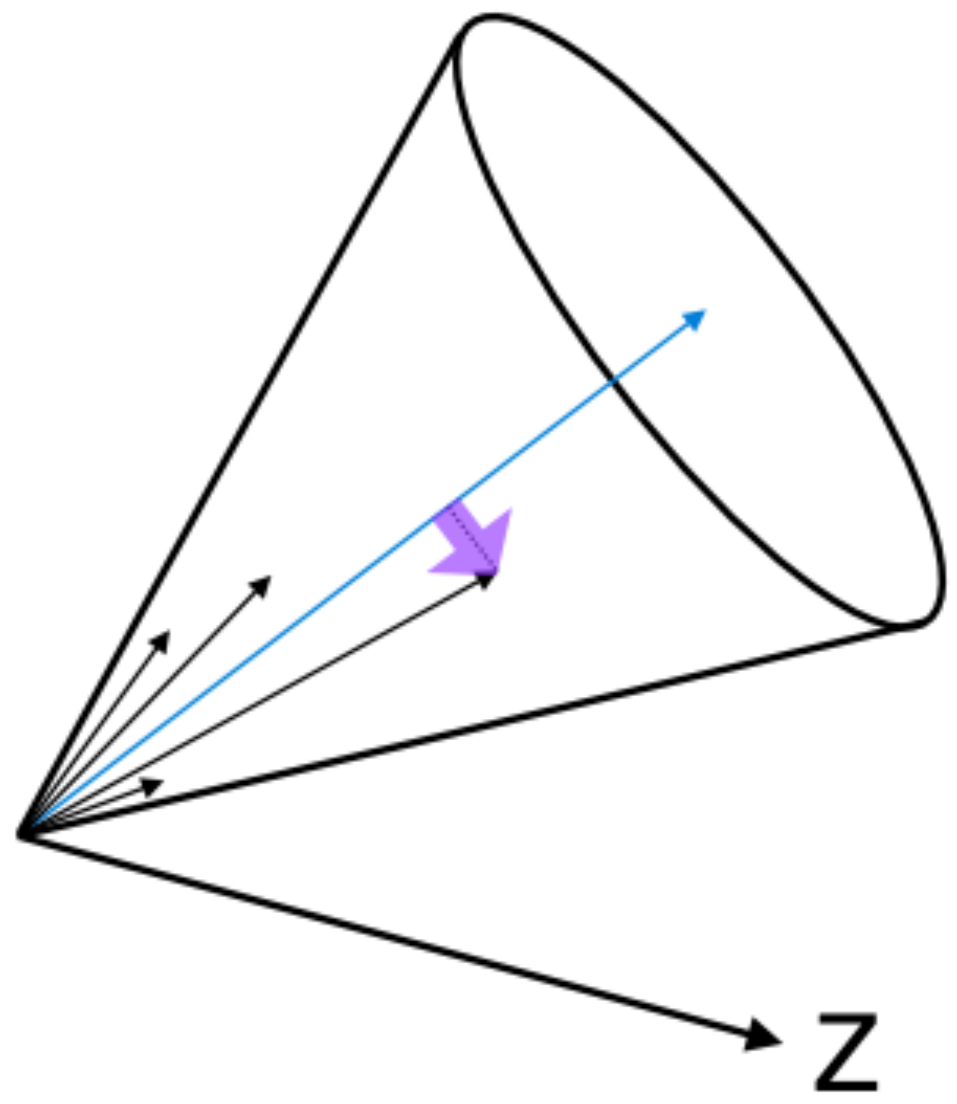

$$j_T = \frac{|\mathbf{p}_{\mathrm{jet}} \times \mathbf{p}_{\mathrm{hadron}}|}{|\mathbf{p}_{\mathrm{jet}}|}$$

Charged Hadrons in Z-tagged Jets

LHCb Collaboration

PHYSICAL REVIEW D 108, L031103 (2023)

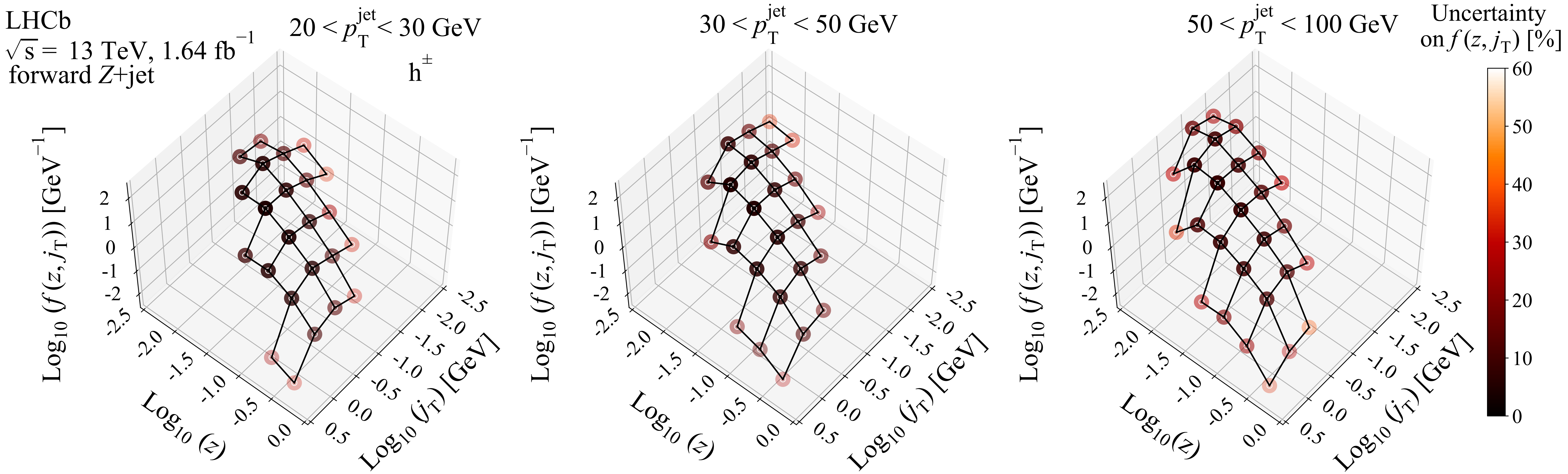

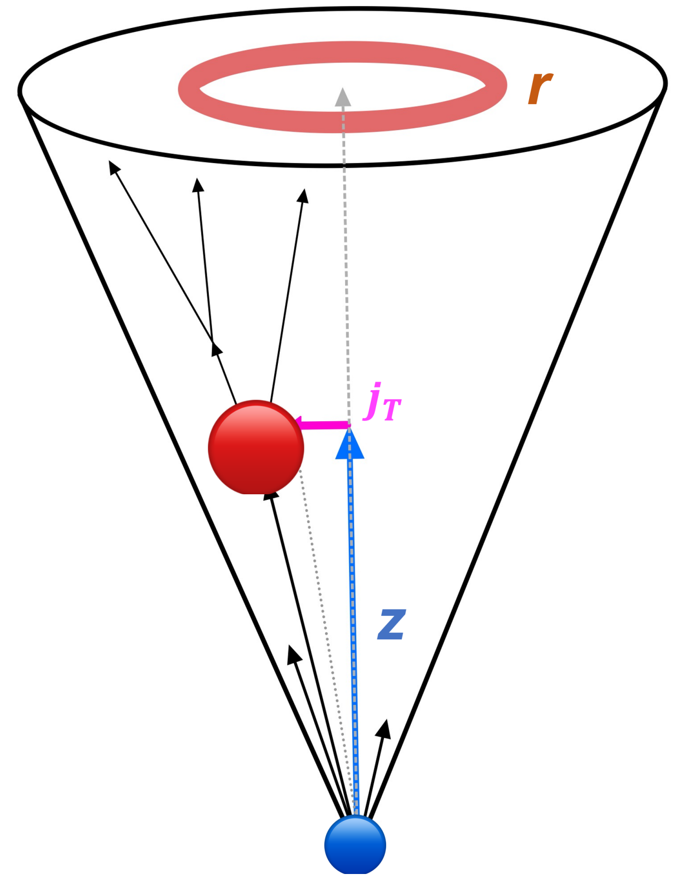

- Hadrons with large z tend to have larger j_T
- Centroid of harder jets moves towards smaller z (softer particle production) and larger j_T (wider jet)
- j_T increases with increasing jet p_T at fixed z. This is consistent with Markov chain fragmentation models (string or cluster models)

Charged Hadrons in Z-tagged Jets

LHCb Collaboration

PHYSICAL REVIEW D 108, L031103 (2023)

arxiv:2208.11691 (accepted by PRD Lett.)

- Charged hadrons are predominantly pions due to their low mass and the flavor content of the initial-state quark

- Heavier hadrons require larger z to form. Delayed scaling behavior for heavier hadrons.

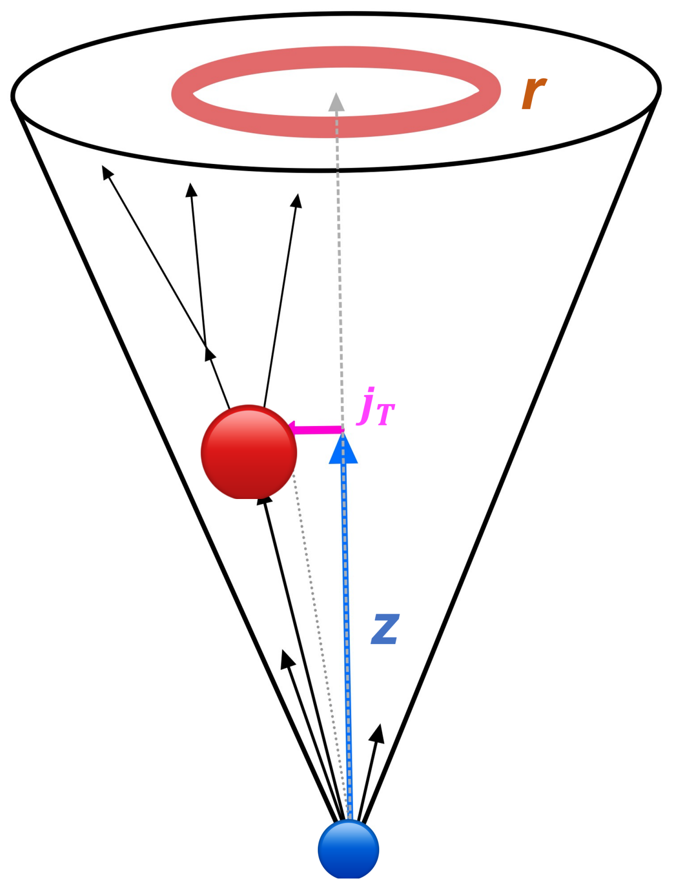

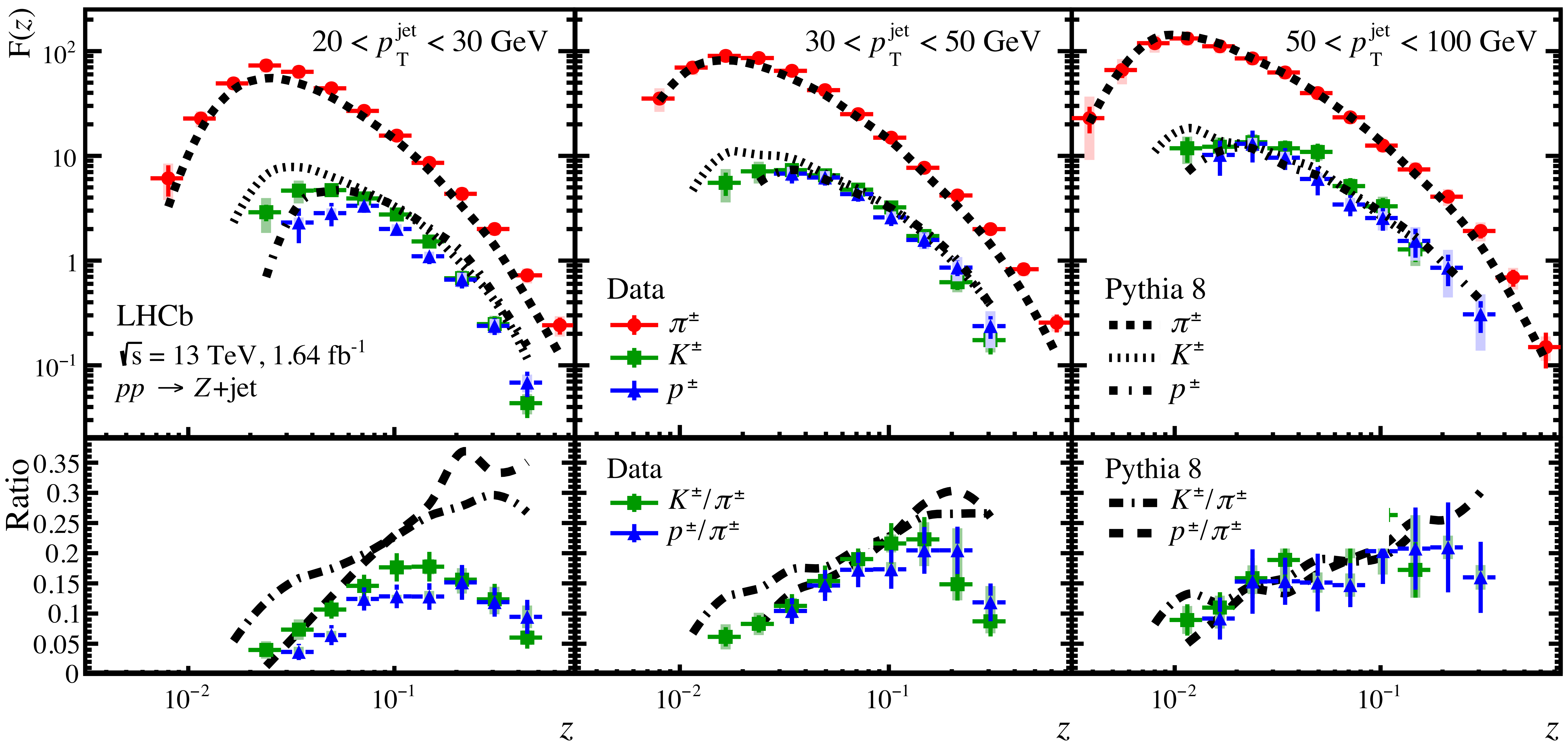

In the lowest jet pT interval:

- Pythia8 overestimates $K^\pm$ and $p^\pm$ production relative to $\pi^\pm$

- Proton production suppressed relative to Kaon at low z

Tagging Higgs events with Machine Learning

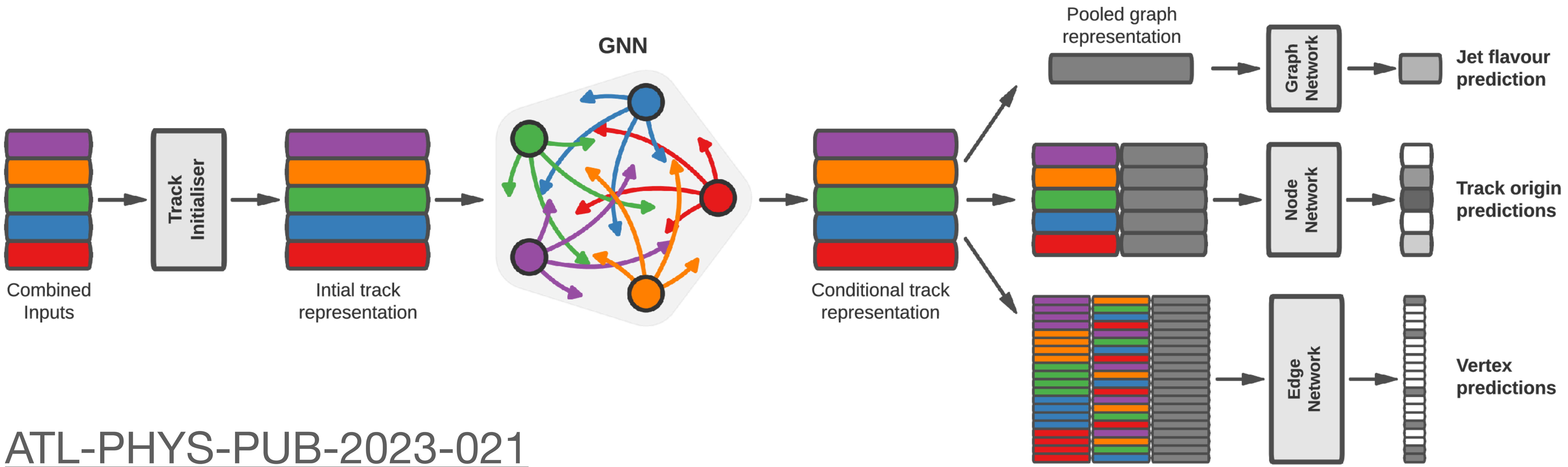

ATL-PHYS-PUB-2023-021

Transformer NN for Boosted Higgs Bosons decaying into $b\bar{b}$ and $c\bar{c}$

ATLAS Collaboration

ATL-PHYS-PUB-2023-021

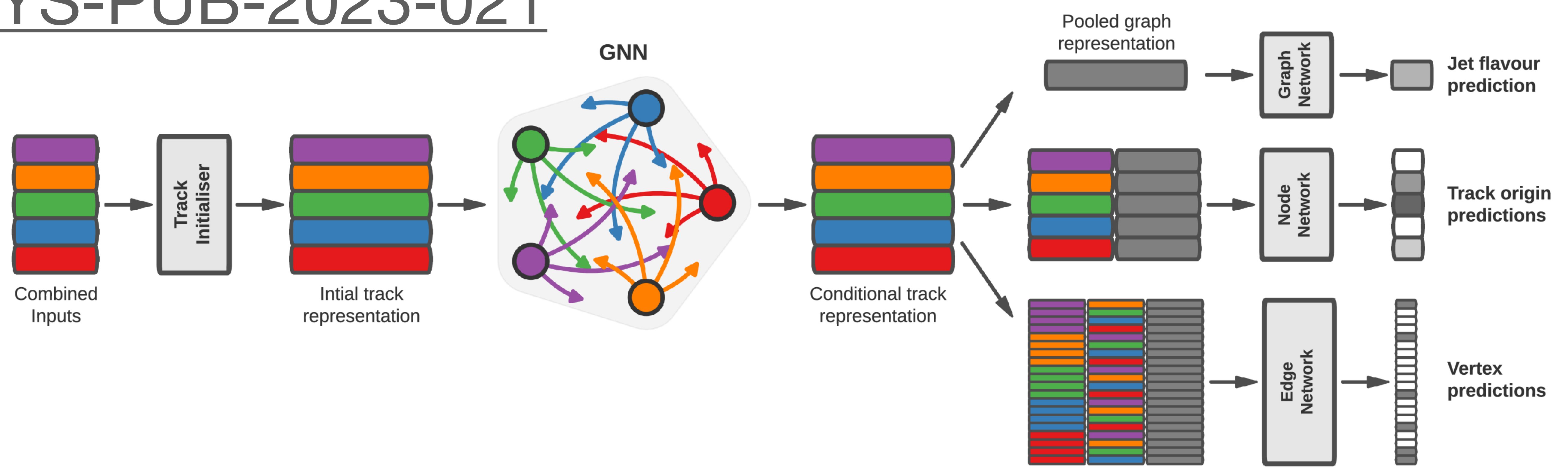

- Tagging is important for Higgs and BSM searches
- Transformer Neural Network (GN2X) based on earlier Graph Neural Network (GN1)
- Trained and validated on simulation using
  - jet p_T, η, m
  - 20 variables for each track (up to 100 tracks)
- Outputs:
  - Jet flavor
  - Track origin
  - Vertex compatibility

Track Input	Description
q/p	Track charge divided by momentum (measure of curvature)
$\mathrm{d}\eta$	Pseudorapidity of track relative to the large-R jet η
$\mathrm{d}\phi$	Azimuthal angle of the track, relative to the large-R jet ϕ
d_0	Closest distance from track to primary vertex (PV) in the transverse plane
$z_0 \sin\theta$	Closest distance from track to PV in the longitudinal plane
$\sigma(q/p)$	Uncertainty on q/p
$\sigma(\theta)$	Uncertainty on track polar angle θ
$\sigma(\phi)$	Uncertainty on track azimuthal angle ϕ
$s(d_0)$	Lifetime signed transverse IP significance
$s(z_0 \sin\theta)$	Lifetime signed longitudinal IP significance
nPixHits	Number of pixel hits
nSCTHits	Number of SCT hits
nIBLHits	Number of IBL hits
nBLHits	Number of B-layer hits
nIBLShared	Number of shared IBL hits
nIBLSplit	Number of split IBL hits
nPixShared	Number of shared pixel hits
nPixSplit	Number of split pixel hits
nSCTShared	Number of shared SCT hits
subjetIndex	Integer label of which subjet track is associated to (GN2X + Subjets only)

Transformer NN for Boosted Higgs Bosons decaying into $b\bar{b}$ and $c\bar{c}$

ATLAS Collaboration

ATL-PHYS-PUB-2023-021

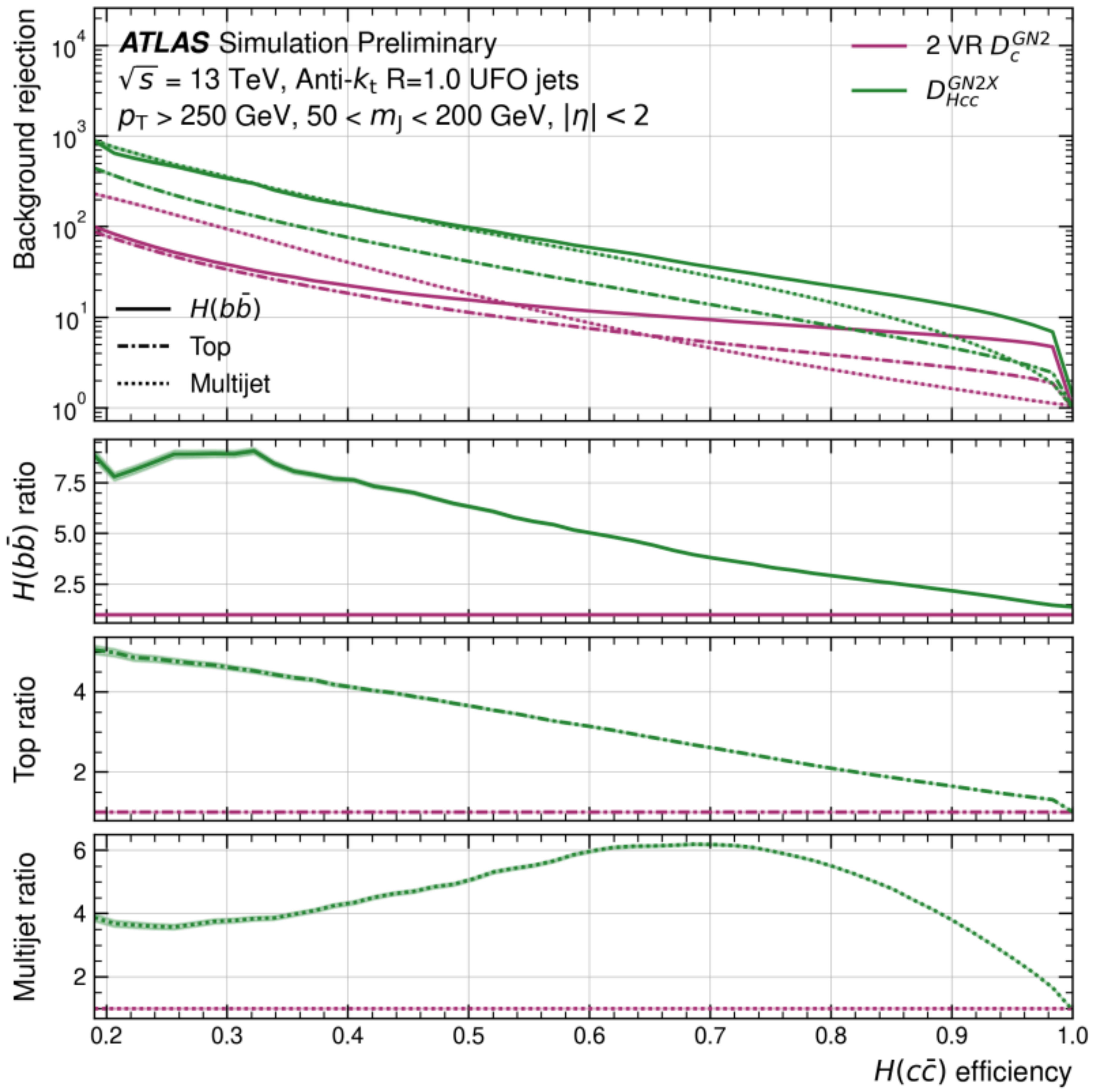

$H(c\bar{c})$ **efficiency**

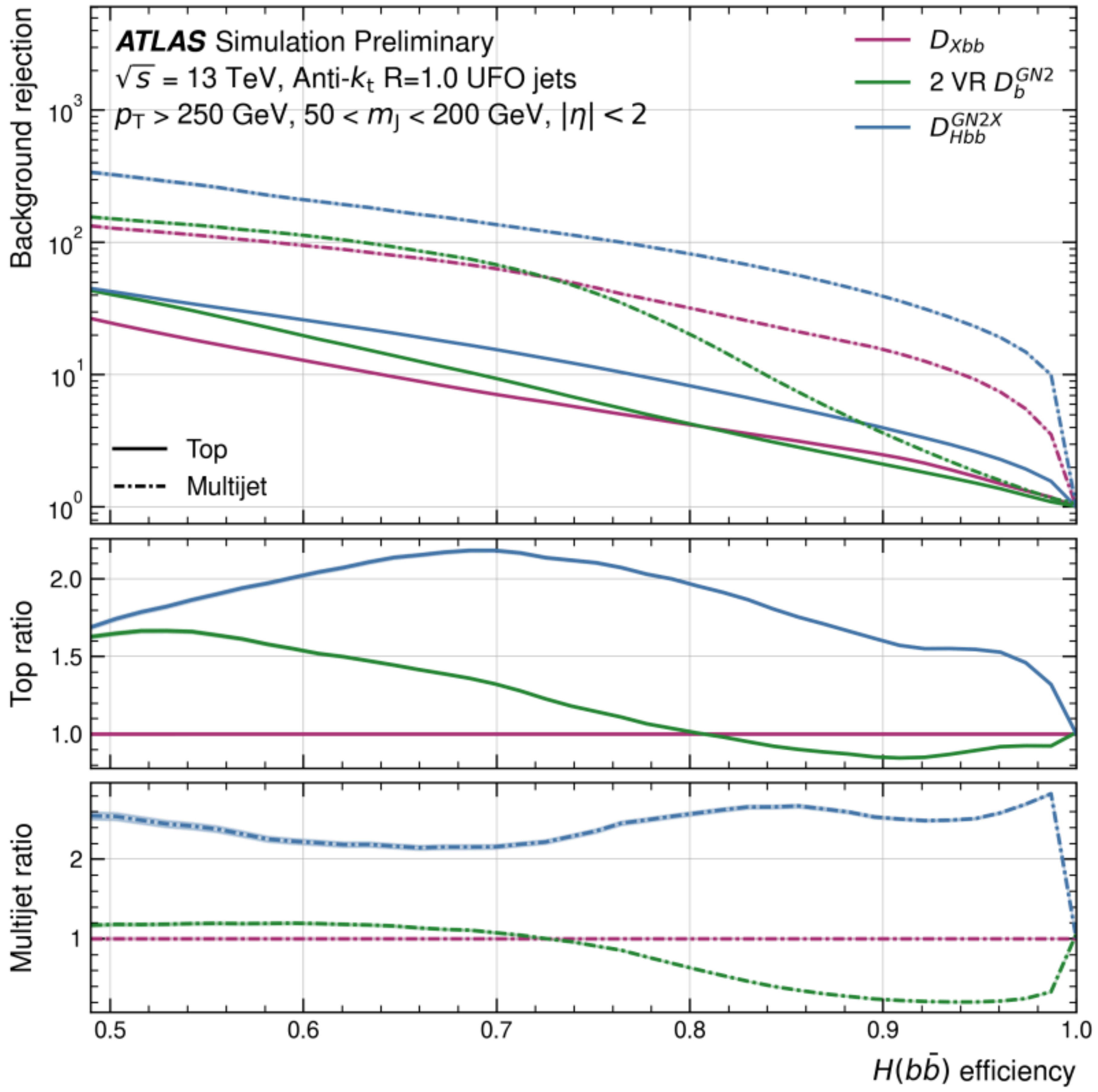

$H(b\bar{b})$ **efficiency**

- For 50% $H(b\bar{b})$ signal efficiency, 1.6x better rejection of top jets and 2.5x better rejection of QCD jets compared to current Xbb tagger
- First of its kind $H(c\bar{c})$ tagger at ATLAS
- For 50% $H(c\bar{c})$ signal efficiency, 3x better rejection of top jets, and 5x better rejection of QCD jets compared to 2-tag variable radius track-jet

Jet Substructure: opening the QCD world

Heavy quark splitting functions

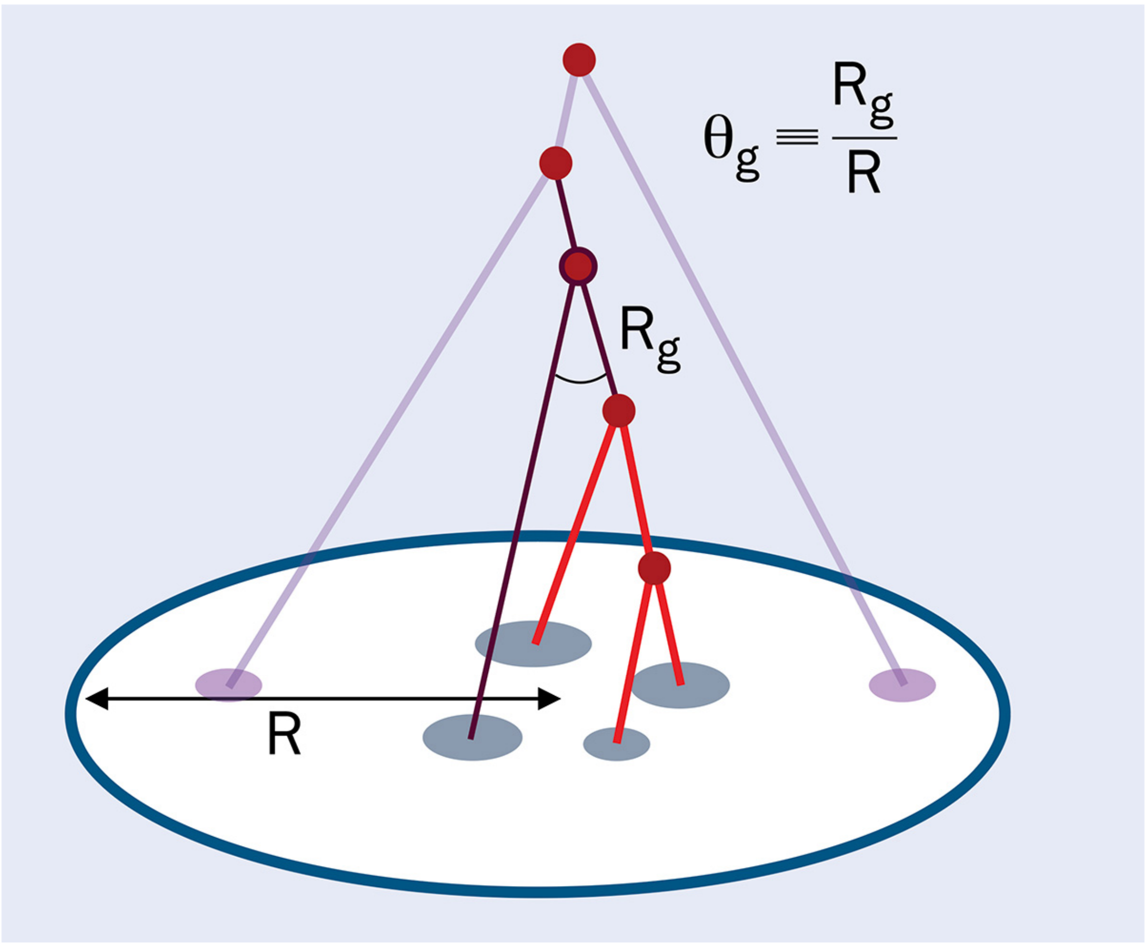

Credit: CERN

Fragmentation of hadrons

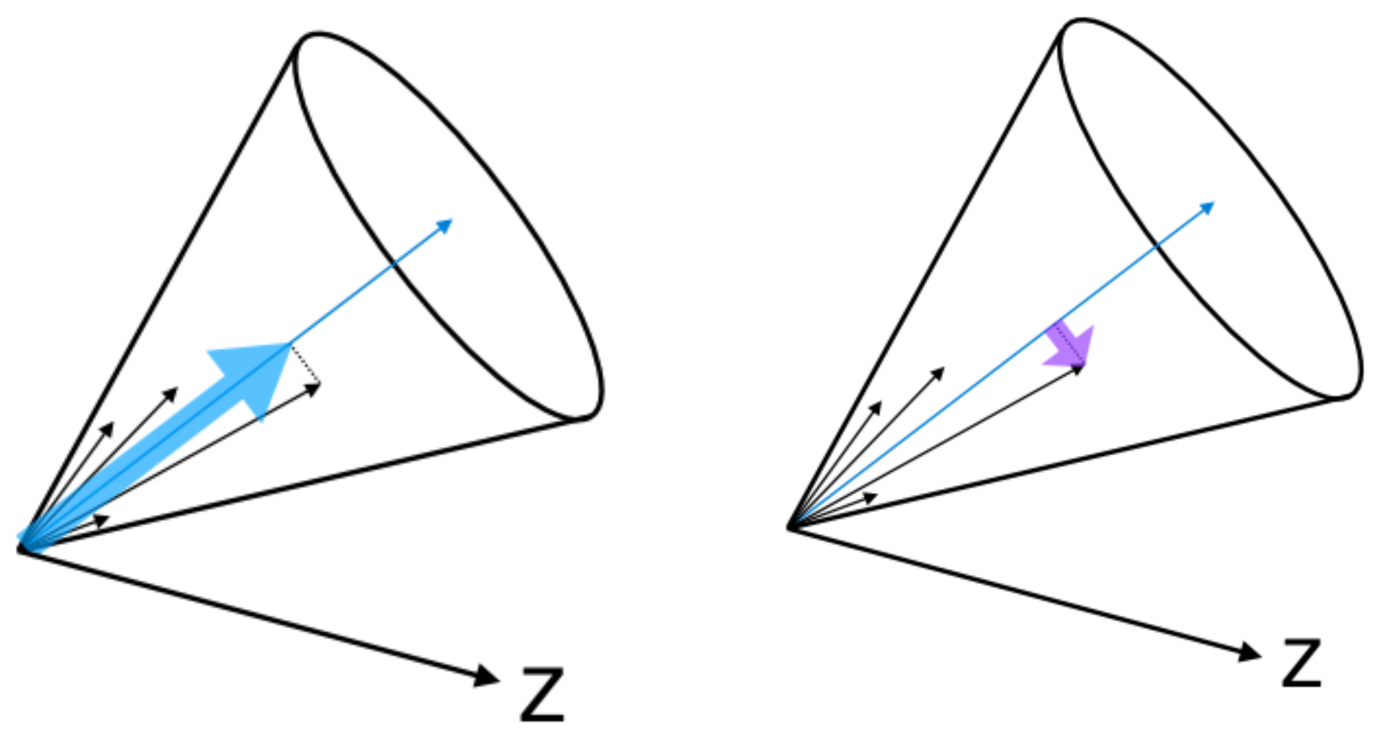

$$z = \frac{\mathbf{p}_{\text{jet}} \cdot \mathbf{p}_{\text{hadron}}}{|\mathbf{p}_{\text{jet}}|^2} \qquad j_T = \frac{|\mathbf{p}_{\text{jet}} \times \mathbf{p}_{\text{hadron}}|}{|\mathbf{p}_{\text{jet}}|}$$

Energy Correlators

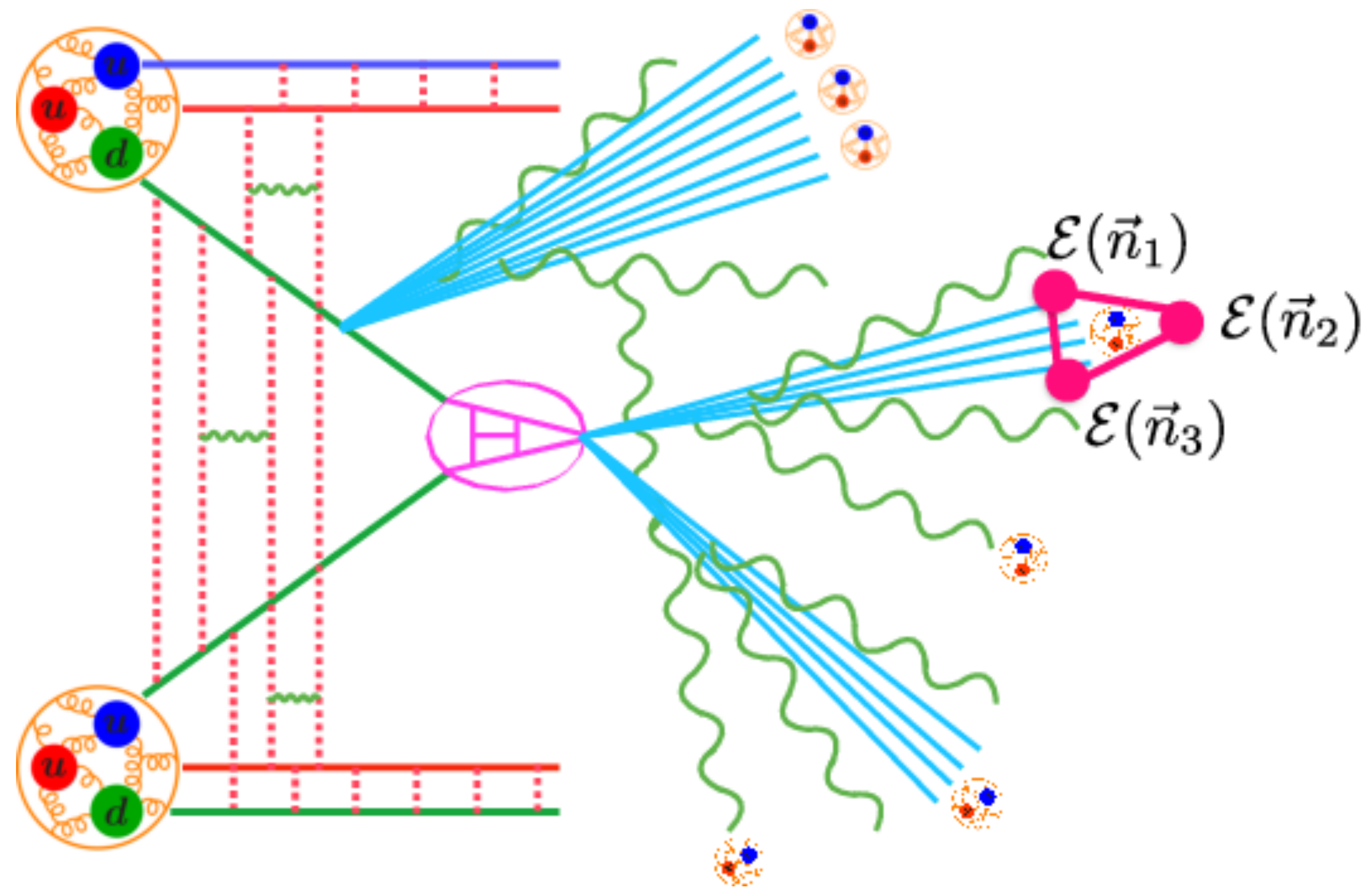

H Chen, I Moult, XY Zhang, HX Zhu , 2020

Boosted heavy-flavor jets

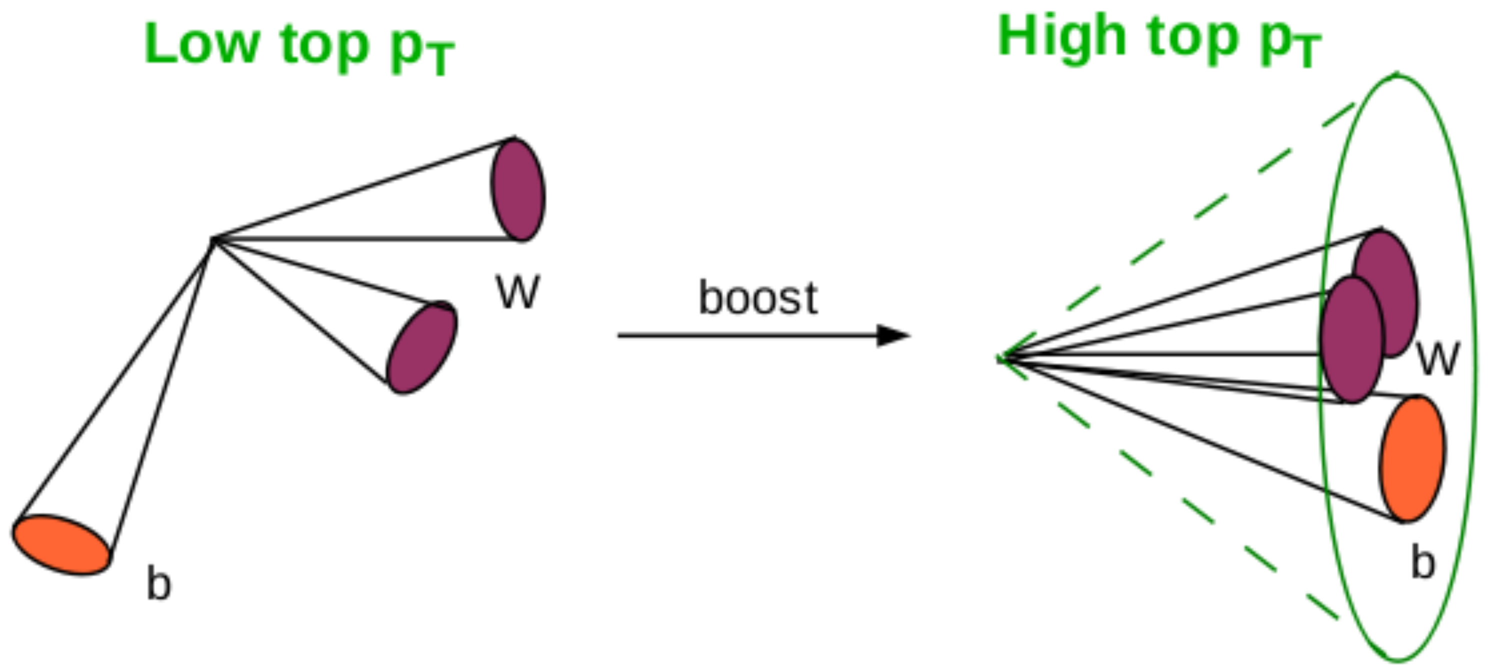

Credit: Matthew Anthony

Jet axes from underlying substructure

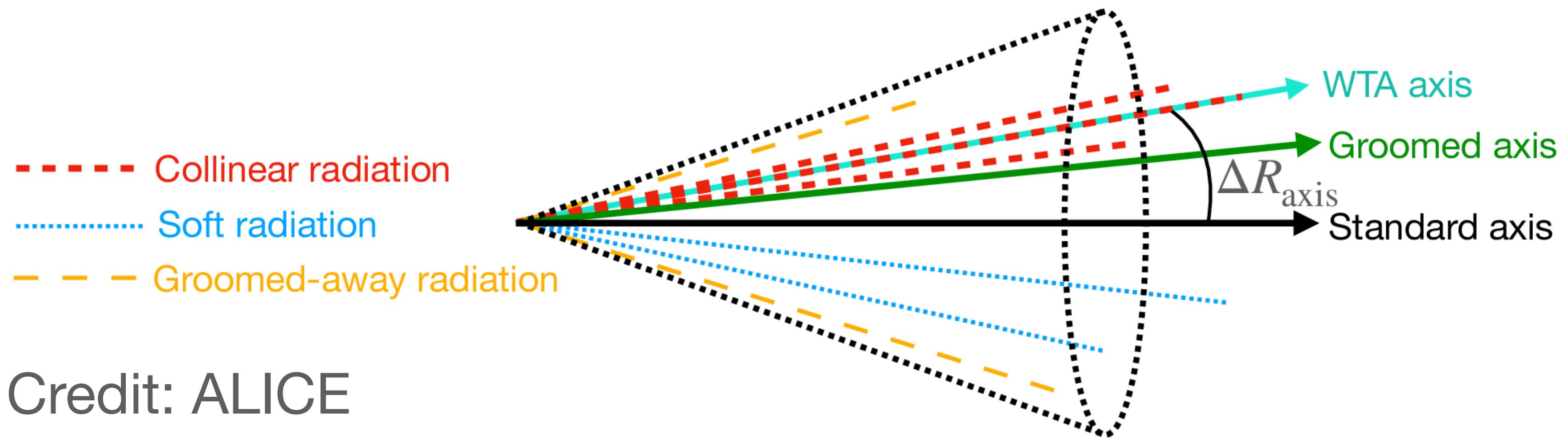

Credit: ALICE

Phase space structure: Lund planes

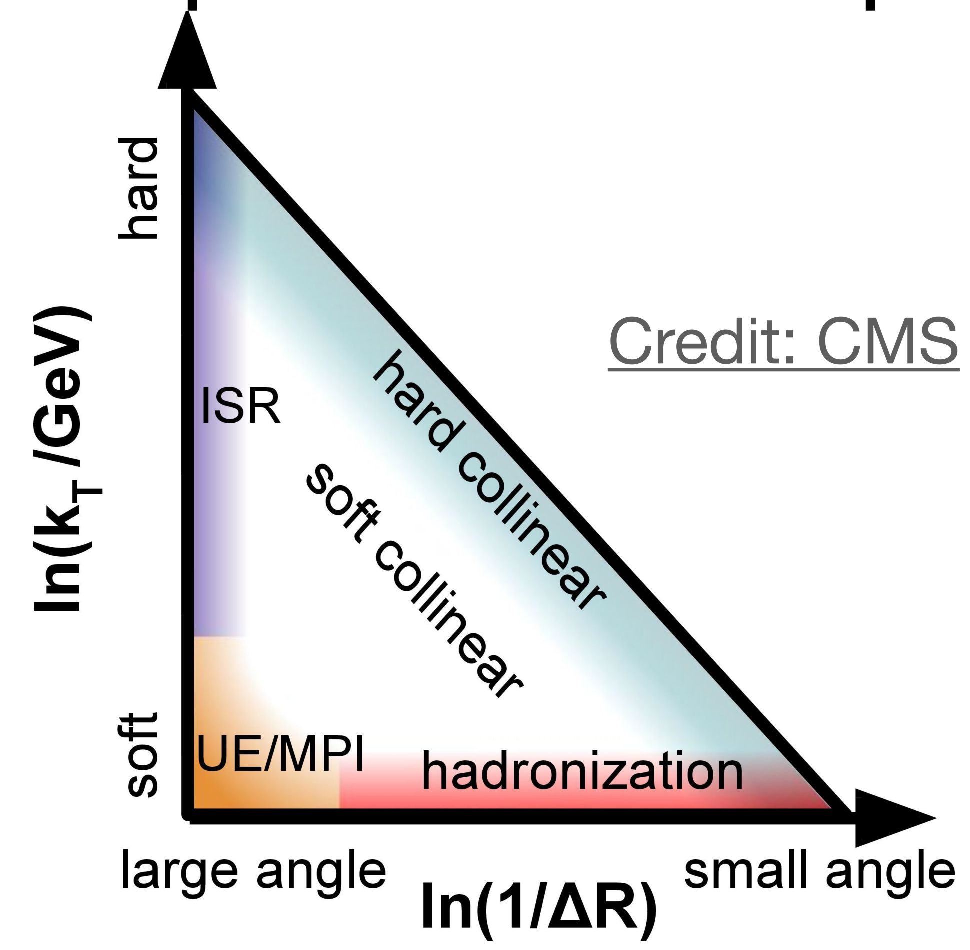

Credit: CMS

References

- ALICE: Measurements of groomed-jet substructure of charm jets tagged by D0 mesons in proton–proton collisions at $\sqrt{s}$ = 13 TeV (https://arxiv.org/abs/2208.04857)
- ALICE: Measurement of the angle between jet axes in pp collisions at $\sqrt{s}$ = 5.02 TeV (https://arxiv.org/pdf/2211.08928)
- ATLAS: Measurement of jet substructure in boosted $t\bar{t}$ events with the ATLAS detector using 140 fb−1 of 13 TeV pp collisions (https://arxiv.org/pdf/2312.03797)
- ATLAS: Transformer Neural Networks for Identifying Boosted Higgs Bosons decaying into $b\bar{b}$ and $c\bar{c}$ in ATLAS (https://cds.cern.ch/record/2866601/files/ATL-PHYS-PUB-2023-021.pdf)
- CMS: Measurement of the primary Lund jet plane density in proton-proton collisions at $\sqrt{s}$ = 13 TeV (https://arxiv.org/pdf/2312.16343)
- CMS: Measurement of energy correlators inside jets and determination of the strong coupling αS (mZ) (https://arxiv.org/pdf/2402.13864)
- CMS: Performance of heavy-flavour jet identification in boosted topologies in proton-proton collisions at $\sqrt{s}$ = 13 TeV (https://cds.cern.ch/record/2866276/files/BTV-22-001-pas.pdf)
- LHCb: Multidifferential study of identified charged hadron distributions in Z-tagged jets in proton-proton collisions at $\sqrt{s}$ = 13 TeV (https://journals.aps.org/prd/pdf/10.1103/PhysRevD.108.L031103)

Backup Slides

Energy Correlators

CMS Collaboration

https://arxiv.org/abs/2402.13864

Experimental Setup and Jet Reconstruction:

- $\sqrt{s} = 13$ **TeV (Run 2)**
- **Back-to-back dijets** $|\Delta\phi| > 2$
- **Full jet reconstruction, tracks and neutrals used**
- **Anti-kt jets with R = 0.4**
- $|\eta_{jet}| < 2.1$
- $p_T^{jet} \in [97,1784]$ **GeV**
- **E2C and E3C are measured from independent samples**

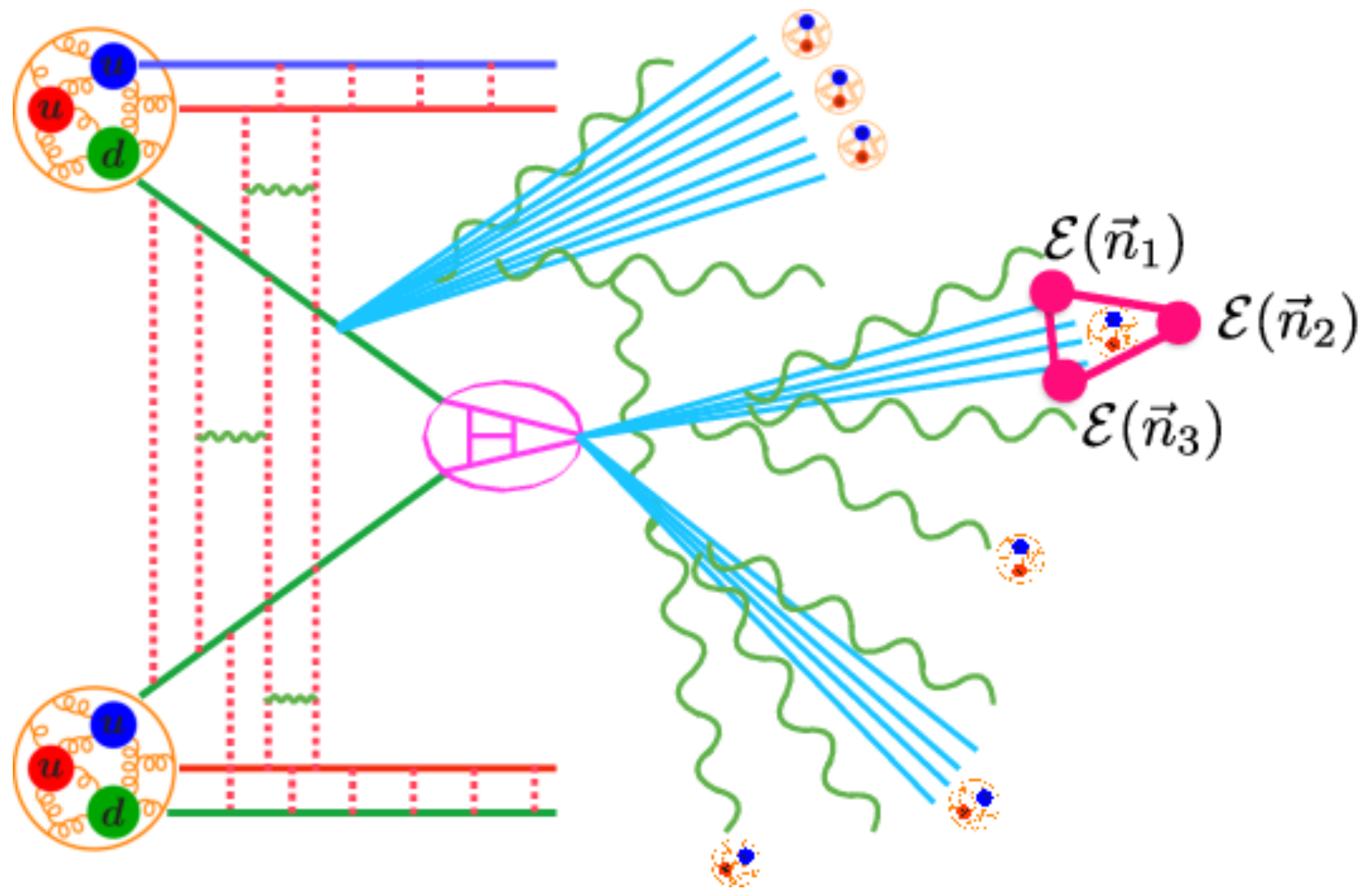

H Chen, I Moult, XY Zhang, HX Zhu , 2020

$$E2C = \frac{d\sigma^{[2]}}{dx_L} = \sum_{i,j}^{n} \int d\sigma \frac{E_i E_j}{E^2} \delta(x_L - \Delta R_{i,j}),$$

$$E3C = \frac{d\sigma^{[3]}}{dx_L} = \sum_{i,j,k}^{n} \int d\sigma \frac{E_i E_j E_k}{E^3} \delta(x_L - \max(\Delta R_{i,j}, \Delta R_{i,k}, \Delta R_{j,k}))$$

- Calculate the angular distance between all pairs of particles ΔR
- Weight each distance by the energies of the two daughters $E_i E_j$
- For E3C, choose the maximum ΔR and weight by $E_i E_j E_k$

Energy Correlators

CMS Collaboration

https://arxiv.org/abs/2402.13864

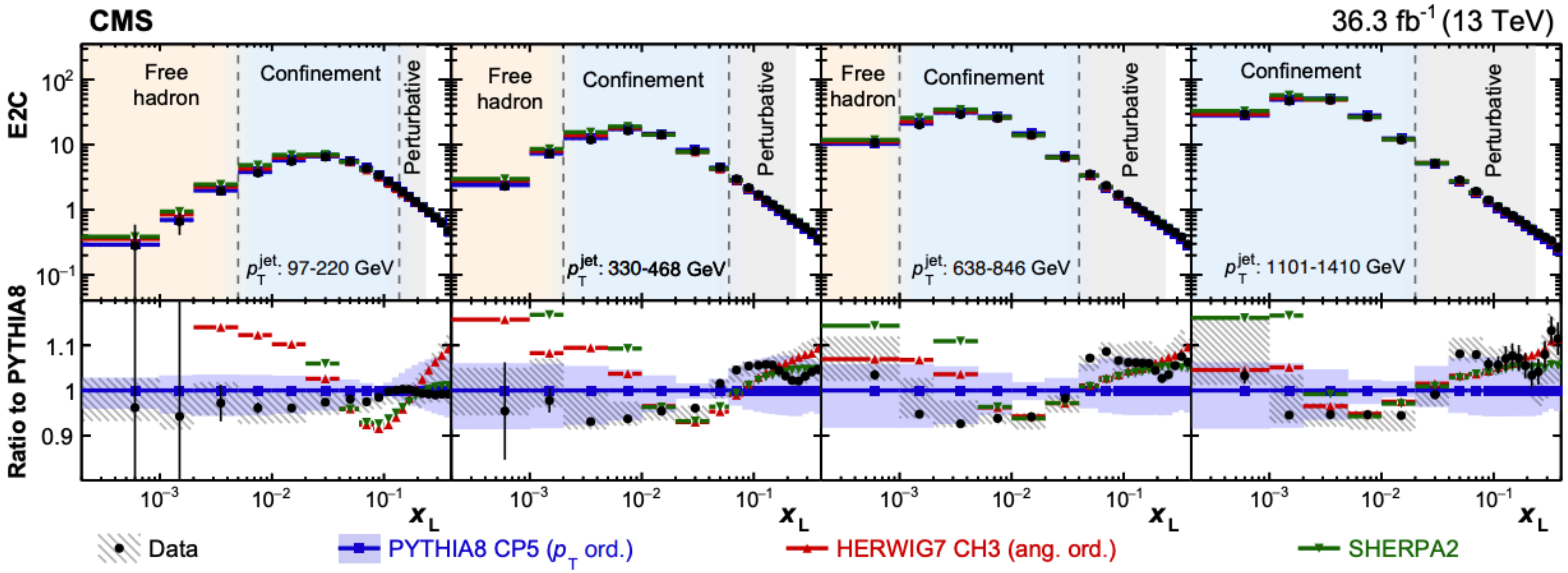

- Clear transition between perturbative emissions, confinement, and free hadron phases
- Pythia8 describes the data quite well
- With larger jet p_T, the confinement region shifts to lower x_L in accordance with transition energy scale $Q = ap_T x_L$ where a is close to 20 GeV from simulation studies.

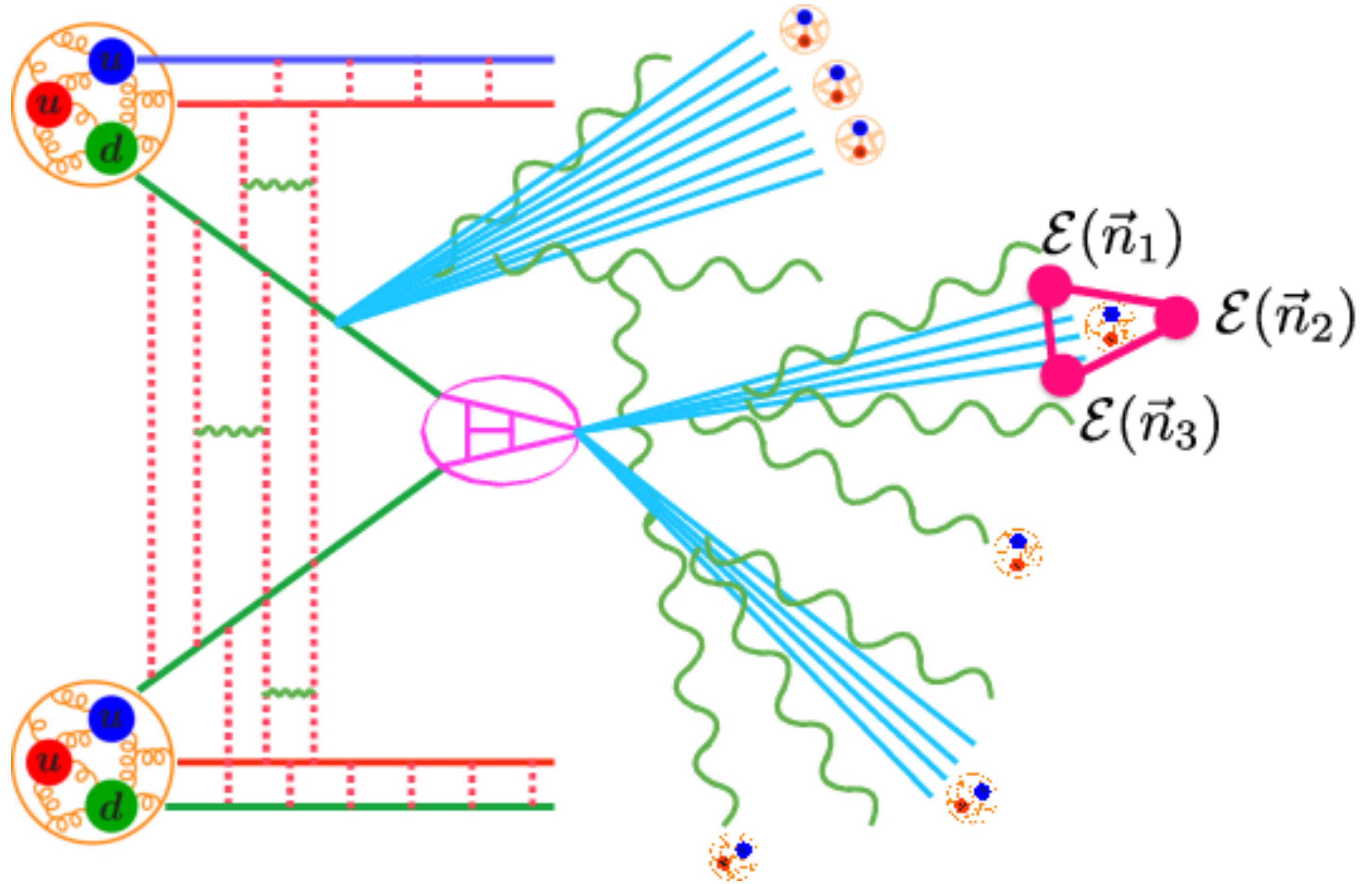

H Chen, I Moult, XY Zhang, HX Zhu , 2020

$$E2C = \frac{d\sigma^{[2]}}{dx_L} = \sum_{i,j}^{n} \int d\sigma \frac{E_i E_j}{E^2} \delta(x_L - \Delta R_{i,j}),$$

$$E3C = \frac{d\sigma^{[3]}}{dx_L} = \sum_{i,j,k}^{n} \int d\sigma \frac{E_i E_j E_k}{E^3} \delta(x_L - \max(\Delta R_{i,j}, \Delta R_{i,k}, \Delta R_{j,k}))$$

- Calculate the angular distance between all pairs of particles ΔR
- Weight each distance by the energies of the two daughters $E_i E_j$
- For E3C, choose the maximum ΔR and weight by $E_i E_j E_k$

Energy Correlators

CMS Collaboration

https://arxiv.org/abs/2402.13864

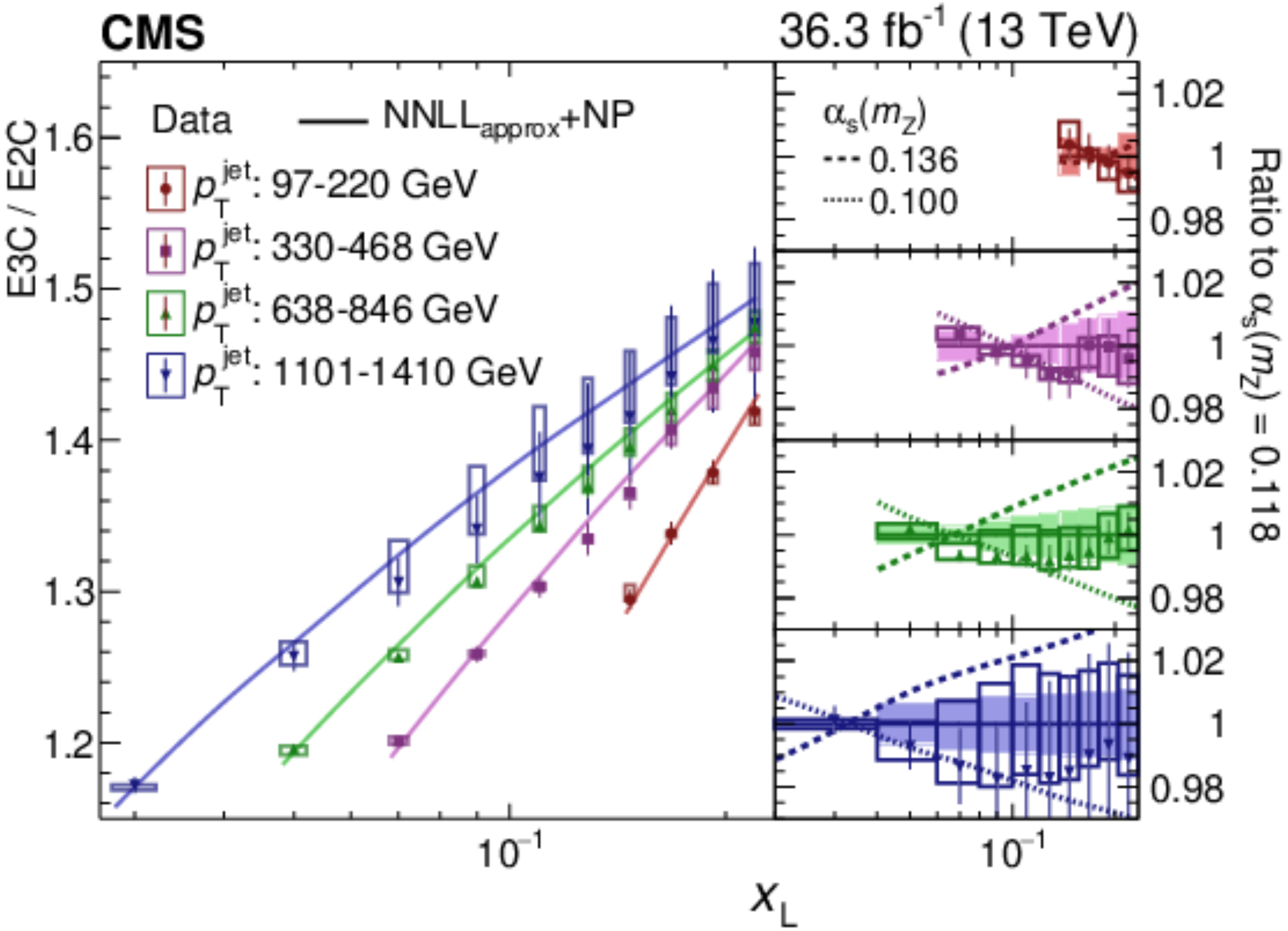

- Ratio of E3C to E2C reveals critical exponents
- Can extract α_S by minimizing χ^2 of the E3C/E2C distributions

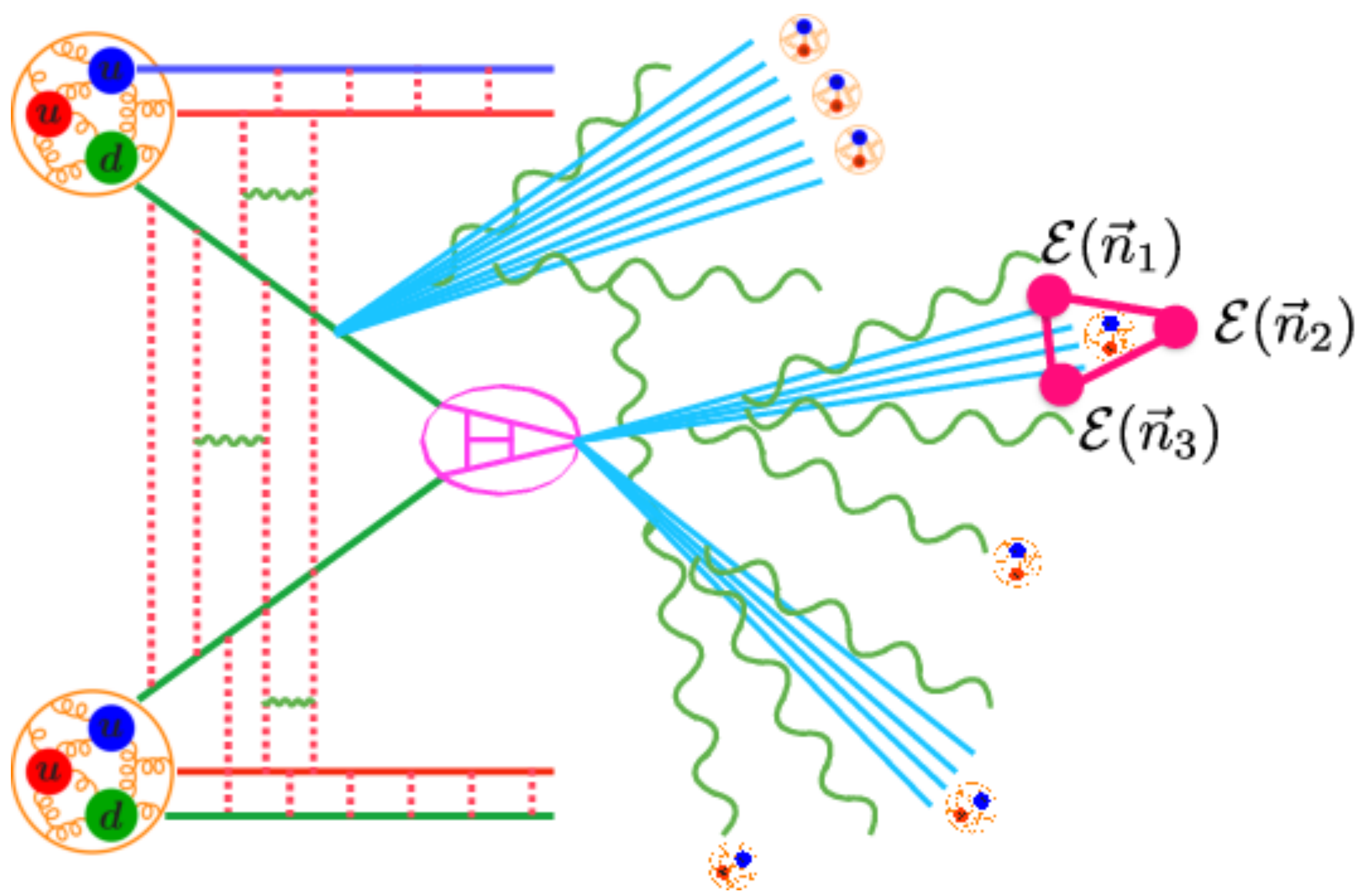

H Chen, I Moult, XY Zhang, HX Zhu , 2020

$$\text{E2C} = \frac{d\sigma^{[2]}}{dx_L} = \sum_{i,j}^{n} \int d\sigma \frac{E_i E_j}{E^2} \delta(x_L - \Delta R_{i,j}),$$

$$\text{E3C} = \frac{d\sigma^{[3]}}{dx_L} = \sum_{i,j,k}^{n} \int d\sigma \frac{E_i E_j E_k}{E^3} \delta(x_L - \max(\Delta R_{i,j}, \Delta R_{i,k}, \Delta R_{j,k}))$$

- Calculate the angular distance between all pairs of particles ΔR
- Weight each distance by the energies of the two daughters $E_i E_j$
- For E3C, choose the maximum ΔR and weight by $E_i E_j E_k$

Energy Correlators

CMS Collaboration

https://arxiv.org/abs/2402.13864

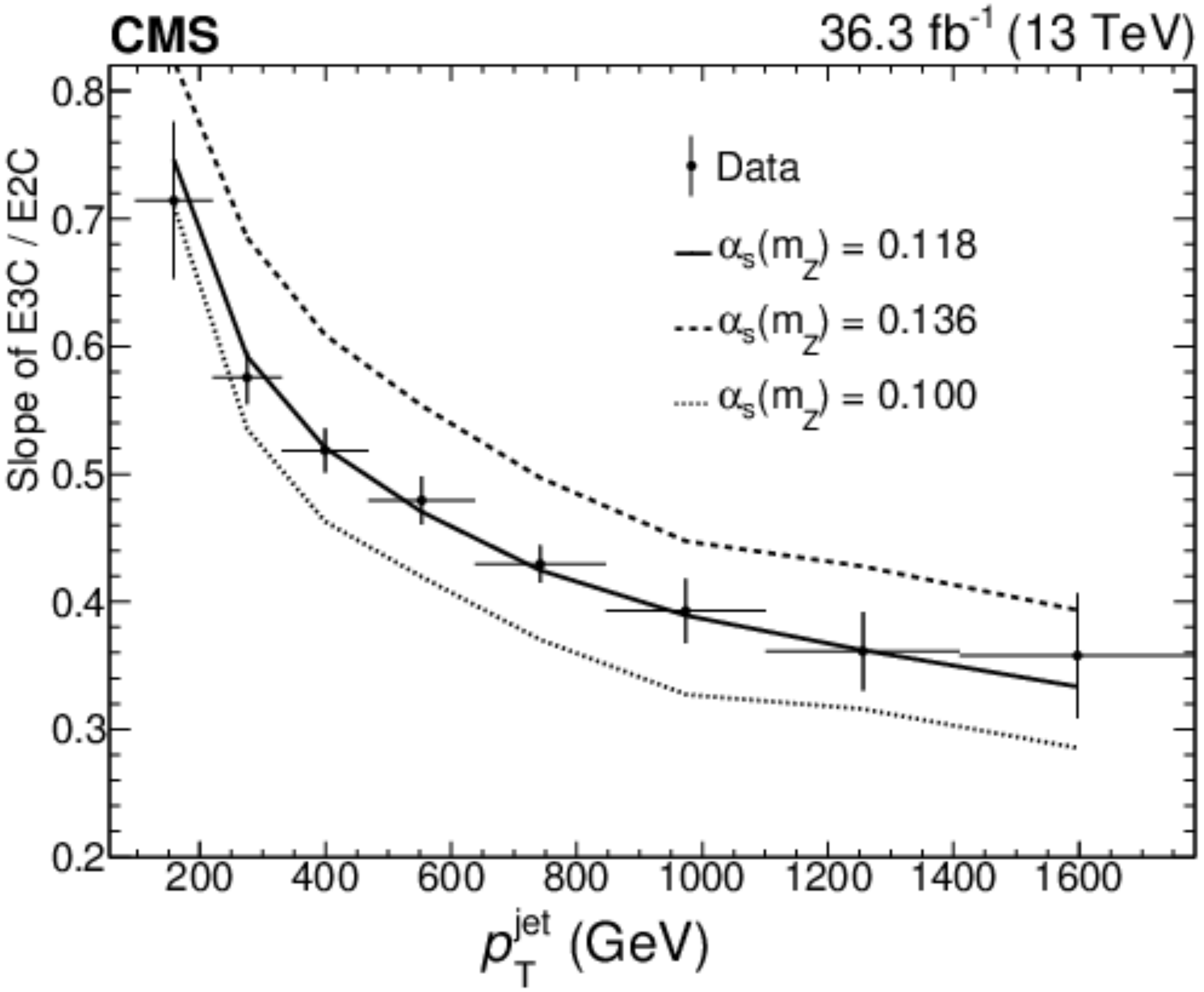

- The “most precise determination of α_S using jet substructure techniques”

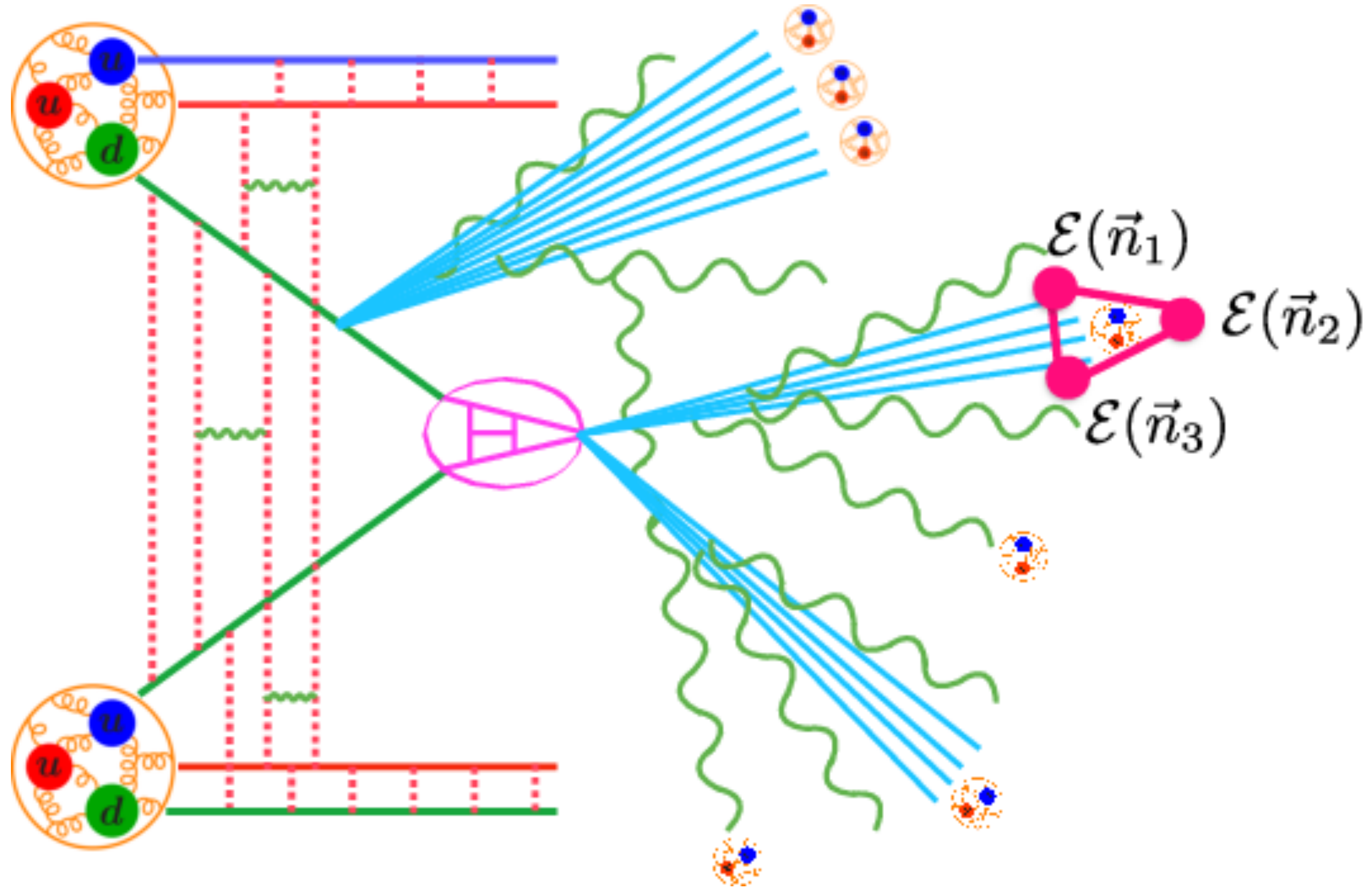

H Chen, I Moult, XY Zhang, HX Zhu , 2020

$$\text{E2C} = \frac{d\sigma^{[2]}}{dx_L} = \sum_{i,j}^{n} \int d\sigma \frac{E_i E_j}{E^2} \delta(x_L - \Delta R_{i,j}),$$

$$\text{E3C} = \frac{d\sigma^{[3]}}{dx_L} = \sum_{i,j,k}^{n} \int d\sigma \frac{E_i E_j E_k}{E^3} \delta(x_L - \max(\Delta R_{i,j}, \Delta R_{i,k}, \Delta R_{j,k}))$$

- Calculate the angular distance between all pairs of particles ΔR
- Weight each distance by the energies of the two daughters $E_i E_j$
- For E3C, choose the maximum ΔR and weight by $E_i E_j E_k$

Energy Correlators

CMS Collaboration

https://arxiv.org/abs/2402.13864

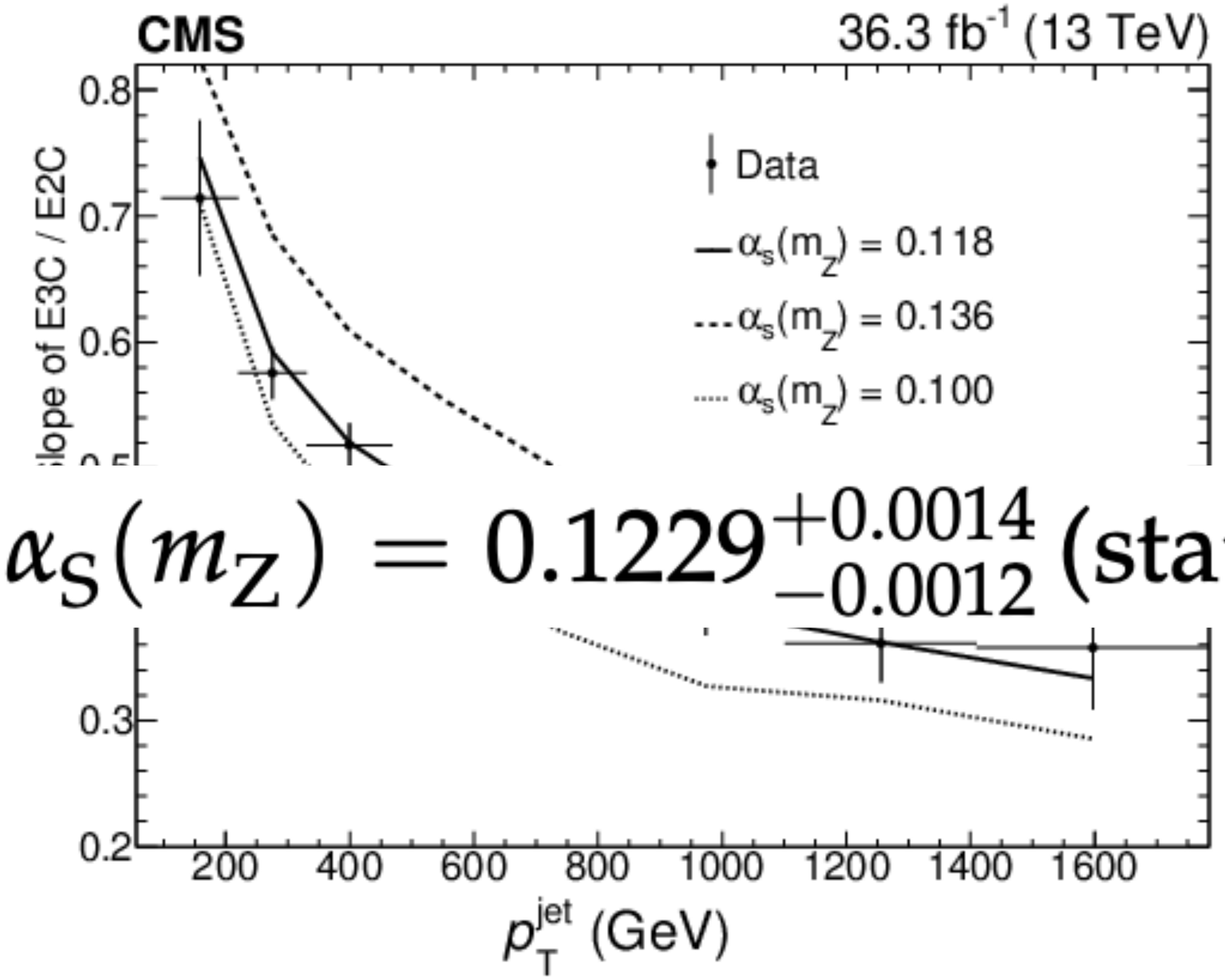

$$\alpha_S(m_Z) = 0.1229^{+0.0014}_{-0.0012}\,(\mathrm{stat})^{+0.0030}_{-0.0033}\,(\mathrm{theo})^{+0.0023}_{-0.0036}\,(\mathrm{exp})$$

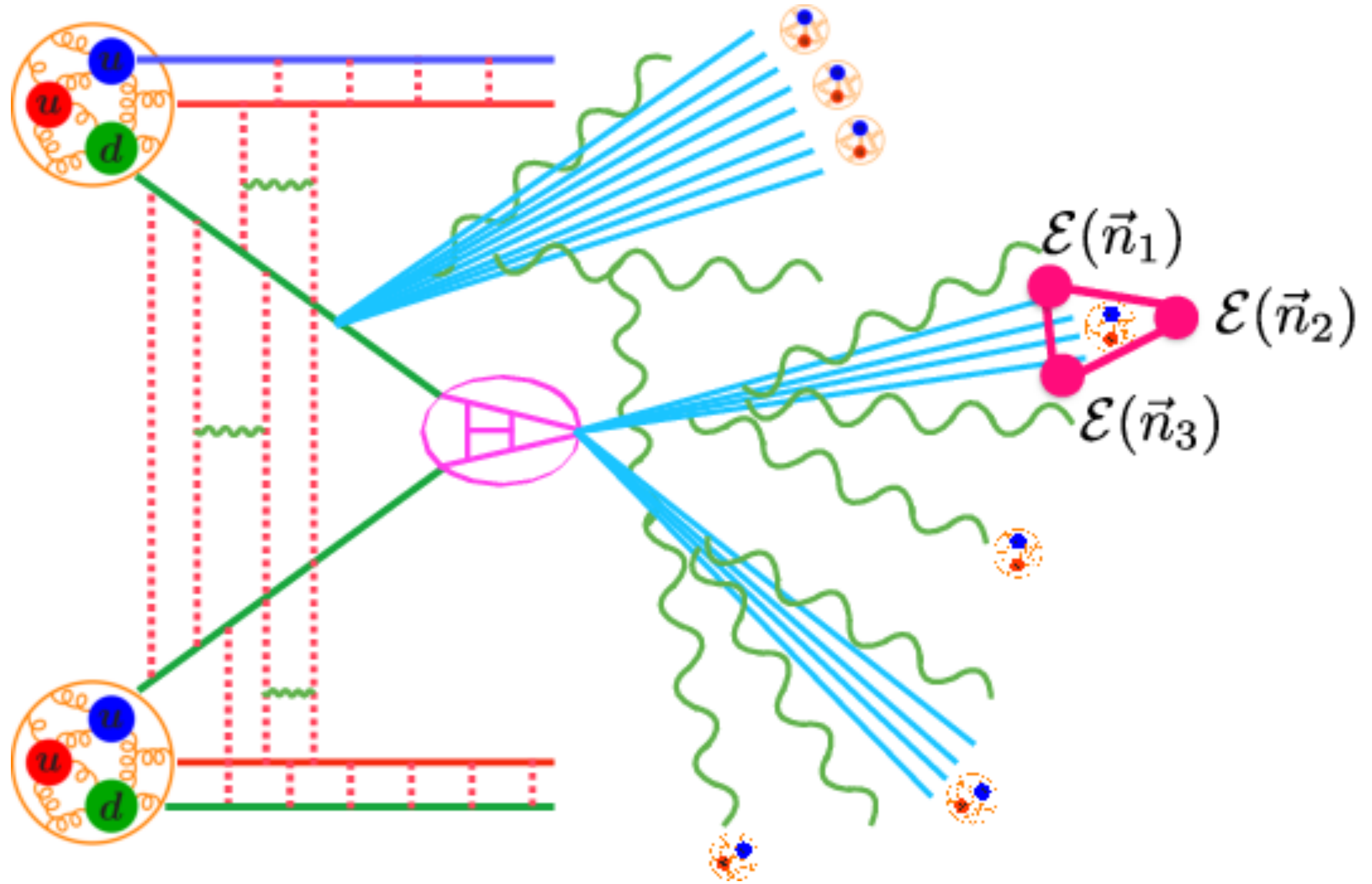

H Chen, I Moult, XY Zhang, HX Zhu , 2020

$\times(\Delta R_{i,j}, \Delta R_{i,k}, \Delta R_{j,k}))$

- Calculate the angular distance between all pairs of particles ΔR
- Weight each distance by the energies of the two daughters $E_i E_j$
- For E3C, choose the maximum ΔR and weight by $E_i E_j E_k$

- The "most precise determination of α_S using jet substructure techniques"

Jet Substructure in Boosted $t\bar{t}$ events

ATLAS Collaboration

arXiv:2312.03797v1

ATLAS EXPERIMENT

Generalized Angularities

$$\lambda_{\beta}^{\kappa} = \sum_{i \in J} z_i^{\kappa} \left(\frac{\Delta R(i, \hat{n})}{R} \right)^{\beta}$$

N-subjettiness

$$\tau_N = \frac{1}{d_0} \sum_k p_{\mathrm{T},k} \min \left\{ \Delta R_{1,k}, \Delta R_{2,k}, \cdots, \Delta R_{N,k} \right\}$$

$$\text{with } d_0 = \sum_k p_{\mathrm{T},k} R_0.$$

Experimental Setup and Jet Reconstruction:

- $\sqrt{s} = 13$ TeV (Run 2)
- $t\bar{t}$ events
- Four types of jets:
  - R = 0.1 Anti-kt calorimeter jets (1)
  - R = 0.4 Anti-kt particle flow jets (2)
  - R = 1.0 reclustered from R = 0.4 jets in (2)
  - p_T dependent variable R jets from tracks

Energy Correlation Functions

$$\mathrm{ECF}(N) = \sum_{i_1 < i_2 < \ldots < i_N \in J} \left(\prod_{a=1}^{N} p_{\mathrm{T},i_a} \right) \left(\prod_{b=1}^{N-1} \prod_{c=b+1}^{N} \Delta R(i_b, i_c) \right)$$

$$C_3 = \frac{\mathrm{ECF}(4)\,\mathrm{ECF}(2)}{\mathrm{ECF}(3)^2},$$

$$D_2 = \frac{\mathrm{ECF}(3)\,\mathrm{ECF}(1)^3}{\mathrm{ECF}(2)^3}.$$

Jet Substructure in Boosted $t\bar{t}$ events

ATLAS Collaboration

arXiv:2312.03797v1

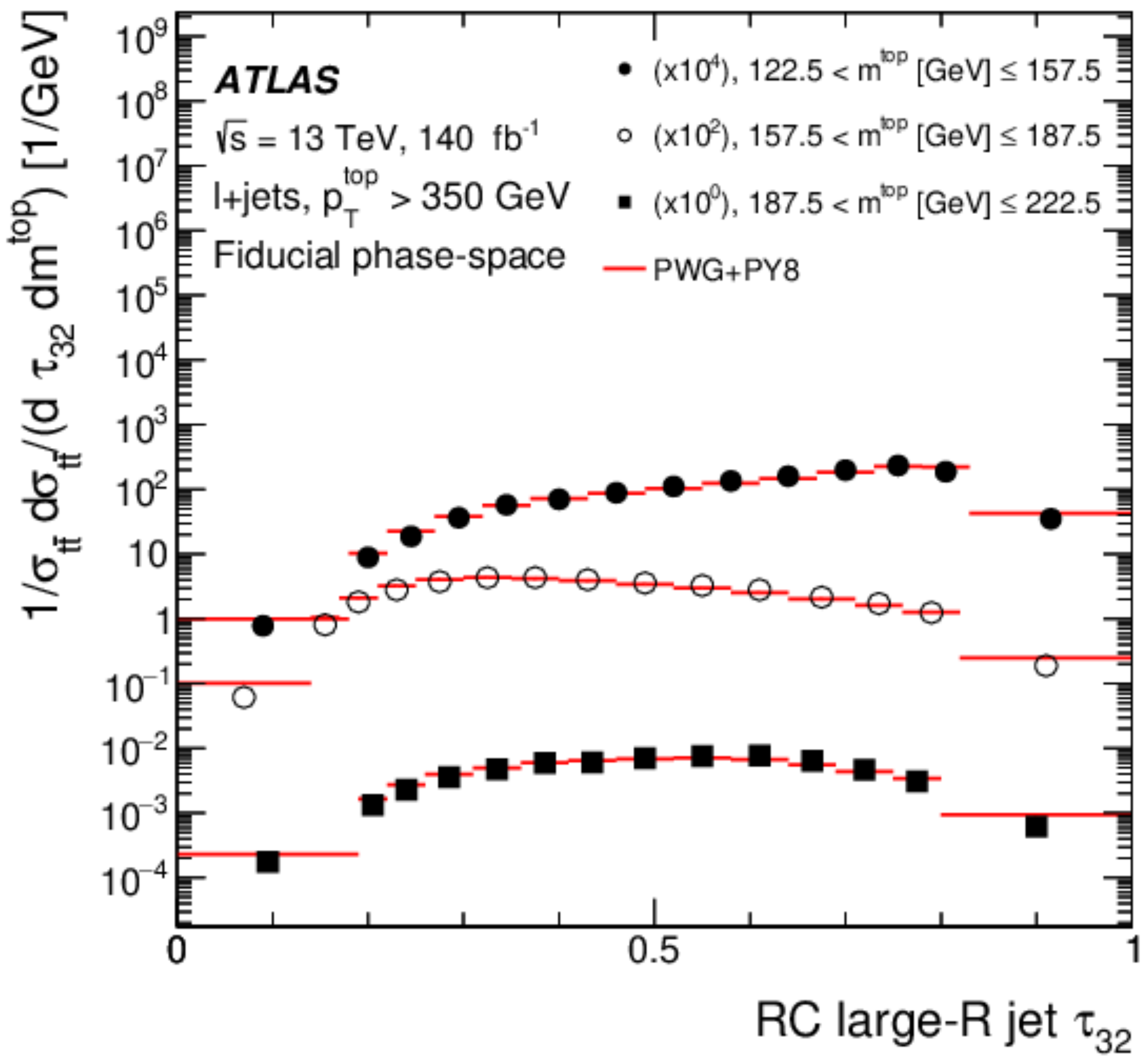

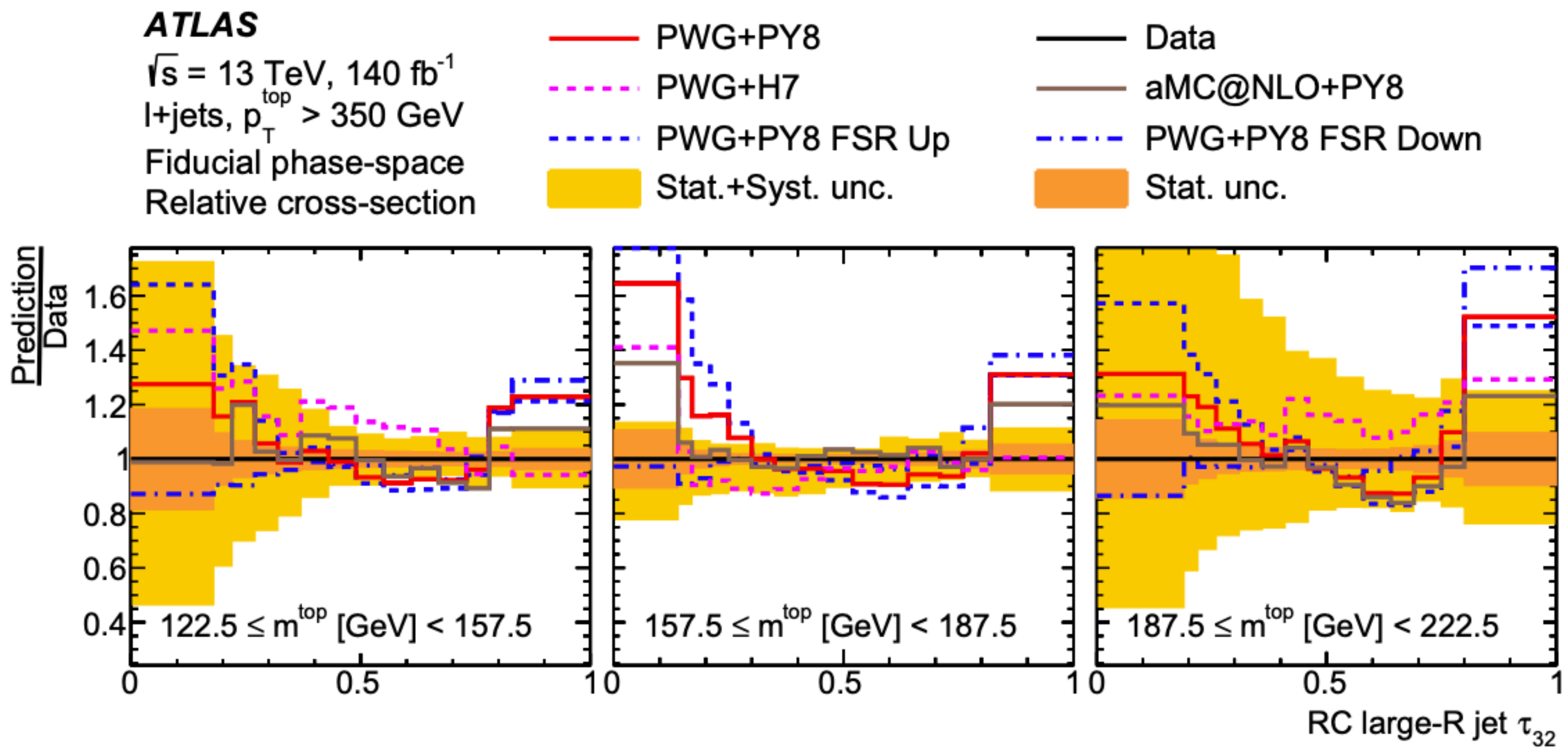

- Ratio of 3-subjettiness to 2-subjettiness τ_{32} for reclustered large R jets as a function of jet mass m^{top}
- τ_{32} discriminates between 2-pronged and 3-pronged jets
- MC generators perform poorly in the middle m^{top} bin

Jet Substructure in Boosted $t\bar{t}$ events

ATLAS Collaboration

arXiv:2312.03797v1

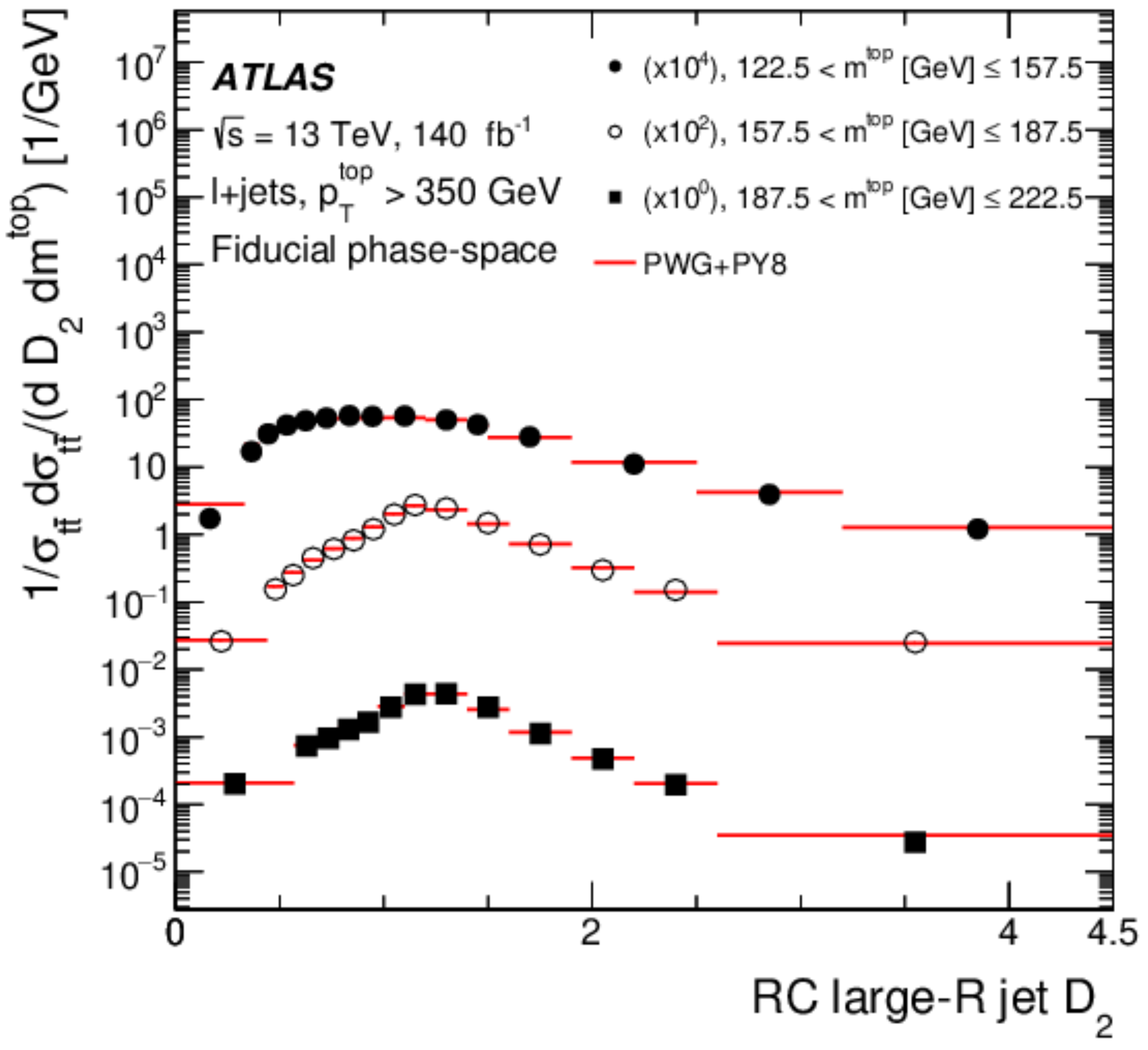

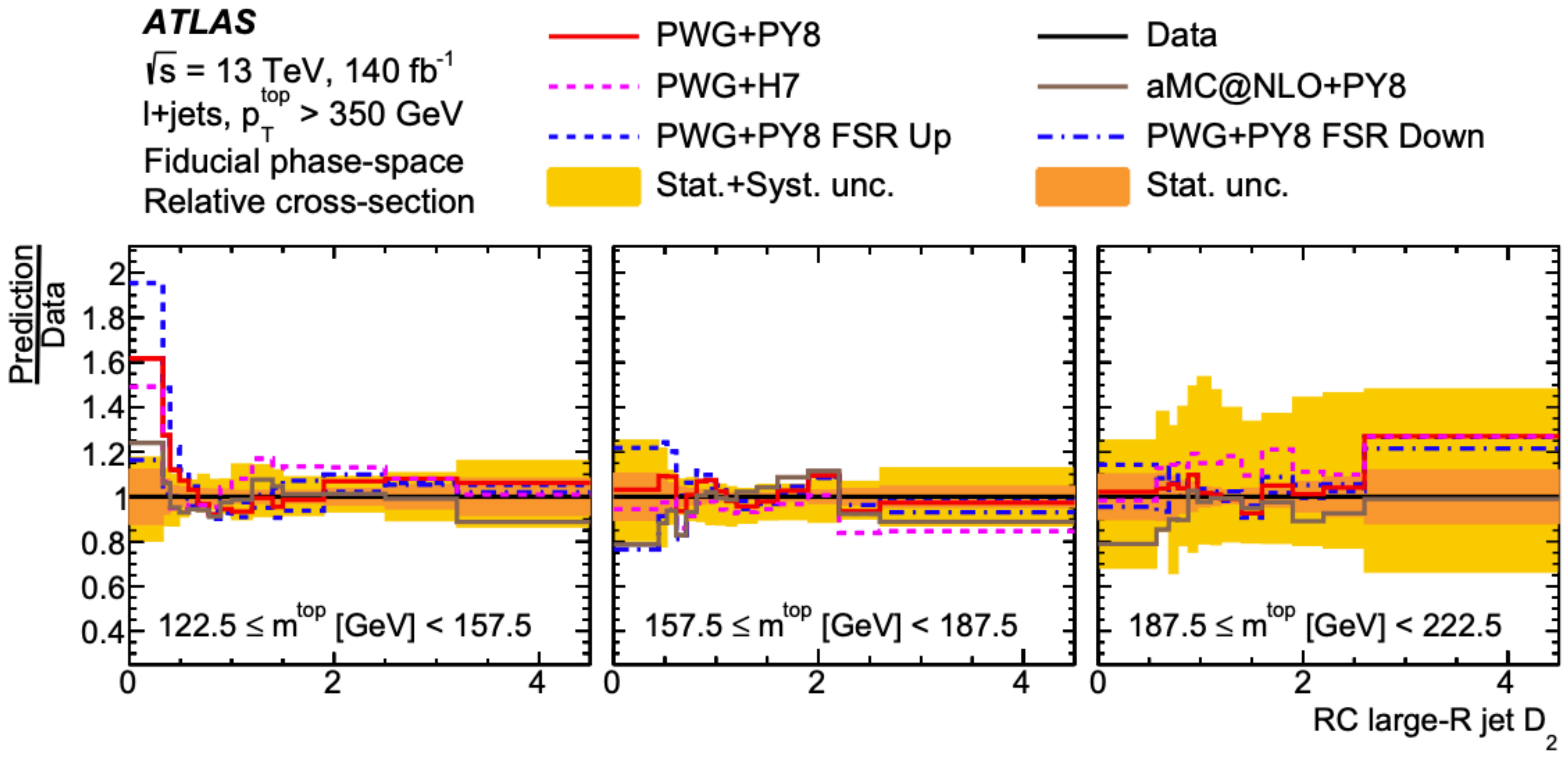

- D_2 is close to 0 for 2-pronged jets
- MC generators perform better in predicting D_2 compared to τ_{32} in bins of m^{top}

Heavy-flavor Jet ID in boosted topologies

CMS Collaboration

CMS PAS BTV-22-001

ParticleNet-MD

- Inputs: particle-flow (PF) objects and secondary vertex (SV) information
- Treat jet as an unordered set of its daughters “particle clouds”

DeepDoubleX

- Inputs: jet observables + PF candidates + SV information
- Complex architecture of convolutional layers and gated recurrent units

DeepAK8-MD

- Inputs: PF objects and SV information
- Takes advantage of correlations between particles through ResNet architecture

Double-b

- Inputs: Track and SV information
- Boosted decision tree to discriminate Higgs to $b\bar{b}$ decays from QCD jets

Studying boosted topologies of heavy resonances $X \rightarrow b\bar{b}/c\bar{c}$ and discriminating them from QCD is important for BSM searches

Heavy-flavor Jet ID in boosted topologies

CMS Collaboration

CMS PAS BTV-22-001

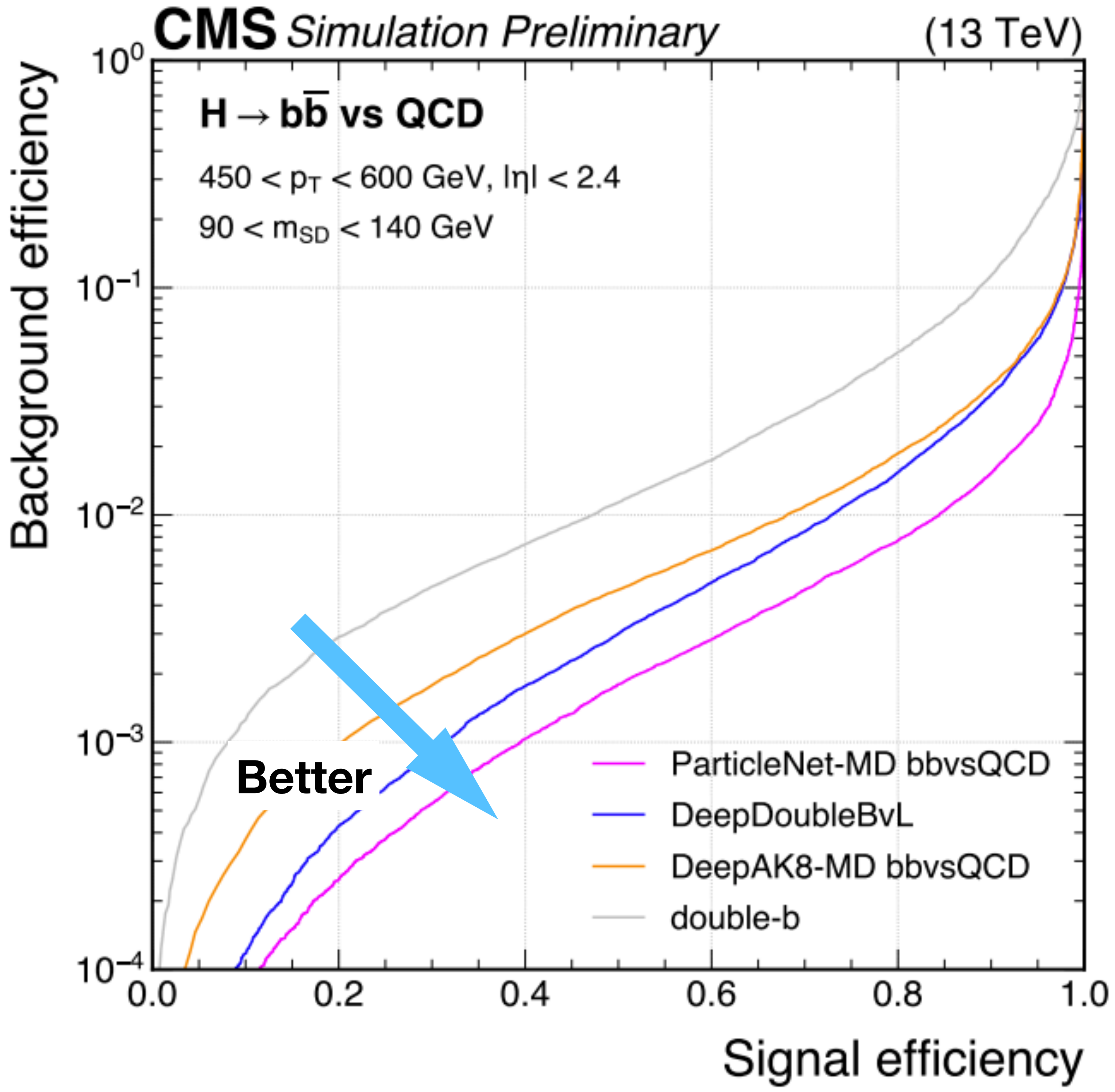

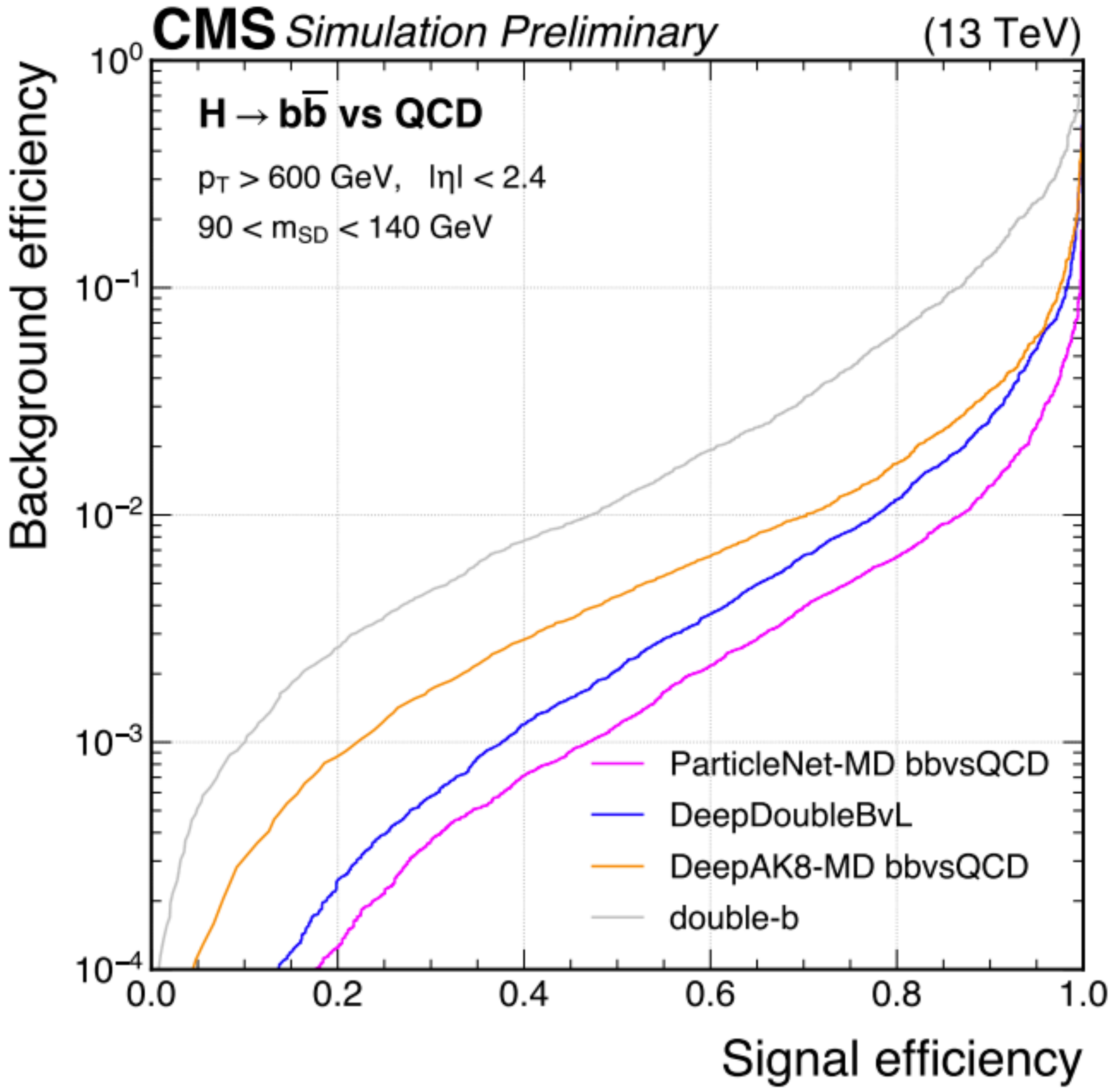

- Receiver operating characteristic (ROC) curve show the signal efficiency versus background rejection
- Neural nets outperform the BDT since they utilize more information from PF objects

Heavy-flavor Jet ID in boosted topologies

CMS Collaboration

CMS PAS BTV-22-001

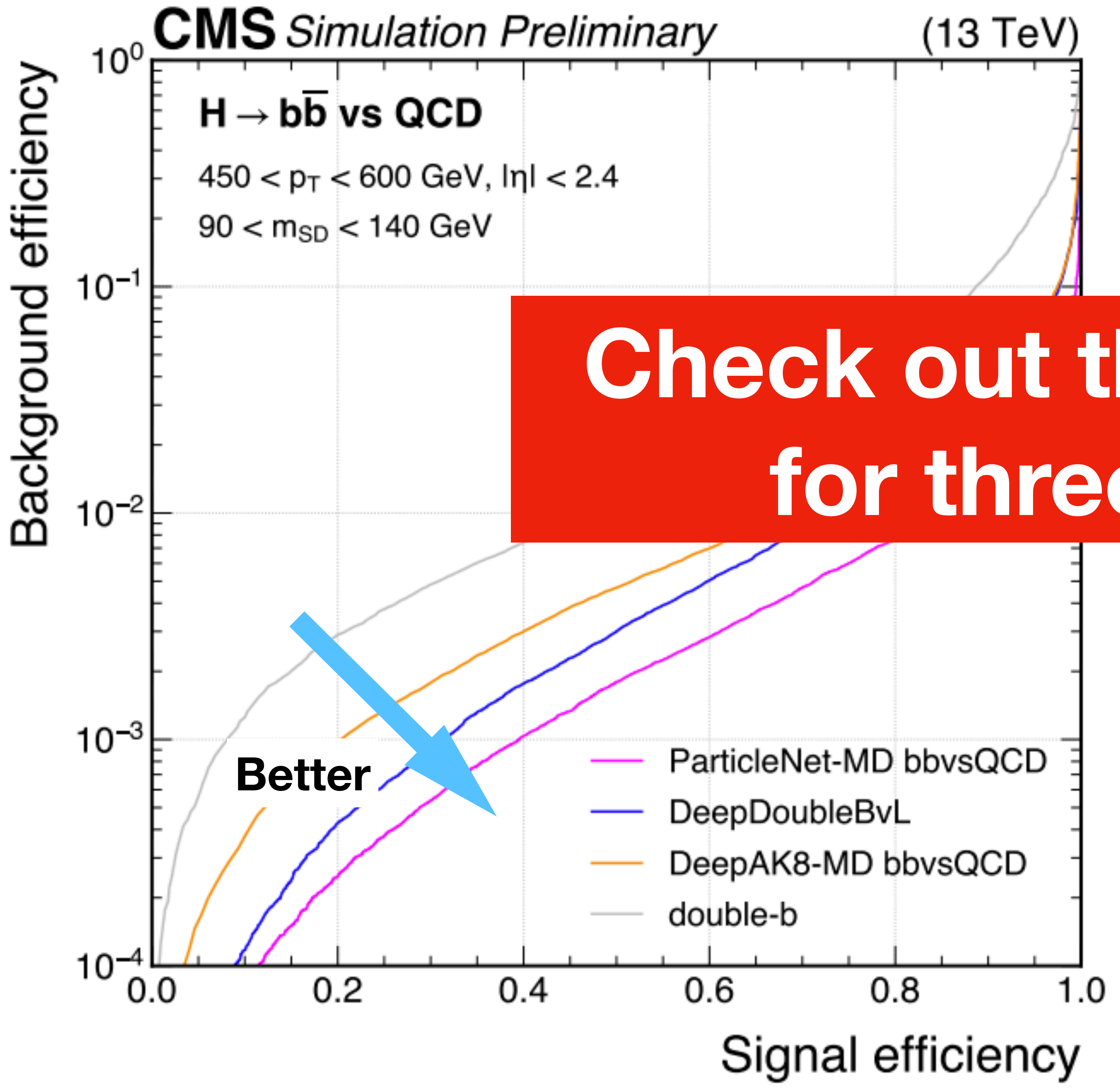

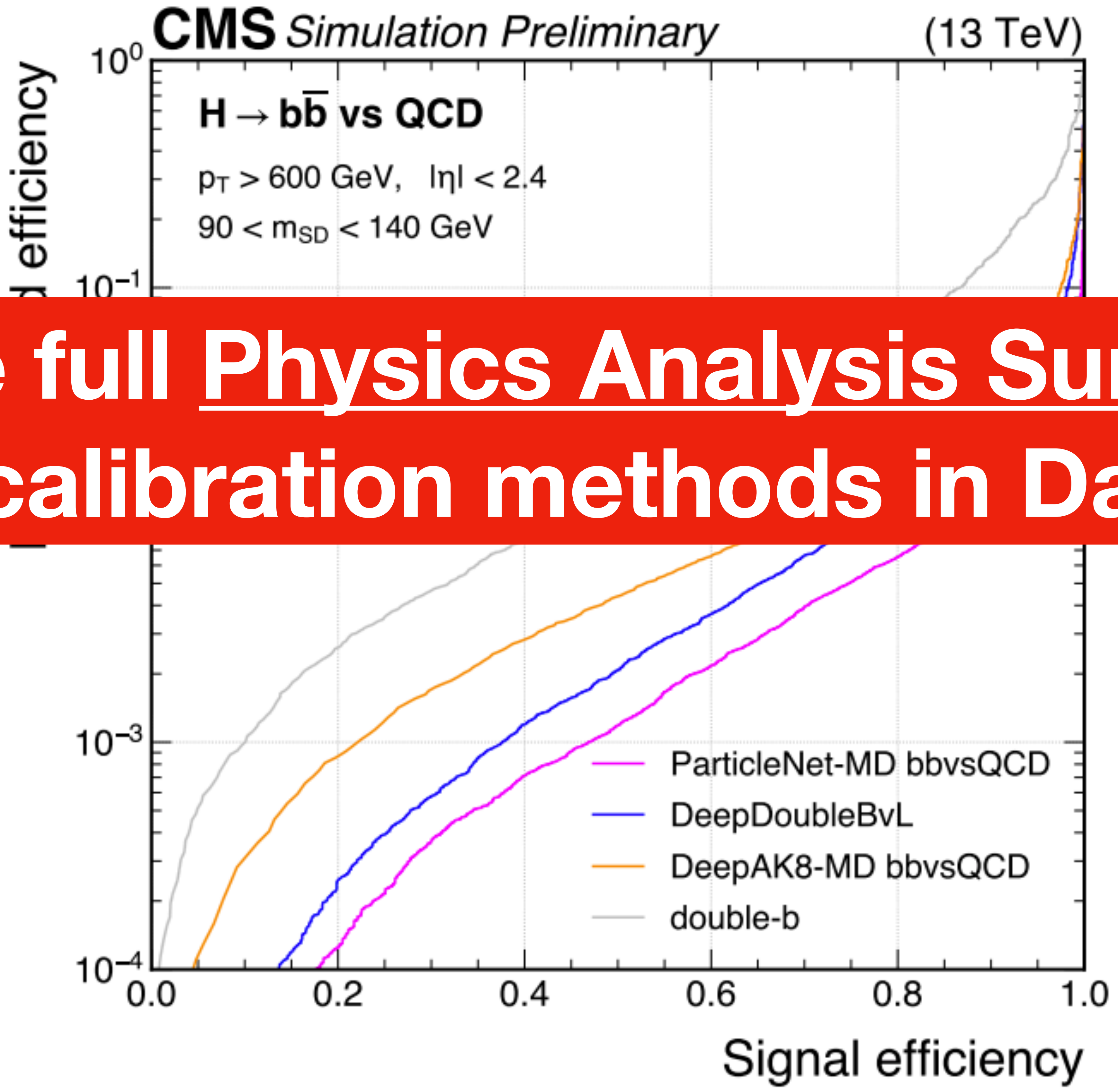

Check out the full Physics Analysis Summary for three calibration methods in Data

- Receiver operating characteristic (ROC) curve show the signal … ncy versus … round rejection
- Neural nets outperform the BDT since they utilize more information from PF objects